Development and Kinetic Analysis of Homogeneous and Heterogeneous Transition Metal Catalysts for the Cleavage of Phosphate Esters in Methanol

by

Mark F. Mohamed

A thesis submitted to the Department of Chemistry

in conformity with the requirements for the

degree of Doctor of Philosophy

Queen's University

Kingston, Ontario, Canada

November, 2010

Abstract

Described here are detailed kinetic studies probing the structural elements which are crucial for the catalytic activity of dinuclear Zn(II) complexes towards phosphate diester cleavage. First, two sets of dinuclear Zn(II) complexes (a member with and without a bridging oxyanion linker group) were synthesized and their ability to promote the cyclization of 2-hydroxypropyl-*p*-nitrophenyl phosphate, a common model for RNA, was compared. Kinetic studies indicated that the complexes without the oxyanion linker were more active in promoting the cyclization in methanol under ${}^{s}_{s}\mathrm{pH}$ controlled conditions at 25 ^{o}C. Quantitative energetics analysis shows that the rate reduction is attributable to a decrease in the second-order rate constant for the cyclization reaction, which adds 3.7 and 6.5 kcal/mol of activation energy to the respective reactions mediated by the complex with the oxyanion linker.

Secondly, we have investigated a series of dinuclear Zn(II) complexes that incorporate various substituents including hydrophobic and hydrogen-bonding ones. Analysis of the data at the ${}^{s}_{s}\mathrm{pH}$ optimum for each reaction indicates that the presence of the H-bonding groups and alkyl groups provides similar increases (at least an order of magnitude) of the k_{cat} terms over the unfunctionalized complex. There is also no clear trend that H-bonding groups or the alkyl groups provide stronger binding to the substrate than the parent complex.

We also describe here the preparation and kinetic analysis of a series of solid supported transition metal catalysts for the cleavage of P=O chemical warfare simulants and P=S pesticides. We report a kinetic study of a 1,10-phenanthroline:Zn(II) complex

immobilized on macroporous polystyrene which is capable of accelerating the cleavage of G-agent and V-agent simulants in methanol at neutral ${}^{s}_{s}\mathrm{pH}$ and ambient temperature by up to 10^5-fold. The materials are recoverable and can be recycled at least ten times.

We have also devised a methodology for simple immobilization of an *ortho*-palladated dimethylbenzylamine complex on macroporous polystyrene and amorphous silica gel. We report the catalyst preparation and a detailed kinetic study of their catalysis of the methanolysis of five P=S pesticides at neutral ${}^{s}_{s}\mathrm{pH}$ and ambient temperature. The polymeric catalysts give over 10^9-fold acceleration compared to the uncatalyzed background reaction at the same ${}^{s}_{s}\mathrm{pH}$.

Acknowledgments

Although mine is the only name on this thesis, it would not have been possible without the support of many friends, family, and colleagues. First and foremost, I owe my deepest gratitude to my supervisor, Dr. R. Stan Brown. I joined Stan's research group as an undergrad and never looked back. There is something contagious about Stan's passion for chemistry and I could not have asked for a better mentor and teacher from whom to learn chemistry. Every time that I started to lose confidence in my projects, it seemed like a five minute chat with Stan was enough to remind me why I love doing chemistry. I am thankful for Stan's guidance and support, and I am sincerely grateful for the confidence that he has continually shown in me.

I am truly indebted to Dr. Alexei Neverov. I would like to thank Alex for his guidance and friendship throughout my time in the lab. Alex's encyclopaedic knowledge of physical organic chemistry and constant willingness to share it are things that I will be grateful for throughout my scientific career. Beyond the science, Alex helped to make working in the Brown group such an enjoyable experience, and has taught me as many lessons on the tennis court as in the lab.

During my time in the Brown group, I have had the opportunity to work with some outstanding scientists whom I am priviledged to call friends. Tony Liu and Chris Maxwell have been there since the beginning and I thank them for making it so much fun to come into the lab every day. I will truly miss all of our scholarly debates (read: arguments) and Friday afternoon musings. I am grateful to Stephanie Melnychuk for her

friendship and support, both as a Brown group member and ever since. Dr. Graham Gibson, my first boss in the Brown group, is thanked for guiding me during those early days. I am grateful for the efforts of Dr. Benoît Didier, who gave me a glimpse into the world of polymers. Dr. Dave Edwards is thanked for many insightful discussions and for spreading his enthusiasm for chemistry. Outside the Brown lab, I am grateful to Jenny Du of the Crudden group for her friendship and motivation, both in and out of the lab.

I owe more to my family than I can possibly do justice in this short space. My father, Fahmy Mohamed, and my sister, Amira Mohamed, have been an unwavering source of support and inspiration. I have known my big sister as long as I have known myself, and I couldn't have wished for a better friend and role model. My father has been a constant source of encouragement, guidance, and is my role model in life. Nothing that I can say here can even begin to express my appreciation for all that he has done. Although she wasn't here to share in the experience, my mother Carol Ann Mohamed has been just as big a part of this journey as anyone. I miss her every day and I know that she is proudly watching over me.

Statement of Originality

To the best of the author's knowledge, the original work in this thesis includes the following:

1. Kinetic study and energetic analysis of the transesterification of the RNA model 2-hydroxypropyl-*p*-nitrophenyl phosphate (HPNPP) catalyzed by **2.6**:$Zn(II)_2$, **2.7**:$Zn(II)_2$, and **2.8**:$Zn(II)_2$ in methanol.

2. Kinetic study of the transesterification of 2-hydroxypropyl-*p*-nitrophenyl phosphate (HPNPP) catalyzed by **3.7**:$Zn(II)_2$ – **3.13**:$Zn(II)_2$ in methanol, including the previously unreported synthesis of compounds **3.10** and **3.11**.

3. Kinetic study of the methanolysis of *O*-ethyl *O*-*p*-nitrophenyl methylphosphonate (**4.7**) and *O*- Ethyl *S*-(3,5-dichlorophenyl) methylphosphonothioate (**4.8**) catalyzed by the complex **4.6**:Zn(II) immobilized on macroporous polystyrene beads.

4. Development of a simple procedure for the preparation palladacycle **5.7** immobilized on the surface of macroporous polystyrene and amorphous silica gel beads.

5. Kinetic study of the methanolysis of fenitrothion (**5.2**), dichlofenthion (**5.4**), coumaphos (**5.5**), diazinon (**5.6**), and malathion (**5.8**) catalyzed by palladacycle **5.7** immobilized on macroporous polystyrene and amorphous silica gel beads.

Table of Contents

List of Figures

List of Tables

List of Schemes

List of Abbreviations

12N3	1,5,9-triazadodecane
Abs	absorbance
BNPP	*bis*(*p*-nitrophenyl) phosphate
CW	chemical warfare
d	doublet
dd	doublet of doublets
DMF	dimethylformamide
DNA	deoxyribonucleic acid
DPA	di(2-picolyl)amine
DVB	divinylbenzene
EI-TOF	electron impact – time of flight
ESI-TOF	electrospray ionization – time of flight
Et	ethyl
HEPES	4-(2-Hydroxyethyl)piperazine-1-ethanesulfonic acid
HPLC	high-performance liquid chromatography
HPNPP	2-hydroxypropyl-*p*-nitrophenyl phosphate
HRMS	high resolution mass spectrometry
Hz	hertz
LD_{50}	lethal dose, 50%
LRMS	Low resolution mass spectrometry
m	multiplet
MHz	megahertz

MNPP	methyl-*p*-nitrophenyl phosphate
NLLSQ	non-linear least square
NMP	N-methyl-2-pyrrolidone
NMR	nuclear magnetic resonance
OP	organophosphorus
OTf	triflate (trifluoromethanesulfonate)
P=O	phosphorus double bonded to oxygen
P=S	phosphorus double bonded to sulphur
RNA	ribonucleic acid
s	singlet
t	triplet
T	temperature
THF	tetrahydrofuran
TMEN	N,N,N'N'-tetramethylethylenediamine
TMPP	2,2,6,6-tetramethylpiperidine
TRIM	trimethylolpropane trimethacrylate
TS	transition state
UpU	uridylyl(3',5')uridine
UV-vis	ultraviolet-visible

Chapter 1 - General Introduction

1.1 – Metal ion catalyzed solvolysis reactions in non-aqueous solvents

Cleavage of the phosphodiester linkage in RNA and DNA by phosphodiesterases under physiological conditions represents one of the most impressive enzymatic transformations known due to the high thermodynamic stability of the phosphate ester bond.[1] A survey of the enzymes responsible for phosphate ester cleavage reveals that many of these enzymes contain multiple metal ions in their active sites,[2] a fact which has sparked intense interest in the study of metal ion promoted phosphate ester solvolysis reactions. The ability of metal ions to catalyze the cleavage of neutral phosphate esters and phosphonates has also been identified as an attractive method for the destruction of toxic neutral organophosphorus compounds which have found widespread use as pesticides and chemical warfare agents.[3] While there have been numerous studies of metal ion catalyzed hydrolysis reactions, a detailed account of these processes has proven problematic due to the poor solubility of metal-hydroxo complexes at high pH. For a metal ion-aquo complex, $M^{x+}(H_2O)_n$, at a pH above the pK_a of a metal-bound water molecule the $M^{x+}(^{-}OH)_n$ complex can oligomerize and precipitate from solution. This undesirable characteristic of metal ions in aqueous solution severely limits the concentration and pH range over which such catalytic systems can be studied. In addition to poor solubility characteristics, the strongly solvating nature and high dielectric constant of water weaken the metal ion:substrate interactions required for catalysis.

Transition into lower polarity protic solvents alleviates many of the limitations imposed by water. In particular, the light alcohols (methanol and ethanol) were found to be

particularly suitable media for metal ion catalyzed phosphoryl transfer. Specifically, methanol is the organic solvent which most closely resembles water in terms of structure and solvation, yet has a dielectric constant which is much lower than that of water (31.5 vs. 78.5 at 25°C).[4] The lower dielectric constant of methanol strengthens electrostatic interactions between charged species in solution which promotes the association of the catalyst and substrate. The Debye-Hückel theory for association of spherical ions in solution predicts that the potential energy of interaction of oppositely charged ions is inversely proportional to the dielectric constant of the medium as given in equation 1.

$$PE = (z_+e)(z_-e)/(4\pi D_0 D_r r) \quad (1)$$

Where z_+e and z_-e are the charges in Coulombs (e = proton charge), r is the distance between the centres of the ions, D_0 is the permittivity of a vacuum, and D_r is the dielectric constant of the medium.[5] Methanol is also advantageous since, unlike the case in water, the metal-alkoxy complexes are generally soluble over a wide pH range. A further benefit of using methanol as a solvent is the improved solubility of organic substrates which often show limited solubility in water.

In addition to the practical benefits of conducting solvolytic processes in alcoholic media is the possibility that the lower dielectric constant medium offers a more realistic representation of an enzyme active site. Although biological reactions involving phosphoryl transfer are hydrolytic, evidence is quickly accumulating which suggests that the active sites of enzymes typically do not exhibit the properties of bulk-water but instead are better approximated as lower polarity organic solvents.[6]

The use of methanol as a reaction medium for solvolytic processes is ultimately hinged upon the ability to accurately control and measure pH. Thanks largely to the recent work of Bosch and coworkers,[7] the pH of a methanol solution can be readily determined by potentiometric means using the relationship ${}^{s}_{s}\mathrm{pH} = {}^{s}_{w}\mathrm{pH} - \delta$ (where ${}^{s}_{s}\mathrm{pH}$ is the pH of a non-aqueous solvent referenced to that solvent, ${}^{s}_{w}\mathrm{pH}$ is the pH of a non-aqueous solvent referenced to water, and δ is a correction constant unique to a given solvent).[i]

In methanol, deLigny and Rehbach[8] previously determined the correction constant to be $\delta = -2.24$ on the molarity scale. Thus, determination of ${}^{s}_{s}\mathrm{pH}$ in methanol is a trivial matter of adding 2.24 to pH readings obtained using a glass electrode calibrated with standard aqueous buffers.

1.2 - Anionic Phosphate Diesters in Nature

Biochemical reactions involving phosphoryl transfer are vital components of normal cellular metabolism and function. This general class of reactions plays a crucial role in many fundamentally important cellular processes including simple metabolism, cell signaling, nucleic acid replication and repair, and gene expression. Arguably the most important biological role of the phosphate diester linkage is the protection of the genetic information stored in the nucleic acid biopolymers, DNA and RNA. Phosphate diesters are highly resistant to solvolytic cleavage and as a result their spontaneous decomposition under physiological conditions is exceedingly slow. The half-life time for the

[i] For the designation of pH in non-aqueous solvents we use the nomenclature recommended by the IUPAC, *Compendium of Analytical Nomenclature. Definitive Rules 1997*, 3rd ed.; Blackwell: Oxford, U.K., 1998.

spontaneous hydrolysis of the simple phosphate diester dineopentyl phosphate at pH = 7.0 and 25 °C was recently estimated to be 31 million years (corresponding to a first-order rate constant of 7×10^{-16} s^{-1}).[1,9] This value is taken as a reasonable approximation of the spontaneous rate of hydrolysis of DNA. The rate of cleavage of RNA is considerably faster due to the presence of the 2'-OH group which acts as an intramolecular nucleophile. Extrapolation of the kinetic data for the base promoted isomerization of the dinucleotide uridylyl(3',5')uridine (UpU, **2** Base = U)[10] allowed for an estimate of 110-years for the half-life of RNA at pH = 7.0 and 25 °C.[11]

1.3 - Phosphate Ester Cleaving Enzymes

While protection of DNA and RNA from damage and unwanted cleavage is essential for sustaining life, many crucial biochemical processes require controlled scission of the phosphate backbone. To counter the exceptionally slow rates of the spontaneous hydrolysis of DNA and RNA (which are far too slow to occur on a biologically relevant time-scale) nature has evolved a series of enzymes specifically designed to accelerate these reactions and allow them to occur at rates which are conducive to cellular activity. A common motif within the active site of phosphate cleaving enzymes is the presence of multiple metal ions.[2] Examples of phosphodiesterase enzymes containing metal ion cofactors include ribonuclease H from HIV reverse transcriptase,[12] 3',5'-exonuclease from DNA polymerase I,[13] P1 and S1 nucleases,[14] and phospholipase C [2] (Figure 1-1). The phosphomonoesterase alkaline phosphatase (which also retains residual phosphodiesterase activity) is the most studied of the metal-containing phosphate cleaving enzymes.[2c,f] Within the active site of metallophosphodiesterases, one typically

finds Zn(II) as the catalytic metal however phosphodiesterases containing Ca(II), Mg(II), Mn(II), and Fe(II) are also known. Next to iron, zinc is the most abundant transition metal in biological systems accounting for up to 3.0 g of the average human body mass.[2a] Many favorable characteristics contribute to the prevalence of Zn(II) as a catalytic metal including its unconstrained coordination geometry, facile ligand exchange, lack of redox chemistry, borderline hard-soft properties (allowing it to bind to a variety of heteroatom ligands), relatively high Lewis acidity, and high bioavailability.[2a]

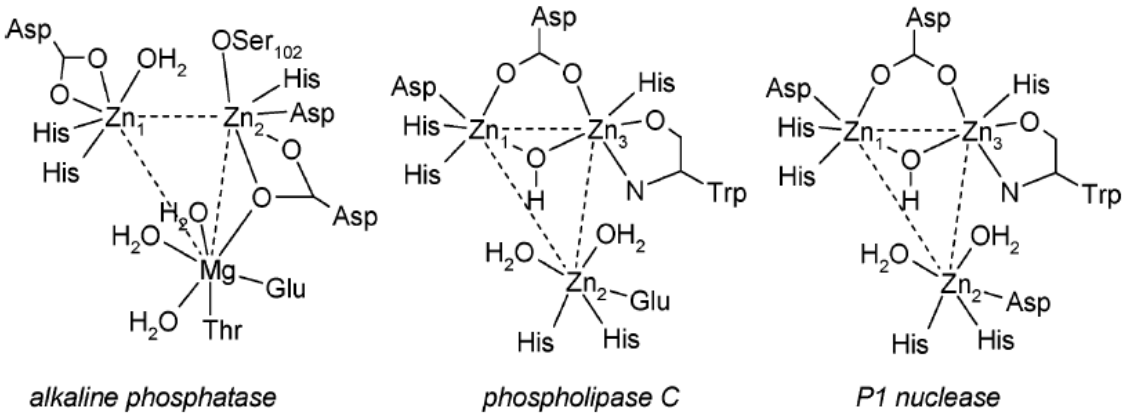

Figure 1-1. Active site structures of three multinuclear metallophosphatases: The phosphomonoesterase alkaline phosphatase, and the phosphodiesterases phospholipase C and P1 nuclease (Reference 2c)

The catalytic role of the Zn(II) ions in phosphoesterases can be divided into two general categories: 1) direct, inner sphere activation; and 2) indirect, outer sphere activation.[11] Direct, inner sphere activation encompasses: a) Lewis acid activation by coordination of the phosphoryl oxygen (**A**, Figure 1-2); b) lowering of the pK_a of a bound nucleophile (H_2O or ROH) to generate higher concentrations of the nucleophilic anion at physiological pH (**B**, Figure 1-2); and c) leaving group assistance through coordination

and stabilization of the developing negative charge (**C**, Figure 1-2). Indirect, outer sphere activation requires the involvement of a metal bound hydroxide as a general base (**D**, Figure 1-2) or a metal bound water as a general acid (**E**, Figure 1-2).

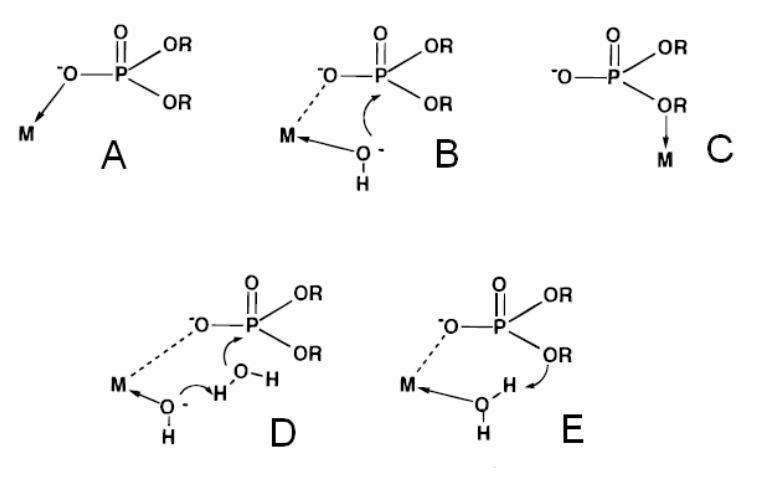

Figure 1-2. Typical modes of metal ion activation in the hydrolysis of phosphate esters. Direct, inner sphere activation (A, B,C) and indirect, outer sphere activation (D,E). (Adapted from Reference 11)

When two or more metal ions are located in close proximity (as in several enzyme active sites), the metal ions may act cooperatively to give rate enhancements which are greater than the sum of the accelerations afforded by the individual metals. When cooperativity is available, the catalytic mechanism may involve combinations of the activation modes depicted in Figure 1-2. Characterization of the cooperative mechanism involving multiple metal-ions is complicated by the fact that many of the possible mechanisms are kinetically indistinguishable.[11]

While the ubiquity and importance of metallophosphatases has been amply demonstrated, exact details as to how these catalysts achieve such huge rate accelerations remain sparse. The non-specific phosphomonoester alkaline phosphatase is by far the most extensively

studied metallophosphatase, and while its mechanism of action is relatively well understood[2,15,16] it is only recently that details concerning the nature of the reaction transition state and the origin of the enzyme's acceleratory power have begun to emerge.[17] In the case of phosphodiesterases, mechanistic details are limited and what is known is based largely on analogy to alkaline phosphatase due to active site homology.[17a,18]

1.4 - Small molecule mimics of dinuclear Zn(II) enzymes in water

The remarkable rate enhancements achieved by enzymes, particularly with respect to phosphoryl transfer, has generated an intense interest in the design and synthesis of synthetic small molecules which mimic the catalytic power of natural systems. The quest to develop synthetic enzyme mimics is largely motivated by academic interest to better understand how enzymes function. In comparison to the situation with enzymes, a mechanistic study involving a small molecule catalyst is a much more tractable problem. Low molecular weight species are much more conducive to systematic structure-activity relationship studies than enzymes and are more amenable to characterization by conventional techniques.[19] In addition to elucidating the fundamental principles of enzyme function, the development of efficient synthetic phosphatases could have important applications as customizable artificial restriction enzymes and other therapeutic agents,[20,21,22,23] and may prove invaluable in the industrial sector where enzyme use is rapidly expanding.

In a discussion of synthetic enzyme models, it is worthwhile to briefly discuss the model substrates against which these catalysts are screened. The use of DNA and RNA as substrates for model enzymes is complicated by the multitude of metal binding sites on the biomolecules which make it difficult to control and characterize the catalyst-substrate interactions. Furthermore, monitoring reactions involving DNA or RNA cleavage generally requires techniques such as gel electrophoresis which are not amenable to real-time reaction analysis. In assessing the efficiency of a model enzyme one would always like to make a comparison between the rate of the catalyzed reaction and the uncatalyzed background reaction. In the case of DNA and RNA, which are notoriously stable towards solvolysis, the accurate determination of an uncatalyzed rate constant has proven very difficult.[24]

As an alternative to natural substrates, a number of convenient reactive models having the same phosphoester linkage have been developed. Model substrates tend to be activated ones whose uncatalyzed solvolysis can be readily measured. The uncatalyzed background reactions for natural substrates are often estimated based on the extrapolation of structure-reactivity relationship data for activated substrates, or based on extrapolation of experimental data collected at high temperature. One must always be conscious of the fact that such estimations are derived from long-extrapolations which may have large inherent errors.[24] In the case of RNA, the most widely used model substrate is 2-hydroxypropyl-*p*-nitrophenyl phosphate (HPNPP, **1.1**) which was developed by Brown and Usher.[25] The hydroxypropyl moiety of HPNPP is representative of the 2'-OH of RNA and the *p*-nitrophenol (or *p*-nitrophenoxide) leaving group is easily observed by

UV-vis spectrophotometry in real-time.[ii] More realistic models of RNA which are often employed are simple dinucleotides (3',5'-BpB, **1.2**, where B = base), but the use of these substrates is made inconvenient by the need for reverse phase HPLC and ^{31}P NMR for reaction analysis which is difficult to perform in real-time. As models for DNA, commonly used examples include *bis*(*p*-nitrophenyl) phosphate (BNPP, **1.3**), and methyl-*p*-nitrophenyl phosphate (MNPP, **1.4**).

[ii] The so-called "*p*-nitrophenyl ester syndrome" advanced by Menger (Menger, F.M.; Ladika, M. *J. Am. Chem. Soc.* **1987**, *109*, 3145) warns that although *p*-nitrophenol is a popular leaving group due to its fast reactions and simple visualization, substrates which incorporate it cannot always be relied upon to give a faithful representation of the much less reactive natural substrates which are being mimicked.

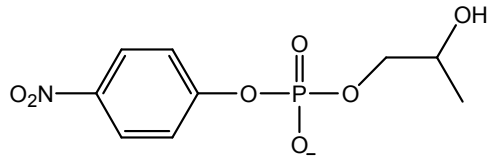

1.1 (HPNPP)

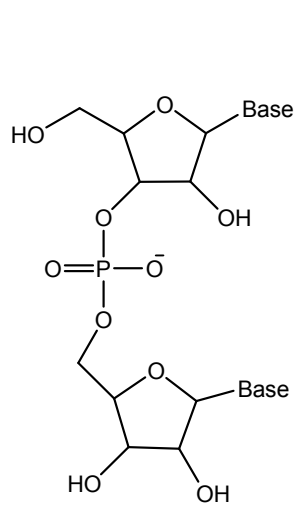

1.2 (3',5'-BpB)

Base =

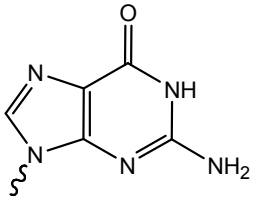

Guanine (G)

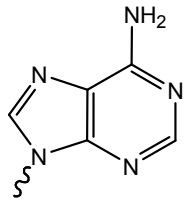

Adenine (A)

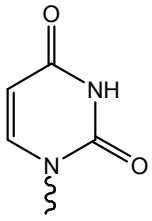

Uracil (U)

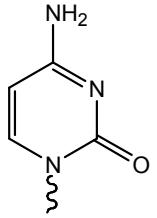

Cytosine (C)

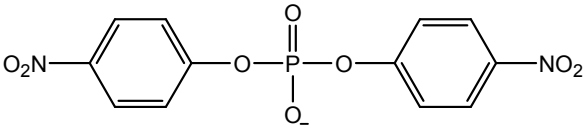

1.3 (BNPP)

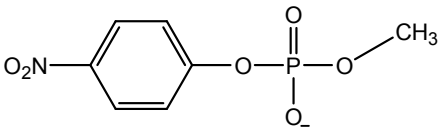

1.4 (MNPP)

Figure 1-3. Structures of anionic phosphate diesters commonly used as models of DNA and RNA.

The challenge of developing synthetic mimics of phosphoesterases, both mononuclear and multinuclear, has been taken up by many research groups, too numerous to list here. The discussion that follows is a brief survey of a limited number of cases which represent

some of the more successful entries in the field as well as some catalytic systems which are particularly pertinent to the original research presented in this dissertation (several specific examples will be discussed in the chapters where they are most relevant). The full extent of the work which has been done concerning synthetic metallophosphatases can be better appreciated in a number of reviews on the subject.[2c,g,19 - 24,26,27] The vast majority of studies on synthetic metallonucleases have been conducted in water, but to date most of these systems have yielded only modest rate accelerations which, with rare exceptions, have second-order rate constants that are not much better than free hydroxide. Furthermore, many of the dinuclear metal complexes are not significantly better than their mononuclear analogs, suggesting that the synergistic effects the two metal ions are not being realized in water.

A measure of success in the development of dinuclear catalyst systems which show metal-ion cooperativity is that the catalyst should exhibit activity which is greater than the sum of its parts. Simply put, a dinuclear catalyst should be more than twice as active as a comparable mononuclear catalyst. One of the first examples of a detailed study of a synthetic dinuclear Zn(II) complex was by Breslow.[28] In comparison to the mononuclear complex **1.5**:Zn(II),[29] a dinuclear complex in which two macrocyclic units were tethered together by a *p*-xylyl spacer (**1.6**:$Zn(II)_2$) was nearly five-fold more active towards the hydrolysis of the phosphate monoester *p*-nitrophenyl phosphate. The dimeric catalyst was seven-times more active than the monomer in the hydrolysis of the carboxylate ester *p*-nitrophenyl acetate. Although metal ion cooperativity was quite limited, the study demonstrated the potential for synthetic systems in which metal ions act in concert. Subsequent structure-activity experiments by Breslow[30] examined the effects of varying

the length and rigidity of the linker between the macrocyclic Zn(II) binding units. The activity of the dinuclear Zn(II) complexes of the ligand series **1.7** – **1.9** was tested towards the hydrolysis of the monoester *p*-nitrophenyl phosphate, the diesters BNPP (**1.3**) and HPNPP (**1.1**), and the dinucleotide UpU (**1.2**, Base = Uracil). It was discovered that certain linkers showed specificity for certain classes of substrates. The dinuclear complex with the long, flexible alkyl spacer (**1.7**:$Zn(II)_2$) was a poor catalyst for all substrates. The short, rigid spacer in complex **1.8**:$Zn(II)_2$ gave the best catalyst for monoester hydrolysis, while the longer (yet still rigid) linker in **1.9**:$Zn(II)_2$ proved most effective for all of the diesters. Although the metal-ion cooperativity in the dinuclear complexes was modest (less than 10-fold acceleration over the mononuclear species), the dinuclear catalysts did offer appreciable acceleration over the background reaction at the same pH (up to three orders of magnitude acceleration in the case of diester **1.1**).

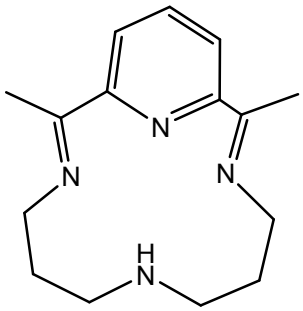

1.5

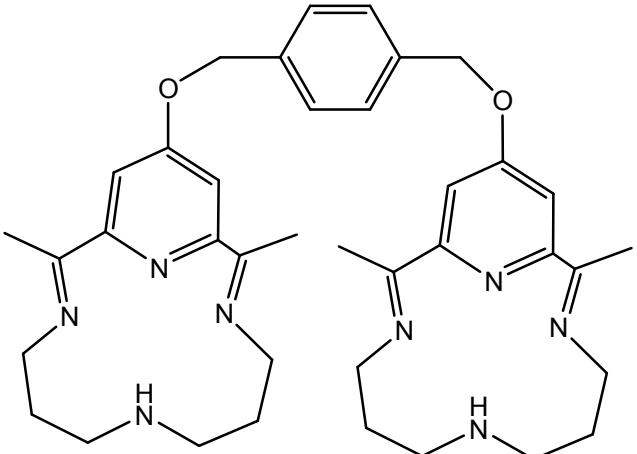

1.6

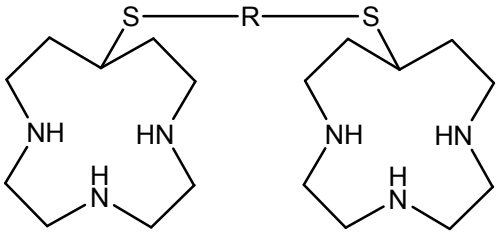

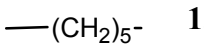

1.7

R =

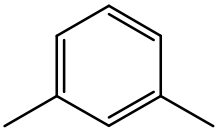

1.8

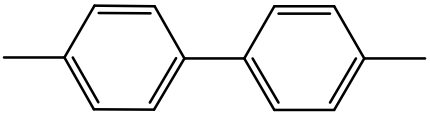

1.9

Richard and Morrow studied a series of dinuclear complexes based on the 1,4,7-triazacyclononane macrocycle (**1.10**) and found that the dinuclear complex **1.11**:$Zn(II)_2$ was several orders of magnitude more active than the mononuclear complexes **1.10**:Zn(II) and **1.12**:Zn(II) towards the intramolecular transesterification of the RNA model HPNPP (**1.1**).[31] In all cases, the authors saw linear kinetics with no indication of binding between the catalyst complexes and the substrate. At near neutral pH in water (pH = 7.6) and 25 ºC, **1.11**:$Zn(II)_2$ was found to catalyze the cyclization of **1.1** with a

second-order rate constant of 0.25 $M^{-1}s^{-1}$ while **1.10**:Zn(II) and **1.12**:Zn(II) achieved only 0.0021 $M^{-1}s^{-1}$ and 0.0013 $M^{-1}s^{-1}$ respectively. Direct comparison of the second-order rate constants showed **1.11**:$Zn(II)_2$ to be 120-fold and 190-fold more active than **1.10**:Zn(II) and **1.12**:Zn(II) respectively. The authors interpreted the enhanced catalytic activity of **1.11**:$Zn(II)_2$ compared to **1.10**:Zn(II) and **1.12**:Zn(II) as evidence of metal ion cooperativity. Interestingly, comparison of the rate of reaction catalyzed by **1.11**:$Zn(II)_2$ with the uncatalyzed background reactions reveals that **1.11**:$Zn(II)_2$ is, in fact, not a very active catalyst relative to free hydroxide. Under high pH conditions (pH = 10) where **1.11**:$Zn(II)_2$ is most active, the second order rate constant of 0.71 $M^{-1}s^{-1}$ for the cyclization of **1.1** is only eleven-fold greater than the second-order rate constant for the base-promoted background reaction (6.5×10^{-2} $M^{-1}s^{-1}$).

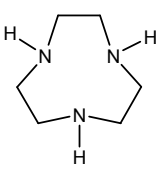

1.10

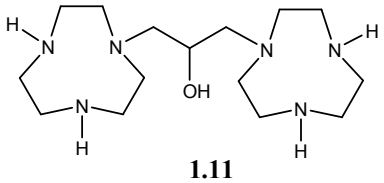

1.11

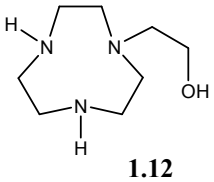

1.12

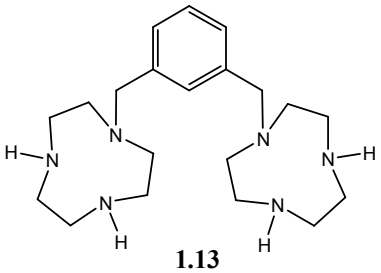

1.13

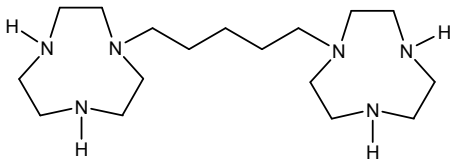

1.14

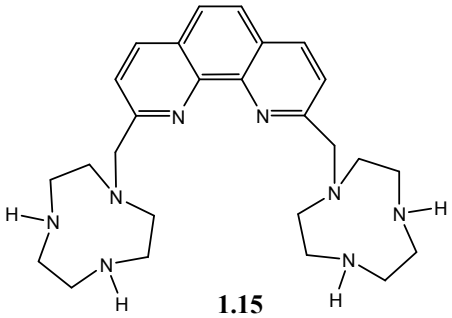

1.15

Richard and Morrow also investigated a series of dinuclear catalysts incorporating the macrocycle (**1.10**) and linkers of varying length and rigidity.[31b] The authors found that unlike the case of **1.11**:$Zn(II)_2$, the dinuclear Zn(II) complexes of **1.13**, **1.14**, and **1.15** displayed catalytic activities which were only slightly more than two-fold greater than the activity of **1.10**:Zn(II), suggesting that in these dinuclear complexes the Zn(II) ions act independent of one another (the complexes were determined to be dinuclear on the basis of NMR titration data). The cooperative behaviour of the metal ions in **1.11**:$Zn(II)_2$ was rationalized on the basis of the propyloxy linker between the macrocycles which is believed to shield the Zn(II) ions from electrostatic repulsion and allow them to come into close enough proximity to act cooperatively.

The first synthetic dinuclear Zn(II) catalyst to show strong binding to a phosphate diester substrate was the calix[4]arene system developed by Reinhoudt.[32] Decoration of the upper rim of a calix[4]arene with two *bis*(dimethylaminomethyl) pyridine units gave ligand **1.16** (the long ethoxyethyl tails on the lower rim of the catalyst were meant to prevent inversion of the macrocyclic core). In a reaction medium composed of acetonitrile/20 mM aqueous HEPES buffer (1:1 v/v), the presence of 0.48 mM **1.16**:$Zn(II)_2$ accelerated the rate of cyclization of substrate **1.1** by a factor of 23,000-fold relative to the background reaction under the same conditions (pH = 7, 25 °C).[32a] The dinuclear catalyst showed saturation kinetics with a maximum rate constant (k_{cat}) of 7.7 x 10^{-4} s^{-1} and an association constant of 5.5 x 10^4 M^{-1}. Importantly, in comparison to the mononuclear Zn(II) complex of **1.17** the dinuclear variant was 50-fold more active, indicative of appreciable metal ion cooperativity. In a comparison between the

mononuclear complex **1.17**:Zn(II) and the complex with the *bis*(dimethylaminomethyl) pyridine in the absence of calix[4]arene (**1.18**:Zn(II)), the former proved to be six-fold more active suggesting that the calix[4]arene macrocycle confers some additional catalytic activity perhaps associated with catalyst conformation.[32a] Although **1.16**:$Zn(II)_2$ gave significant rate accelerations for the cyclization of diester **1.1**, it proved ineffective for the hydrolysis of the triester diethyl-*p*-nitrophenyl phosphate, the DNA model ethyl-*p*-nitrophenyl phosphate, and the monoester *p*-nitrophenyl phosphate.

Reinhoudt later expanded the calix[4]arene system to incorporate a third Zn(II) ion (**1.19**:$Zn(II)_3$), but the trinuclear complex gave only an additional 40% activity compared to the dinuclear complex for the intramolecular cyclization of **1.1**.[32b] Further iterations on the dinuclear ligand **1.16** led to the incorporation of dimethylamine groups between the metal centres (**1.20**) which were intended to act as internal general bases.[32c] While **1.20**:$Zn(II)_2$ was generally effective towards the transesterification of **1.1**, the amine substituents appeared to have an adverse effect, dropping the saturating rate (k_{cat}) by a factor of two and the substrate binding constant by a factor of 30 relative to **1.16**:$Zn(II)_2$. The dimethyamine groups, while acting as internal general bases were also believed to sterically encumber the substrate (accounting for the decrease in the association constant) as well as perturb the conformation of the macrocyclic catalyst and disrupt the catalytically competent binding mode.[32c,e]

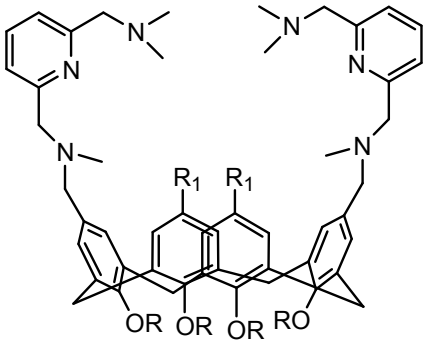

R_1 = H **1.16**
R_1 = -$(CH_2)N(CH_3)_2$ **1.20**

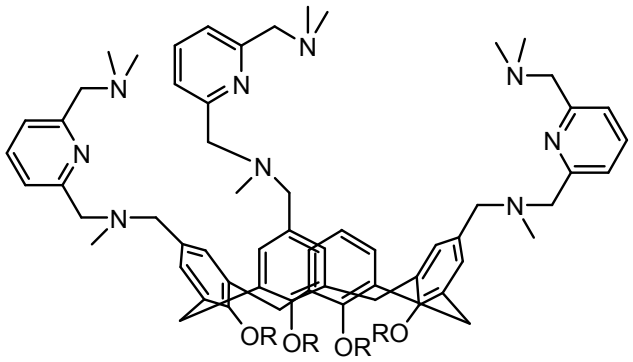

1.19

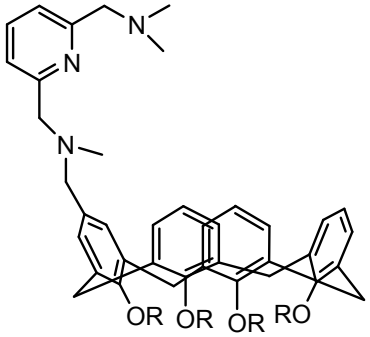

1.17

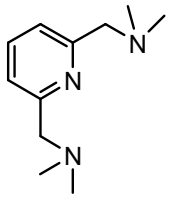

1.18

1.5 - Small molecule mimics of dinuclear Zn(II) enzymes in alcohol

While studies on the cleavage of phosphate esters catalyzed by synthetic dinuclear complexes in water has met with varying degrees of success, none of the examples even begin to approach the rate accelerations achieved by the enzymes they aim to mimic.[33] Recent work from this laboratory has been directed towards the cleavage of simple phosphate diesters catalyzed by metal ion complexes in the light alcohols (methanol and ethanol). As previously discussed, the light alcohols offer several practical advantages for studying metal-catalyzed processes and provide a medium which may better approximate

the chemical environment within an enzyme's interior. Prior to investigating dinuclear catalysis of phosphate diester cleavage in methanol, our research group conducted detailed studies on the metal-ion catalyzed methanolysis of carboxylate esters,[34] activated amides,[35] phosphate triesters,[36] phosphonates,[37] phosphorothioates,[38] and phosphonothioates.[39] While the catalyzed cleavage of these substrates will not be elaborated on here, these studies revealed the potential for methanol to act as a cooperative medium for metal ion promoted cleavage reactions. Furthermore, concurrent potentiometrtic experiments helped reveal the speciation of metal ions and their complexes in alcohol solvent which gave us the ability to elucidate the catalytically active species in solution.[40]

The study of dinuclear catalysis in the Brown research group began with the initial studies of the cleavage of the RNA model **1.1** catalyzed by the mononuclear complex **1.21**:Zn(II).[41] The plot of the pseudo first-order rate constant, k_{obs}, vs. [**1.21**:Zn(II)]$_{total}$ for the methanolysis of **1.1** showed upward curvature at high [**1.21**:Zn(II)] indicative of a rate term which was second-order in **1.21**:Zn(II) (Figure 1-4). The second-order behaviour was interpreted as a cooperative interaction between two molecules of **1.21**:Zn(II). The kinetic data were fit according to the equation $k_{obs} = k_2$[**1.21**:Zn(II)] + k_3[**1.21**:Zn(II)]^2 to give $k_2 = 18.9\ M^{-1}s^{-1}$ and $k_3 = 1.8 \times 10^3\ M^{-2}s^{-1}$. The large value of k_3 suggested that the reaction pathway involving two catalyst molecules was quite efficient and that a dimeric ligand in which two **1.21**:Zn(II) units were covalently linked should give a highly active, pre-organized dinuclear complex.

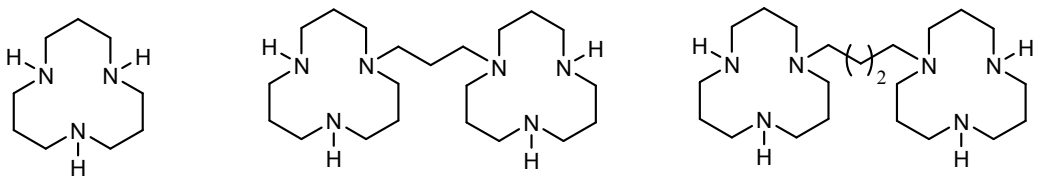

1.21 **1.22** **1.23**

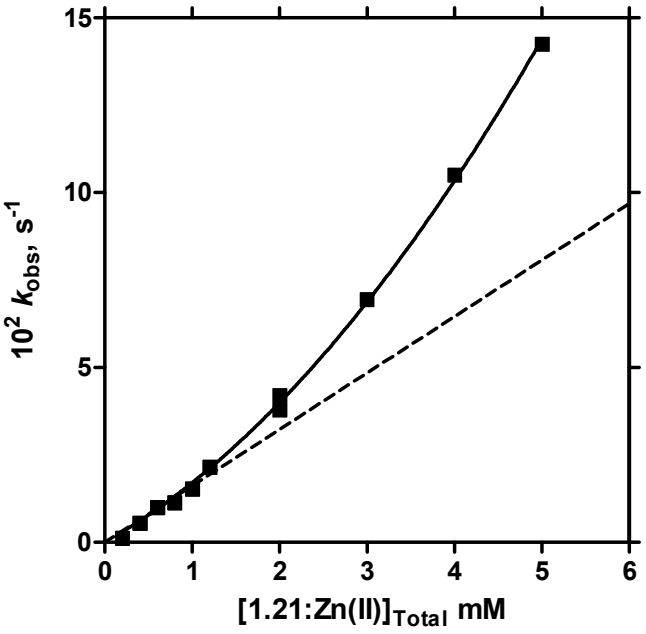

Figure 1-4. A plot of k_{obs} vs. [**1.21**:Zn(II)] at [$^{-}OCH_3$]/[Zn(II)]$_{total}$ = 0.5 for the methanolysis of **1.1** (2 x 10^{-5} M), $^{s}_{s}$pH 9.30 and T = 25 °C. Dotted line is the linear regression of [**1.21**:Zn(II)] ≤ 1.2 x 10-3 M, whereas the solid line is NLLSQ fitted throughout the [Zn(II)]$_{total}$ range.

Attachment of the two macrocycles via a propyl linker gave ligand **1.22**. Although the dinuclear Zn(II) complex **1.22**:Zn(II)$_2$ was previously described, it was found to be very ineffective in water for the hydrolysis of *bis*(2,4-dinitrophenyl)phosphate and *p*-nitrophenyl phosphate.[42] The rate constant for the hydrolysis of the highly activated DNA model *bis*(2,4-dinitrophenyl)phosphate were very slow (k_{obs} = 8.2 x 10^{-6} s^{-1}, 1.0 mM catalyst, pH = 7.0, 34 ºC) and the dinuclear complex was found to be no better than

the mononuclear complex **1.21**:Zn(II), suggesting no metal-ion cooperativity in water. The situation in methanol was found to be dramatically different. In the presence of 1.0 mM **1.22**:$Zn(II)_2$ and 1.0 mM $NaOCH_3$ (which buffers the solution at ${}^{s}_{s}pH = 9.5$), the observed rate constant for the cleavage of **1.1** was found to be $k_{obs} = 275\ s^{-1}$ which corresponds to a half-life time of 2.5 ms and to an acceleration of 2×10^{12}-fold over the background reaction at the same ${}^{s}_{s}pH$.[41] The active form of the catalyst was found to be the species comprising one ligand, two Zn(II) ions, and one methoxide ion (**1.22**:$Zn(II)_2$:$^{-}OCH_3$). The plot of k_{obs} vs. [**1.22**:$Zn(II)_2$] for the cleavage of **1.1** was linear with a gradient of $k_2 = 275{,}000\ M^{-1}s^{-1}$. In comparison to the second-order rate constant for the methoxide promoted cleavage of **1.1** ($k_2^{-OMe} = 2.6 \times 10^{-3}\ M^{-1}s^{-1}$), the complex **1.22**:$Zn(II)_2$ was found to be 1.1×10^{8}-fold more reactive. The dinuclear complex was also able to catalyze the methanolysis of the DNA model **1.4**, exhibiting Michaelis-Menten kinetics indicative of binding between the catalyst and substrate. As in the case of the RNA model, in terms of second-order rate constants, **1.22**:$Zn(II)_2$ was found to be 1.2×10^{8}-fold more reactive than methoxide for the methanolysis of the DNA model **1.4**.[41]

The huge rate accelerations afforded by **1.22**:$Zn(II)_2$ prompted our research group to undertake a detailed mechanistic investigation. The **1.22**:$Zn(II)_2$ catalyzed cleavage of a series of 2-hydroxypropyl-aryl phosphates (**1.24a-g**) was studied and it was found that the linear plots of k_{obs} vs. [**1.22**:$Zn(II)_2$] observed for substrates with good leaving groups (**1.24a,b**) transformed into curved Michaelis-Menten type kinetics for substrates with poorer leaving groups (**1.24c-g**).[43] Figure 1-5 shows a reaction pathway consistent with the observed kinetic data. The linear behaviour with active substrates (**1.24a,b**) results

from a fast k_{cat} term which is greater than k_{-2}, leaving linear second-order kinetics with k_2 being rate-limiting. In the case of slower reacting substrates (**1.24c-g**), cleavage of the leaving group (k_{cat} term) becomes rate limiting resulting in saturation kinetics.

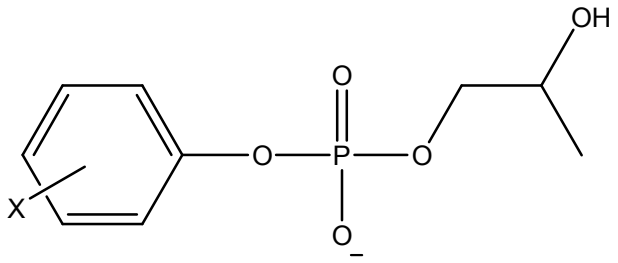

1.24 **a = 1.1**, X = 4-NO_2
b, X = 4-NO_2, 3-CH_3
c, X = 3-NO_2
d, X = 4-Cl
e, X = 3-OCH_3
f, X = H
g, X = 4-OCH_3

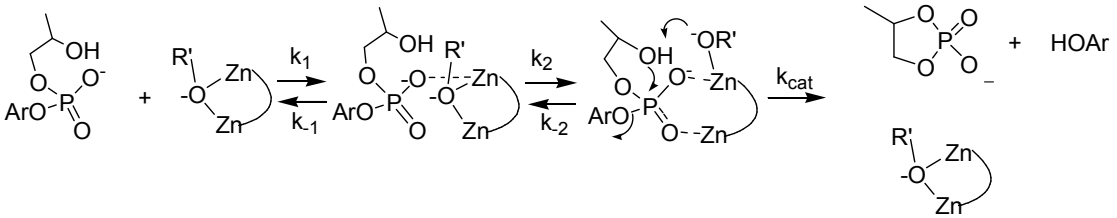

Figure 1-5. Proposed pathway for the cleavage of phosphate diesters **1.24a-g** promoted by **1.22**:$Zn(II)_2$.

Ligand **1.23**, a variant of **1.22** with a four carbon linker between the macrocycles, was prepared in order to study whether a slightly more flexible catalyst might show even greater activity.[44] The catalytic activity of the **1.23**:$Zn(II)_2$ complex towards the cleavage of phosphate diesters **1.24a-g**, while substantial, was found to be slightly less than the activity of **1.22**:$Zn(II)_2$. Catalyst **1.23**:$Zn(II)_2$ exhibited the same general kinetic behaviour as **1.22**:$Zn(II)_2$ (transition from linear to saturation kinetics upon worsening of

the leaving group), but the reactions were noticeably slower. Experiments involving **1.23**:$Zn(II)_2$ were also complicated by the limited solubility of the complex in methanol as well as very strong inhibition by the trifluoromethanesulfonate (triflate) anion which was introduced with the Zn(II) ions as the $Zn(OTf)_2$ salt. In the case of substrate **1.1**, the second-order rate constant for the **1.23**:$Zn(II)_2$ catalyzed cleavage was found to be 2.1 x 10^4 $M^{-1}s^{-1}$ which is 13-fold less than the second-order rate constant obtained with **1.22**:$Zn(II)_2$. Although catalyst flexibility was expected to increase catalytic activity, the added degrees of freedom in the catalyst may retard the catalyst-substrate rearrangement step (k_2, Figure 1-5) and could account for the lower reactivity of **1.23**:$Zn(II)_2$ relative to **1.22**:$Zn(II)_2$.[44]

1.6 - Neutral phosphate esters as chemical warfare agents and pesticides

Many neutral organophosphate triesters and phosphonate esters (of general structure **1.25**) where the leaving group has a pK_a of ~8 or less exhibit extreme toxicity due to their potent inhibition of acetylcholinesterase, the enzyme responsible for the hydrolysis of the neurotransmitter acetylcholine in the synaptic cleft.[45] The inhibitory mechanism involves phosphorylation of the hydroxyl group of the serine moiety of acetylcholinesterase, thus rendering it incapable of nucleophilic attack on acetylcholine. The accumulation of un-hydrolyzed acetylcholine leads to muscle spasm, paralysis, and eventually death from asphyxiation.[3]

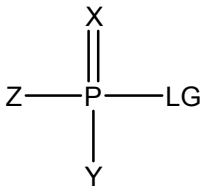

X = O, S
Z = OR
Y = OR, R
LG = OR, SR, F, CN

1.25

While the toxicity of organophosphorus esters was first investigated for crop protection as pesticides (modern examples of which include malathion **1.26**, parathion **1.27**, paraoxon **1.28**, and fenitrothion **1.29**)[46], the lethal nature of the compounds quickly led to their development as chemical warfare (CW) agents. This culminated in the development of the so-called G-agents (e.g. Sarin **1.30**, Soman **1.31,** Tabun 1.**32**) and later the much more toxic V-agents (eg. VX **1.33**, Russian VX **1.34**).[47] With an estimated LD_{50} (the amount required to kill 50% of the test subjects) in humans of 0.009 mg/kg, VX (**1.33**) is widely regarded as the deadliest man-made poison known.[48]

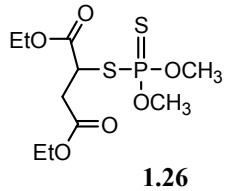

1.26

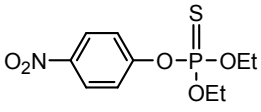

1.27

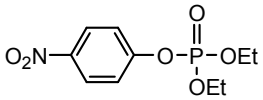

1.28

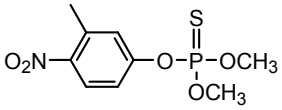

1.29

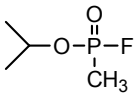

1.30

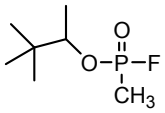

1.31

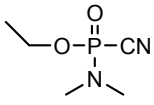

1.32

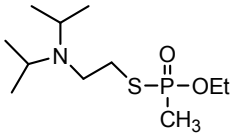

1.33

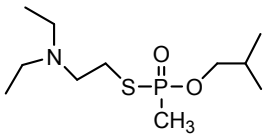

1.34

Unfortunately, despite the fact that CW agents have been prepared and stockpiled on the kilo-ton scale,[47] and that nearly 500,000 tons of organophosphorus pesticides are used each year,[49] the existing strategies for the large scale decontamination or demilitarization

of these poisonous materials suffer from important drawbacks. The currently employed methods are not effective against all species of organophosphorus toxins and may take long periods of time to give complete detoxification. In addition, the methodologies currently in use for the destruction of such noxious chemicals rely primarily on hydrolytic or oxidative processes which suffer from poor efficiency, harsh reaction conditions, and in some cases produce products which are as toxic as the starting materials.[47] The controlled decomposition of organophosphorus esters into non-toxic products remains an ongoing challenge with a growing need for fast, safe, and efficient methodologies.

1.7 - Methodologies for the decontamination of toxic organophosphorus esters

1.7.1 - Simple Hydrolysis

Ideally, a viable decomposition methodology should be effective against a wide range of compounds, be catalytic with high turnover, be inexpensive, proceed at near neutral pH and ambient temperature, and most importantly, convert the poisonous materials to non-toxic products. Rapidity of decomposition is also of utmost importance, particularly in the case of CW agents where the oft quoted "McKay criterion" dictates that the material should be decomposed "within a cigarette break."[50]

Hydrolysis would seem to be the most attractive decontamination strategy for toxic organophosphorus compounds since it uses a solvent (water) which is environmentally benign and in large supply. The susceptibility of the G-agents to hydrolysis has been

known for some time.[51,52,53] Indeed, Martell[54] and Ackerman[55] found that Sarin and Soman are relatively soluble in water and hydrolyze under basic conditions (Figure 1-6) at 25˚C with second-order rate constants (k_2^{OH}) of 23.7 $M^{-1}s^{-1}$ and 10.0 $M^{-1}s^{-1}$ respectively, meaning that at pH = 10, hydrolysis is complete (to at least ten half-life times) in 40 to 120 minutes.

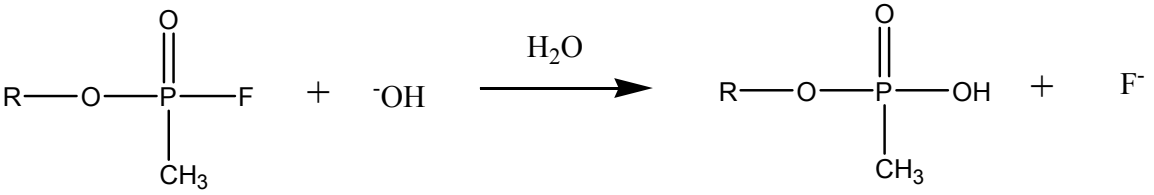

Sarin, R = $CH(CH_3)_2$
Soman, R = $CH(CH_3)C(CH_3)_3$

Figure 1-6. The hydroxide promoted hydrolysis of G-agents Sarin and Soman.

However, the hydrolysis products of the phosphonofluoridate G-agents are a phosphonic acid and fluoride. The generation of acid requires that large excesses of base be supplied in order to maintain the rate of hydrolysis. Since the attack of neutral water on Sarin or Soman is slow or non-existent, hydrolytic decontamination of G-agents requires relatively concentrated caustic solutions, which are corrosive and difficult to dispose of.

While hydrolysis of the G-agents and their simulants is relatively straightforward, hydrolysis of the much more toxic VX (and other phosphonothioate V-agents) is a much greater challenge.[47b] The immediate problem with V-agent hydrolysis is the low solubility of the compounds in alkaline aqueous solution and the slow inherent rate of hydroxide promoted hydrolysis. VX is hydrolyzed (Figure 1-7) in 0.1 M NaOH solution

with a half-life time of over 30 minutes (roughly 6200 times slower than Sarin under the same conditions). In acidic solution where VX is N-protonated and much more soluble, the hydrolysis reaction is exceedingly slow. More alarming however is the fact that one of the products of VX hydrolysis remains highly toxic but is much more resistant to further hydrolysis. The hydrolysis of VX (**1.33**) leads to 75-90% of the desired P-S cleavage to give the non-toxic O-ethyl methylphosphonic acid (**1.33a**, EMPA), however the process also yields 10-25% of the thioic acid **1.33b** (from P-O cleavage, known as EA-2192) which is anionic and thus much more stable towards base promoted hydrolysis while maintaining considerable toxicity. It was also found that the P-S/P-O cleavage ratio decreases (more of the toxic thioic acid is produced) with increasing hydroxide concentration.[47b]

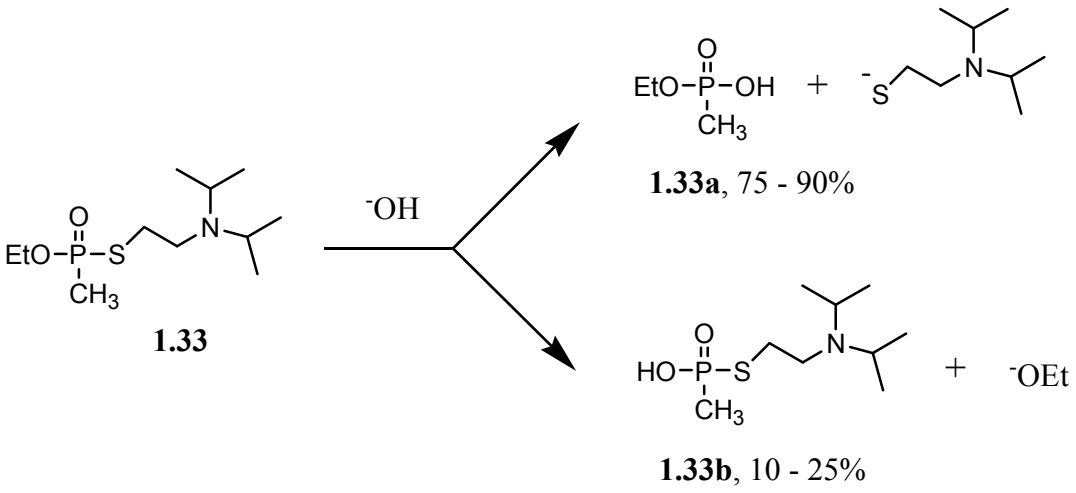

Figure 1-7. The hydroxide promoted hydrolysis of VX.

Later studies showed that perhydrolysis of VX (substitution at phosphorus by the HO_2^- anion) is 40 times faster than the reaction with hydroxide and leads exclusively to P-S cleavage.[56] This process is however not truly catalytic, requires a large excess of peroxide (which presents an explosion hazard when used on large scale) and still requires rather

basic conditions. Other α-effect nucleophiles such as oximate[56b] and *o*-iodosobenzoate[47c,57] anions have been investigated and while they do destroy VX, they are not catalytic and must be used in large excess.

1.7.2 – Metal ion catalyzed hydrolysis of CW agents and pesticides

The prevalence of metal ions in phosphate cleaving enzymes has inspired the use of metal ions as catalysts for the decomposition of toxic organophosphates. The effects of transition metal salts on the hydrolysis of G-agents and their simulants was first investigated by Wagner-Jauregg[51] and subsequently by Martell.[53,54] Both groups examined the effects of adding a variety of transition metal salts (and their complexes with chelating ligands) to the hydrolysis of Sarin or the Sarin simulant diisopropylfluorophosphate (**1.35**). They independently found Cu(II) to be the most catalytically active metal, particularly when complexed to a bidentate amine ligand such as 2,2'-bipyridine or N,N,N'N'-tetramethylethylenediamine (TMEN). Martell showed that the Cu(II):(TMEN) complex (**1.36**) led to hydrolysis of an excess of Sarin at pH = 7.4 with a half-life time of five minutes. In comparison with the half-time for the uncatalyzed attack of neutral water on Sarin (based on the observed rate constant for the attack of neutral water on Sarin, 5×10^{-6} s^{-1})[54] which is 2310 minutes, complex **1.36** afforded 4.6×10^2-fold acceleration for the hydrolysis of Sarin. Similar results were observed with Soman,[47a] the hydrolysis of which was accelerated by an order of magnitude in the presence of 1.0 mM $CuSO_4$.

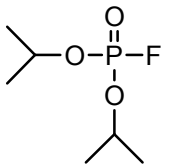

1.35

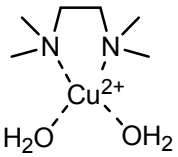

1.36

The metal catalyzed hydrolysis of VX encountered little success. The Cu(II) catalysts which were effective for the G-agents gave only modest acceleration for VX, possibly due to the substrate binding to copper via the diisopropylamino group rather than the phosphoryl group.[47a] Furthermore, upon hydrolysis of the P-S bond, the resulting thiol(ate) product can potentially bind to Cu(II) leading to reduction of Cu(II) to Cu(I) and the formation of disulfides.

The majority of organophosphorus insecticides currently in use are phosphorothionate triesters with P=S functionality (**1.25**, X=S, Z = OR, Y = OR, LG = OR, SR).[48] Unfortunately, phosphorothionate pesticides are known to hydrolyze much more slowly than their P=O (or "oxon") counterparts, primarily as a result of the decreased electrophilicity at phosphorus due to the lower electronegativity of sulphur as compared to oxygen.[58] The catalytic hydrolysis of organophosphorus pesticides has not been investigated thoroughly and only a few examples of metal catalyzed hydrolyses are known. A molybdenocene compound[59] gave only modest acceleration of the hydrolysis of parathion (**1.27**), while the presence of softer divalent transition metals such as Cu(II), Pb(II), and Hg(II) were more promising.[60] The use of lead and mercury salts is not feasible, however, since these metals are themselves quite toxic. The most effective metal

catalysts for pesticide hydrolysis are the cyclometalated Pt(II) and Pd(II) ketoximes (**1.37**) developed by Ryabov.[61]

The cyclometallated compounds were used effectively for the hydrolysis of parathion (**1.27**), methyl parathion (**1.40**), coumaphos (**1.41**), and demeton-S (**1.42).**

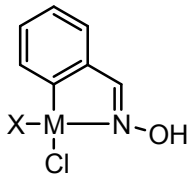

1.37

M = Pt, Pd

X = Py, DMSO

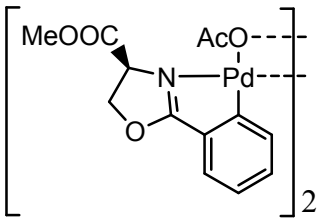

1.38

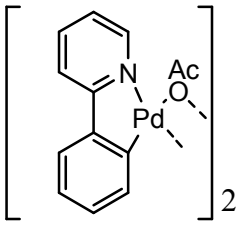

1.39

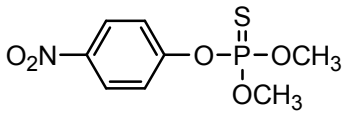

1.40

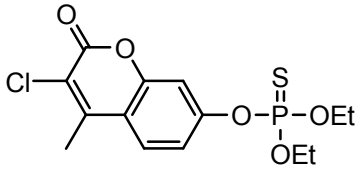

1.41

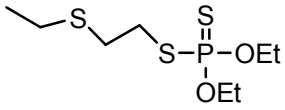

1.42

The cycloplatinated complex (**1.37**, M = Pt) gave up to 10^9-fold acceleration for the hydrolysis of parathion relative to the background reaction at pH = 8.5. The catalytic mechanism was believed to involve transient coordination of the P=S to the platinum centre followed by intramolecular attack of the oximate supernucleophile.[61a] Later work by Gabbaï[62] investigated similar cyclopalladated species and corroborated the high activities reported by Ryabov. Further studies by Gabbaï showed that the dimeric palladium complexes **1.38** and **1.39**, which lack the internal oxime supernucleophile, maintained high reactivity towards the hydrolysis of methyl parathion, suggesting that the internal nucleophile was not a critical aspect of the catalytic mechanism.[63]

1.7.3 – Metal ion catalyzed decomposition of CW agents and pesticides in methanol

As with our research group's use of metal ions in methanol to mimic biological systems, metal ions dissolved in alcohol have proven very effective for the decomposition of neutral organophosphates. In fact, our interest in the metal ion promoted methanolysis of phosphate esters has its origins in decontamination research. Despite the advantages of performing decontaminations in water, and the wealth of information concerning these reactions, there exist many important limitations associated with hydrolytic processes. First and foremost is the limited solubility of many toxic organophosphorus compounds in aqueous solution. Despite the common reference to "nerve gas", most of the toxic organophosphorus agents are viscous oils at room temperature and must be aerosolized in order to be dispersed or sprayed. While the phosphonofluoridate G-agents exhibit fair solubility in water,[51-55] the more toxic V-agents and the environmentally persistent pesticides have rather low solubility in water under neutral or basic conditions. Furthermore, although water is an environmentally benign ("green") solvent, upon hydrolysis of organophosphorus agents the waste solution is either highly caustic or contains metal ions. The solution thus requires further processing before it can be safely disposed into the environment. Unlike organic waste, aqueous effluent cannot be incinerated and must eventually be returned to the biosphere.

Under metal ion promoted conditions, the reaction products are also an important consideration. Unlike hydrolysis, which transforms a neutral phosphate ester into a phosphoric/phosphonic acid, methanolysis converts the neutral ester into another neutral ester. The generation of phosphoric acids is undesirable because it necessitates the use of large excesses of base to maintain a sufficiently high pH for the hydrolysis reaction to

occur. Furthermore, in the presence of a metal ion catalyst, the anionic phosphate product is expected to bind to the metal ion and inhibit catalysis. The product of the methanolysis reaction is not expected to bind to a metal ion catalyst with any greater affinity than did the stating material.

The first experiments examining the methanolysis of organophosphates involved the La(III)-catalyzed methanolysis of the pesticide (and widely used G-agent stimulant) paraoxon (**1.28**).[36a] Lanthanum(III) was investigated because of its proven ability to catalyze the methanolysis of carboxylate esters and activated amides.[34,35] Lanthanum(III) was found to be an exceptional catalyst for the breakdown of paraoxon in methanol, with maximum activity at ${}^{s}_{s}\mathrm{pH} = 8.5$. It was found that at a total La(III) concentration of 2.0 mM and ${}^{s}_{s}\mathrm{pH} = 8.5$, the methanolysis of paraoxon had a half-life time of 20 seconds, as compared to half-life time of 600 years under base promoted conditions at the same ${}^{s}_{s}\mathrm{pH}$ which corresponds to a 10^9-fold acceleration. Previous studies with La(III) showed the active species to be a dimer, with the general form $La^{3+}{}_2(^{-}OCH_3)_n$.[34,35] Correlation of the kinetic data for the methanolysis of paraoxon with the species distribution for $La^{3+}{}_2(^{-}OCH_3)_n$ (Figure 1-8) showed the $La^{3+}{}_2(^{-}OCH_3)_2$ dimer (**1.43**) to be the most catalytically active form.

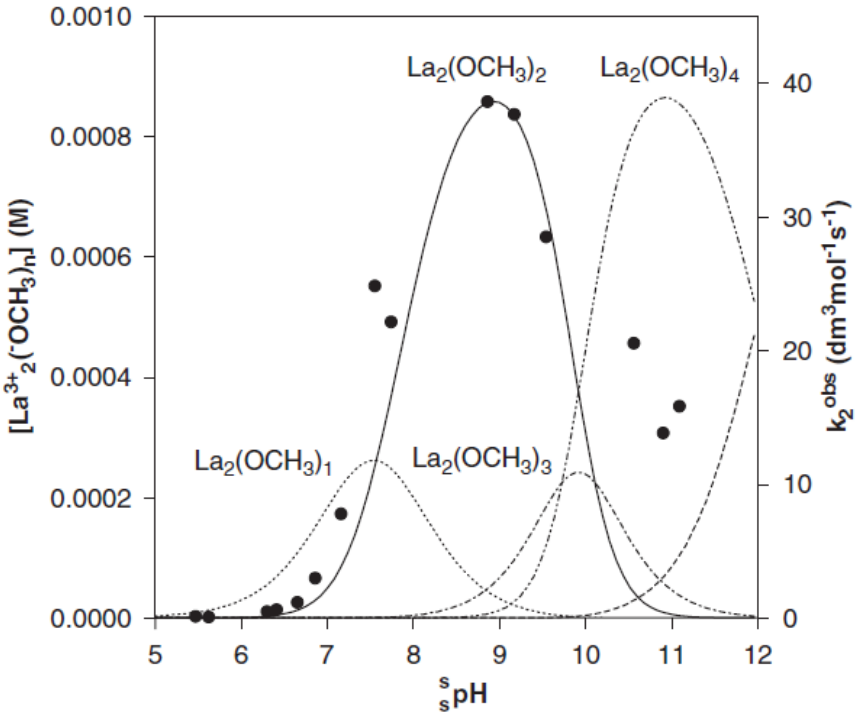

Figure 1-8. Speciation diagram for the distribution of $La^{3+}{}_2(^{-}OCH_3)_n$, n = 1- 5, as a function of ${}^{s}_{s}pH$. The solid circles represent the second-order rate constants for the methanolysis of paraoxon catalyzed by La(III) as a function of ${}^{s}_{s}pH$. (Reference 26)

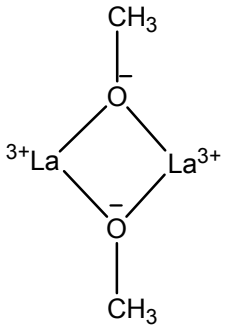

1.43

In addition to La(III), our research group has found the **1.21**:Zn(II):$^{-}OCH_3$ complex to be effective for the destruction of P=O toxins.[36b,39a] The mechanistic details surrounding the methanolysis of G-agent[37a] and V-agent[37b] simulants catalyzed by La(III) and **1.21**:Zn(II):$^{-}OCH_3$ have been studied through structure-activity relationship experiments,

and in all cases the catalyzed reaction has been found to proceed through a concerted pathway with nucleophilic attack and leaving group departure occurring simultaneously.

Although La(III) proved to be an exceptional catalyst for the degradation of P=O substrates, it offers virtually no benefit over the background reaction for P=S pesticides.[39a] The effectiveness of a metal ion in promoting the phosphoryl transfer is intimately tied to its ability to bind (if only transiently) to the phosphoryl group and activate it towards nucleophilic attack. The hard La(III) cation has very low affinity for the soft sulfur atom of P=S substrates.[39b] Early efforts identified **1.21**:Zn(II):$^{-}OCH_3$ as a moderately effective catalyst for the methanolysis of the pesticide fenitrothion (**1.29**),[39a] giving a 67-fold rate enhancement over the background reaction in terms of second-order rate constant. Slightly better catalysis (1100-fold acceleration) was observed with the Zn(II) complex of 2,9-dimethylphenanthroline.[39a]

Due to the importance of hard/soft interactions in catalysis, Zn(II) was later replaced with the softer metal ion Cu(II). At a concentration of 1.0 mM at $^{s}_{s}pH = 8.75$, the complex **1.22**:Cu(II):$^{-}OCH_3$ was found to accelerate the methanolysis of **1.29** by a factor of 8.4 x 10^8-fold over the background reaction at the same $^{s}_{s}pH$.[39b]

Expanding on the work of Ryabov,[61] we have also explored the use of cyclopalladated complexes for the decomposition of P=S pesticides in methanol. Our group identified the *ortho*-palladated complex **1.44** as a highly effective catalyst for the methanolysis of a series of phosphorothioate substrates including fenitrothion (**1.29**), coumaphos (**1.41**), dazinon, (**1.45**), dichlofenthion (**1.46**), and quinalphos (**1.47**).[39c] In methanol solution, the

triflate ligand of complex **1.44** is replaced by a solvent molecule which is deprotonated under basic conditions with an observed kinetic $^{s}_{s}pK_a$ of 10.9.

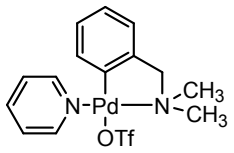

1.44

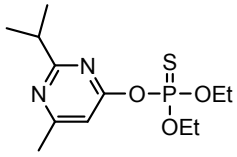

1.45

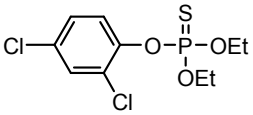

1.46

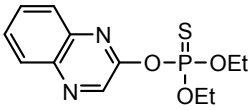

1.47

For the methanolysis of fenitrothion (**1.29**) at $^{s}_{s}pH = 11.5$, catalyst **1.44** gives a second-order rate constant of 3.3 x 10^3 $M^{-1}s^{-1}$ (as compared to the base promoted reaction which has a second-order rate constant of 7.2 x 10^{-4} $M^{-1}s^{-1}$). Under more desirable neutral conditions in methanol, when operating at $^{s}_{s}pH = 8.75$ catalyst **1.44** affords an impressive 4.9 x 10^9-fold acceleration over the background reaction at that $^{s}_{s}pH$.

The effectiveness of metal ions in promoting the solvolysis (both hydrolysis and alcoholysis) of organophosphorus toxins has been amply demonstrated, but the use of these catalytic systems for large scale decontamination projects is limited by the inability to recycle the catalyst, the generation of metal-contaminated waste which may pose an environmental hazard, and the high cost of some of the catalytic species (particularly palladium and platinum). Many of these problems can be overcome through the use of heterogeneous varieties of the catalytic species.

1.8 – Solid Supported Catalysis

Since the development of solid-phase peptide synthesis by Merrifield in 1963[64] there has been ever growing interest in heterogeneous synthesis[65] and catalysis.[66] Catalysts immobilized on solid surfaces have the distinct advantage of simple removal from the reaction solution by filtration, the ability to be recycled, and the ability to use catalysts in solvents in which they might otherwise not be soluble. The ability to recover and recycle the catalyst is particularly important when the immobilized species is valuable (eg. precious metal species or complex organic molecules) or when the catalytic species represents an environmental hazard whose disposal is otherwise difficult.[67] Heterogeneous catalysis does however present a unique set of challenges and disadvantages. The flow of solution within the polymer matrix is retarded by high viscosity, even within highly porous materials.[67] The slow transport of solution through the polymer matrix often leads to the rates of chemical reactions being limited by surface penetration rather than some chemical process. For this reason, reactions catalyzed by immobilized catalysts are generally slower than the same reaction conducted under homogeneous conditions. The problem of mass transport is worsened by the fact that the methods used to functionalize the polymer surface often result in an inhomogeneous distribution of the catalytic species throughout the polymer matrix and can leave catalytic sites buried deep within the polymer matrix where they are inaccessible to the reaction solution. In the case of immobilized metal catalysts, metal leeching is also a constant concern which results in loss of activity of the heterogeneous catalyst upon recycling, and contamination of the resulting reaction solution with unwanted metal species.[68]

The nature of the solid support to which a catalytic unit is affixed can have a profound effect on both the physical and chemical properties of the heterogeneous catalyst. The most widely used organic framework is polystyrene or polystyrene-divinylbenzene co-polymer solid support. Polystyrene polymers are attractive due to their chemical inertness, good thermal stability, and resistance to degradation under extreme pH conditions.[69] The properties of polystyrene polymers are generally modulated by the degree of cross-linking. Low levels of divinylbenzene (DVB) cross-linking (0.5-2%) leads to materials having a densely packed polymer backbone through which diffusion is very slow. Swelling of the polymer in an appropriate solvent can create larger porosity which facilitates molecular diffusion into the polymer matrix, but this is typically limited to low polarity organic solvents.[70,71] Much higher DVB cross-linking (10-80%) and the addition of a porogen in the polymerization process generates macroporous polymers with large permanent porosity, but diffusion of molecules into the polymer matrix is still limited.[71]

Typically, functionalized organic polymers are prepared using one of two general methods: a) substitution of an organic molecule onto a pre-modified polymer (eg. chloromethylpolystyrene); or, b) preparation of an organic molecule bearing a polymerizable functionality (eg. a vinyl group) and subsequent copolymerization with another co-monomer (eg. styrene). While the latter may lead to greater incorporation of the desired molecule into the polymer framework, the situation is complicated by the fact that the different rates of incorporation of the monomers into the polymer chain often lead to co-polymers of ill-defined composition.[70]

A second important class of solid supports comprises the inorganic oxides, particularly amorphous and mesoporous silica.[72] Silica based materials have the advantage of very large surface areas accessible to solvent, and well ordered pores with well defined size. Unlike organic polymers, inorganic materials tend to be less susceptible to thermal degradation and their hydrophilic backbone structures make them more amenable to reactions in aqueous or high polarity solvents. Functionalized silicas also have the advantage of relatively easy preparation. Silica functionalized with organic molecules can be prepared in one of two ways: a) grafting of alkyl trialkoxysilanes ($(RO)_3SiR'$, where R' is the catalytically relevant unit) onto pre-formed silica beads via reactions with the surface silanol groups; or, b) the so called "sol-gel" method, in which the silica monomer, tetraethylorthosilica, is co-condensed with alkyl trialkoxysilanes in the presence of a structure-directing agent (typically an ionic surfactant). For the incorporation of organic molecules into silica, the sol-gel method is generally thought to be superior since it leads to higher loading and more uniform distribution of the organic group in the silica matrix.[71,72] The major drawback of silica gels as solid supports is their relative instability under high pH conditions and the presence of surface silanol groups which, if left uncapped, can participate in acid-base reactions or coordinate to metal species in ways which are deleterious to the desired reaction.

1.9 – Hydrolysis of Phosphate Esters Catalyzed by Immobilized Metal Ion Catalysts

The first example of a polymer supported catalyst for the hydrolysis of toxic phosphorus esters was reported by Menger and Tsuno,[73] drawing on the work of Wagner-Jauregg[51] and Martell,[53,54] which demonstrated that Cu(II) complexes of several chelating polyamine ligands promote the hydrolysis of Sarin and the simulant diisopropylphosphonofluoridate (**1.35**).

Martell had previously found that the Cu(II) complex of tetramethylethylenediamine (**1.36**) promoted the hydrolysis of Sarin with 4.6 x 10^2-fold acceleration over the background reaction. Using commercial chloromethylated polystyrene and substituting the benzylic chloride with amine ligands, Menger was able to generate immobilized equivalents of Martell's Cu(II) complex (Figure 1-9).

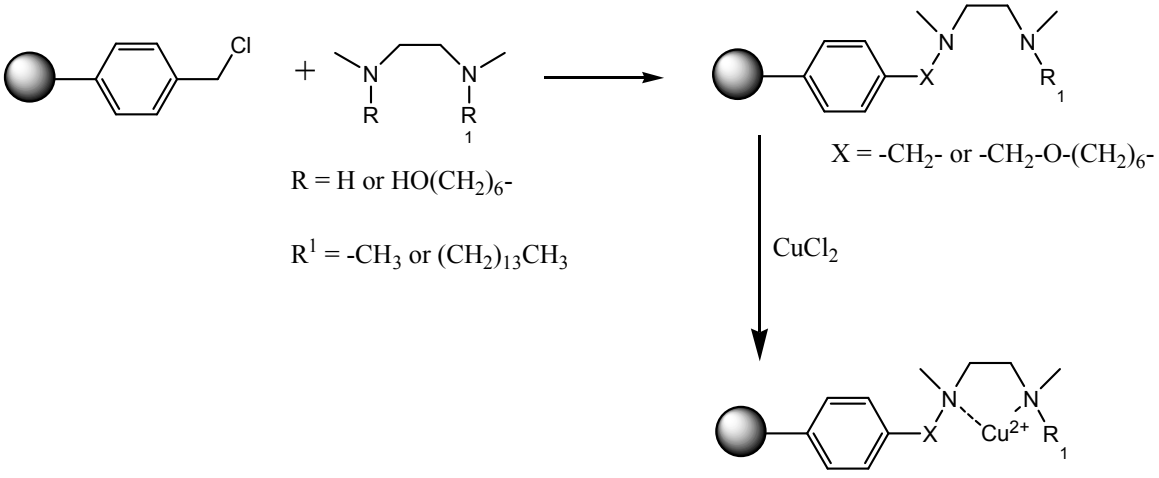

Figure 1-9. Polystyrene loaded with Cu(II)-ethylenediamine complexes for the methanolysis of organophosphorus compounds (Ref. 73).

The copper loaded materials were used as catalysts for the hydrolysis of the G-agent simulants *p*-nitrophenyl isopropylphenylphosphinate (NPIPP, **1.48**) and *p*-nitrophenyl diphenyl phosphate (NPDPP, **1.49**) in water buffered at pH = 8.

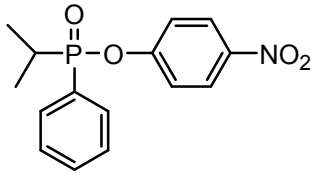

1.48

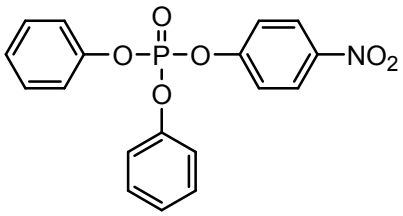

1.49

In the best case scenario, with 1.8 mg of a polymer containing roughly 1.7 mmol Cu(II) per gram, the hydrolysis of **1.48** was accelerated by a factor of 1460 relative to the reaction at the same pH in the absence of polymer. Under the same conditions, the hydrolysis of **1.49** was accelerated by a factor of 360. Higher metal loadings were shown to lead to greater catalysis and the materials were found to be truly catalytic, with the ability to completely hydrolyze an amount of substrate in ten-fold excess of the Cu(II) content.

By varying the distance of the catalytic group from the polymer surface (going from $X = CH_2$ to $X = O(CH_2)_6$, Figure 1-9), it was found that extending the catalyst away from the polymer conferred greater catalytic activity. The hydrolysis of **1.48** was enhanced a further 8-fold with the addition of the spacer molecule, while the hydrolysis of **1.49** was enhanced 10-fold. The amelioration of the catalytic activity of solid supported reagents and catalysts with long spacers between the active group and the solid matrix is a well known phenomenon.[66c,74] Extension of the catalyst away from the solid surface is thought

to allow easier access of the substrate to the reactive centre, and greater mobility of the catalytic species which allows it to behave more "solution-like" than when it is firmly anchored close to the polymer surface.

Interestingly, the inclusion of a hydrocarbon layer between the catalyst and surrounding solution ($R^1 = (CH_2)_{13}CH_3$, Figure 1-9) decreased the reactivity of the material, in some cases dropping the rate of hydrolysis 20-fold. It was originally believed that by creating a non-polar outer layer of hydrocarbon, the relatively non-polar substrates would diffuse more readily from the water phase into the proximity of the catalyst. This however proved not to be the case.

Plots of k_{obs} as a function of pH for the hydrolysis of **1.48** showed that for a change in pH of 2.5 units (pH = 6.0 - 8.5), the rate of hydrolysis changed only by a factor of 2.5, suggesting that hydrolysis was insensitive to hydroxide concentration and hence hydroxide was not the nucleophilic species. This was deemed consistent with a mechanism in which Cu(II) plays a dual Lewis-acid role: 1) binding to and activating the phosphoryl group and 2) delivering a metal-bound hydroxide.

Despite the apparent success of Menger's polymer supported hydrolysis catalysts, relatively little work has been done to expand the scope of immobilized metal species for the hydrolysis of organophosphorus agents. The few examples which exist have had limited success.

Again using the Cu(II)-polyamine motif, Chang *et. al.*[75] prepared the Cu(II) complexes of alkylamino styrene monomers **1.50** – **1.52** and copolymerized these materials with

trimethylolpropane trimethacrylate (TRIM, **1.53**) to generate insoluble TRIM polymers loaded with Cu(II) for the hydrolysis of the monoester, *p*-nitrophenyl phosphate.

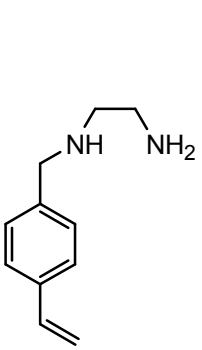

1.50

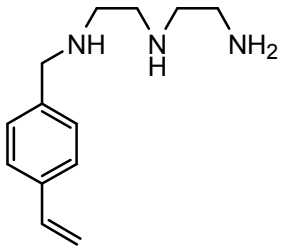

1.51

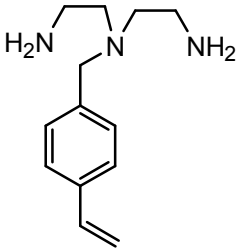

1.52

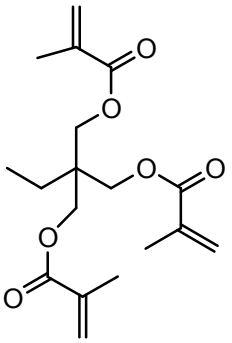

1.53

It was found that only the polymers loaded with the Cu(II) complexes of **1.50** and **1.52** were catalytically active, with true catalytic turnover. The observed catalysis was, however, not substantial. Relative to the uncatalyzed reaction at pH = 8.5, 0.05 g of the polymer loaded with **1.50**:Cu(II) accelerated the hydrolysis of the substrate by a factor of 28 while the same weight of polymer containing **1.52**:Cu(II) gave only two-fold acceleration. Perhaps the most noteworthy aspect of this study was the observation that while the polymeric forms of **1.50**:Cu(II) and **1.52**:Cu(II) were catalytically active, the homogeneous complexes of **1.50**:Cu(II) and **1.52**:Cu(II) were not, a rare observation in heterogeneous catalysis. The activity of the polymeric material was attributed to the change of the local environment of the catalytic species (perhaps to a less polar environment) as well as a distortion of the coordination geometry of Cu(II) in the polymeric form as compared to the monomer.

Chang later extended the scope of the work to include TRIM polymers containing a bipyridine-Cu(II) complex.[76] The insoluble copper loaded polymer was prepared by

copolymerizing the Cu(II) complex of 4-vinyl-4'-methyl-2,2'-bipyridine (**1.54**) (Cu(II) was introduced as $Cu(NO_3)_2$) with trimethylolpropane trimethacrylate (**1.53**). Using this technique, a polymer with a Cu(II) loading of 0.25 mmol/g was achieved. The polymer was used to catalyze the hydrolysis of three substrates: *p*-nitrophenyl phosphate, *bis*(*p*-nitrophenyl) phosphate (**1.3**), and the organophosphorus pesticide methyl parathion (**1.40**).

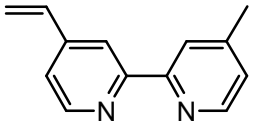

1.54

In an 85:15 water/methanol mixture at pH = 8.1, the Cu(II)-loaded polymer gave several orders of magnitude acceleration for all three substrates, the most impressive of which was the 7 x 10^5-fold acceleration of the hydrolysis of methyl parathion. In addition to the impressive rate enhancements, the polymeric materials displayed true catalytic turnover as well as some other interesting characteristics. As with the previous polymers prepared by Chang *et. al.,*[75] the catalytic activity of the polymeric material was greater than that of the monomeric Cu(II)-**1.54** complex in homogeneous solution. The authors argued that the enhanced catalytic activity of the polymeric material must indicate that the polymer matrix creates an environment around the catalytic site which is able to stabilize the reaction transition state better than in solution. While this argument may be a contributing factor, it might also be hypothesized that anchoring of the catalyst onto a polymer support prevents the formation of catalytically inactive dimers, as observed for Zn(II) and Cu(II) complexes of 1,10-phenanthroline and bipyridine in methanol solution.[39a,b] It was also noted that the polymeric catalysts had significantly stronger binding, as evidenced by a

much lower Michaelis constant, for the hydrolysis of all substrates. It was proposed that the substrates were physically absorbed into the polymer, thus increasing the local concentration of the substrate on the polymer surface. Concentrating the substrate on the polymer results in the maximum activity being achieved at a lower total substrate concentration than would be expected in homogeneous solution, thus resulting in a lower observed value of the Michaelis constant.

Chang also examined the effects of loading macrocyclic polyamines into insoluble TRIM polymers. Many examples exist of the hydrolysis of phosphate esters promoted by divalent metal complexes of 1,4,7-triazacyclononane (**1.10**)[77] or its N-alkylated derivatives.[31,78] Burstyn[77d,e] showed that while the **1:10**:Cu(II):$(H_2O)_2$ complex is catalytically active for the hydrolysis of phosphate diesters, it is in equilibrium with the catalytically inactive hydroxo bridged dimer (which is favoured at high concentration). In order to prevent the dimerization and increase the concentration of the catalytically active monomer, Chang *et. al.*[79] prepared a series of 1,4,7-triazacyclononane ligands which were N-alkylated with 4-vinylbenzyl groups (**1.55 –** 1.**57**) and copolymerized with trimethylolpropane trimethacrylate (**1.53**).

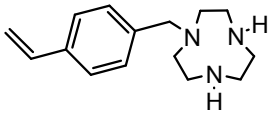

1.55

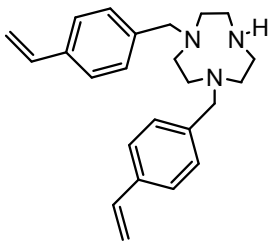

1.56

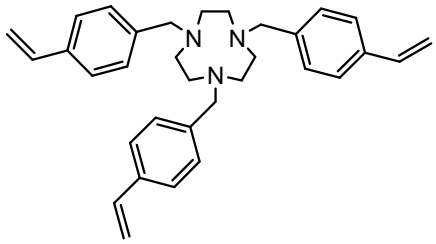

1.57

In addition, polymerization of ligand **1.57** without TRIM gave a cross-linked polymeric material composed entirely of catalytically active monomers. The reactive polymers were used as catalysts for the hydrolysis of *bis*(*p*-nitrophenyl) phosphate (**1.3**), and methyl parathion (**1.40**). Again, the authors found that the polymeric catalysts loaded with the Cu(II) complexes of **1.55 – 1.57** were more active than the monomeric complexes in solution. The best polymer was one which was prepared by first polymerizing **1.57** to form a soluble core, followed by the addition of TRIM to create an insoluble outer layer. In an 85:15 water/methanol mixture buffered at pH = 8.1, this polymer gave accelerations of 3.3×10^5-fold and 5.9×10^5-fold for the hydrolysis of **1.40** and **1.3** respectively relative to the background reactions at the same pH.

A few other examples of heterogeneous metal catalysts exist for organophosphorus ester hydrolysis including polystyrene "Chelex" resins loaded with Fe(III),[80] silver-exchanged zeolites,[81] ion-exchange resins loaded with Cu(II) complexes of 2,2'-bipyridine or TMEN,[82] and naturally occurring clays.[83] Unfortunately, none of these materials gave rate accelerations which allowed the organophosphorus agents to be destroyed at satisfactory rates.

Aside from metal-based catalysts, the only other immobilized catalysts to show promise in the destruction of poisonous organophosphorus agents are the immobilized *o*-iodosobenzoates developed by Moss *et. al.* *o*-Iodosobenzoate (**1.58**) is the conjugate base of *o*-iodosobenzoic acid (**1.59**), a hypervalent iodine compound which is known to

be a powerful α-nucleophile and oxidant.[47c] The *o*-iodosobenzoate anion has been shown to be a turnover catalyst for the hydrolysis of organophosphorus esters (Figure 1-10).[47c]

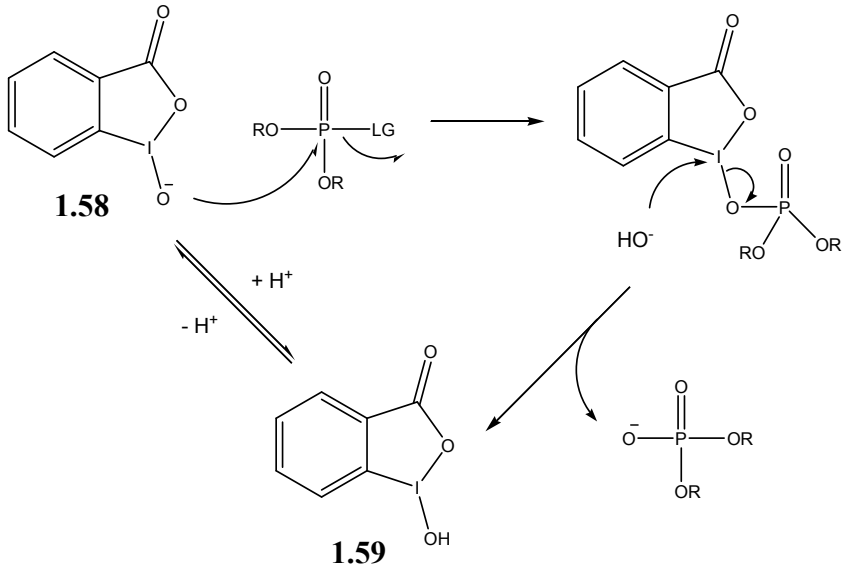

Figure 1-10. The catalytic mechanism for the hydrolysis of phosphate esters catalyzed by the *o*-iodosobenzoate anion.

Moss *et. al.* successfully anchored **1.59** on polymer supports of polystyrene and polyacrylate[84] and these materials effectively catalyzed the hydrolysis of Soman and substrate **1.49**. The observed rates were however significantly slower than the rates observed for the same catalysts in aqueous solution in the presence of a surfactant (the optimal conditions for the catalyst).[85] The reduced activity of the polymeric catalyst was thought to be due to the hydrophobic polymer matrix which did not allow access of the aqueous solution to the active sites. To improve the "wetability" of the immobilized catalyst, the authors moved to a silica gel support which is more hydrophilic and amenable to aqueous reactions.[86] The silica support did increase the reactivity of the immobilized catalyst, but these materials were still more than ten times slower than the optimal solution reaction. The catalyst was later immobilized on Amberlite[87], titanium

dioxide (Titania), and nylon.[88] While these materials proved effective for the hydrolysis of the G-agents and their simulants, the *o*-iodosobenzoate is not catalytic for the destruction of V-agents. It is believed that upon release of the thiol(ate) leaving group from VX, *o*-iodosobenzoate oxidizes sulphur and is converted to *o*-iodobenzoic acid.[57b] There are also no results to suggest that these materials are effective towards the destruction of phosphorothionate pesticides.

1.10 – Proposed Research

1.10.1 – Structure activity relationships in dinuclear Zn(II) complexes which catalyze the cleavage of phosphate diesters.

The importance of the phosphate diester bond as the robust linker that allows construction of the polymeric guardians of the genetic code, RNA and DNA, and the biological importance of reactions which cleave this bond has inspired an intense interest in studying the mechanism by which enzymes perform these transformations. Current understanding of enzymes which cleave phosphate diesters has largely failed the most important test: creating mimics which rival the activity of the natural systems. Our research group's work with complex **1.22**:$Zn(II)_2$ in methanol[41,43] has found this catalyst to be the most active synthetic dinuclear catalyst reported to date; however, our understanding of the origin of the unprecedented catalysis remains very limited. Given the diversity of dinuclear complexes which have been studied for the cleavage of phosphodiesters, we selected a few of these examples and aimed to study the structural elements, particularly of the organic ligand, that influence catalytic activity.

A very common structural motif among dinuclear Zn(II) catalysts which show metal-ion cooperativity in water is the presence of an oxy-anion bridge between the two metal ions.[31,89,90] We believed that the necessity for an anionic bridge was a consequence of the aqueous medium and that it is not an essential requirement for catalysis under all conditions. This hypothesis could not be tested in water, however, since dinuclear complexes lacking the oxy-anion bridge do not show any significant catalysis, perhaps as a result of the inability to form the complex with two Zn(II) ions or as a consequence of Zn(II)--Zn(II) repulsion forcing the two metal ions too far apart for cooperative interactions. In light of our previous work with **1.22**:$Zn(II)_2$ in methanol, where we were able to form a highly active dinuclear complex in the absence of an oxy-anion in the linker, we were eager to undertake studies to fully understand the catalytic effect of the anionic ligand. Chapter 2 of this thesis describes a detailed kinetic study of a series of dinuclear Zn(II) complexes with and without an anionic oxygen atom between the metal centers to determine the effect of this group on the rate of cleavage of RNA model **1.1**. We have also performed energetics calculations based on the kinetic data to shed light on the origin of the effect.

We have also been intrigued by the recent reports of hydrogen-bond donors being incorporated into metal complexes to enhance catalysis.[90,91] We were interested to see if the proposed hydrogen-bonding interactions which are thought to accelerate reactions in water would be enhanced in lower-dielectric constant solvents such as methanol. We were also curious to gain better insight into the role of the hydrogen-bond donating substituents, since little conclusive evidence exists for the exact mechanism by which these groups enhance catalysis. Chapter 3 describes a structure activity study examining

the effect of various substituents (both hydrogen-bonding and simple alkyls) on a series of dinuclear Zn(II) complexes which catalyze the cleavage of the phosphate diester **1.1**.

1.10.2 – Solid supported transition metal catalysts for the decomposition of neutral organophosphorus esters.

In addition to acting as the backbone for the nucleic acids, organophosphate esters (most importantly neutral phosphate esters) have found widespread use as chemical warfare (CW) agents and pesticides. We previously demonstrated that lanthanide ions (e.g. La(III)), and complexes of various transition metals (e.g. Zn(II), Cu(II), Pd(II)) are exceptional catalysts for the decomposition of neutral organophosphorus esters in methanol solution.[36-39] Some of the homogeneous systems involving complexes of Zn(II) and Cu(II) suffered from dimerization of the catalyst, resulting in the concentration of the active monomeric forms being very low under the reaction conditions.[39a] In particular, the 1,10-phenanthroline complex of Zn(II):$^{-}OCH_3$ was found to be highly active for the methanolysis of phosphate triesters, but was found to be thermodynamically most stable in the catalytically inactive dimeric form. To circumvent this problem, we aimed to affix the catalytic complex onto a solid polymer support, thereby preventing dimerization. This would also have the added benefit of generating an insoluble catalyst which could be easily recovered from the reaction mixture and reused multiple times. Chapter 4 describes our work towards the immobilization of the Zn(II):phenanthroline complex onto polystyrene supports and the activity of these heterogeneous catalyst towards the methanolysis of simulants of the G-agents and V-agents.

In addition to controlling the speciation of the metal-ion catalyst, immobilization on solid support is an attractive method to preserve expensive or precious catalysts. We had previously found the palladacycle complex **1.44** to be an extremely effective catalyst for the methanolytic destruction of P=S pesticides.[39c] Despite the large rate accelerations provided by the catalyst, the high cost of palladium may curtail its large scale use as a decontamination strategy. We were eager to develop a simple method to anchor the palladacycle complex onto solid supports to generate recoverable, recyclable catalysts which would prevent the loss of the expensive metal. Chapter 5 is an account of our development of a simple strategy to form a palladacycle on the surface of polystyrene and silica gel particles. We also demonstrate that these heterogeneous catalysts are highly efficient for the methanolysis of a series of P=S pesticides at ambient temperature and neutral $^{s}_{s}$pH .

1.11 - References

1) Wolfenden, R. *Chem. Rev.* **2006**, *106*, 3379.

2) a) Lipscomb, W.N.; Sträter, N. *Chem. Rev.* **1996**, *96*, 2375. b) Cowan, J.A. *Chem. Rev.* **1998**, 98, 1067. c) Weston, J. *Chem. Rev.* **2005**, *105*, 2151. d) Cleland, W.W.; Hengge, A.C. *Chem. Rev.* **2006**, *106*, 3252. e) Sträter, N.; Lipscomb, W.N; Klabunde, T.; Krebs, B. *Angew. Chem. Int. Ed.* **1996**, *35*, 2024. f) Wilcox, D.E. *Chem. Rev.* **1996**, *96*, 2435. g) Krämer, R. *Coord. Chem. Rev.* **1999**, *182*, 243.

3) Yoy, A.D.; Walsh, E.N. *Phosphorus Chemistry in Everyday Living*, 2nd 3ed.; American Chemical Society: Washington, DC, 1987; Chapters 18-20.

4) Harned, H. S.; Owen, B. B. *The Physical Chemistry of Electrolytic Solutions*, 3rd ed.; ACS Monograph Series 137; Reinhold Publishing: NewYork, 1957; p 161.

5) Levine, I. N. *Physical Chemistry*, 4th ed.; McGraw-Hill, Inc.; U.S.A., 1978; pp 276-281.

6) a) Cleland, W.W.; Frey, P.A.; Gerlt, J.A. *J. Biol. Chem.* **1998**, *273*, 25529. b) Antonsiewicz, J.; McCammon, J.A.; Gilson, M.K. *Biochemistry*. **1996**, *35*, 7819.

7) (a) Bosch, E.; Rived, F.; Roses, M.; Sales, J. *J. Chem. Soc., Perkin Trans.2*. **1999**, 1953. (b) Rived, F.; Roses, M.; Bosch, E.. *Anal. Chim. Acta*. **1998**, *374*, 309. (c) Bosch, E.; Bou, P.; Allemann, H.; Roses, M.. *Anal. Chem*. **1996**, 3651.

8) deLignym C.L.; Rehbach, M. *Recl. Trav. Chim.* **1960**, *79*, 727.

9) a) Schroeder, G.K.; Lad, C.; Wyman, P.; Williams, N.H.; Wolfenden, R. *Proc. Natl. Acad. Sci. USA*. **2006**, *103*, 4052. b) Lad, C.; Williams, N.H.; Wolfenden, R. *Proc. Natl. Acad. Sci. USA*. **2003**, *100*, 5607.

10) Järvinen, P.; Oivanen, M.; Lönnberg, H. *J. Org. Chem.* **1991**, *56*, 5396.

11) Williams, N.H; Takasaki, B.; Wall, M.; Chin, J. *Acc. Chem. Res.* **1999**, *32*, 485.

12) Davies, J.F.;Hostomska, Z.; Hostomsky, Z; Jordan, S.R.l Matthews, D.A. *Science*. **1991**, *252*, 88.

13) Beese, L.S.; Steitz, T.A. *EMBO.* **1991**, *10*, 25.

14) Lahm, A.; Volbeda, S.; Suck, D. *J. Mol. Biol.* **1990**, *215*, 207.

15) Kim, E.E. ; Wyckoff, H.W. *J. Mol. Biol.* **1991**, *218*, 449.

16) Coleman, J.E. *Annu. Rev. Biophys. Biomol. Struct.* **1992**, *21*, 441.

17) a) Zalatan, J.G.; Fenn, T.D.; Brunger, A.T.; Herschlag, D. *Biochemistry* **2006,** *45*, 9788. b) Zalatan, J.G.; Herschlag, D. *J. Am. Chem. Soc.* **2006,** *128*, 1293. c) Nikolic-

Hughes, I.; Rees, D.C.; Herschlag, D. *J. Am. Chem. Soc.* **2004**, *126*, 11814. d) Zalatan, J.G.; Catrina, I.; Mitchell, R.; Grzyska, P.K.; O'Brien, P.J.; Herschlag, D.; Hengge, A.C. *J. Am. Chem. Soc.* **2007**, *129*, 9789. e) Zalatan, J.G.; Fenn, T.D.; Herschlag, D. *J. Mol. Biol.* **2008**, *384*, 1174.

18) Lassila, J.K.; Herschlag, D. *Biochemistry*. **2008**, *47*, 12853.

19) Parkin, G. *Chem. Rev.* **2004**, *104*, 699.

20) Hegg, E.L.; Burstyn, J.N. *Coord. Chem. Rev.***1998**, *173*, 133.

21) Cowan, J.A. *Curr. Op. Chem. Biol.* **2001**, *5*, 634.

22) Morrow, J.R.; Iranzo, O. *Curr. Op. Chem. Biol.* **2004**, *8*, 192.

23) Lönnberg, T.; Lönnberg, H. *Curr. Op. Chem. Biol.* **2005**, *9*, 665.

24) Kirby, A.J.; Hollfelder, F. *From Enzyme Models to Model Enzymes*. ; The Royal Society of Chemistry: Cambridge, UK, 2009; p.31.

25) Brown, D.M.; Usher, D.A. *J. Chem. Soc.* **1965**, 6558.

26) Brown, R.S.; Neverov, A.A. *Advances in Physical Organic Chemistry.* **2008**, *42*, 271.

27) Brown, R.S.; Lu, Z.-L.; Liu, C.T.; Tsang, W.Y.; Edwards, D.R.; Neverov, A.A. *J. Phys. Org. Chem.* **2010**, *23*, 1.

28) Breslow, R.; Singh, S. *Bioorg. Chem.* **1988**, *16*, 408.

29) Prince, R.H.; Stotter, D.A.; Wooley, P.R. *Inorg. Chim. Acta.* **1974**, *9*, 51

30) Chapman Jr., W.H.; Breslow, R. *J. Am. Chem. Soc.* **1995**, *117*, 5462.

31) a) Iranzo, O.; Kovalevsky, A.Y.; Morrow, J.R.; Richard, J.P. *J. Am. Chem. Soc.* **2003**, *125*, 1988. b) Iranzo, O.; Elmer, T.; Richard, J.P.; Morrow, J.R. *Inorg. Chem.* **2003**, *42*, 7737.

32) a) Molenveld, P.; Kpsabelis, S.; Engbersen, J.F.J.; Reinhoudt, D.N. *J. Am. Chem. Soc.* **1997**, *119*, 2948. b) Molenveld, P. Stikvoort, W.M.; Kooijman, H.; Spek, A.L.; Engbersen, J.F.J.; Reinhoudt, D.N. *J. Org. Chem.* **1999**, *64*, 3896. c) Molenveld, P.; Engbersen, J.F.J.; Reinhoudt, D.N. *Eur. J. Org. Chem.* **1999**, 3269. d) Molenveld, P.; Engbersen, J.F.J.; Reinhoudt, D.N. *Angew. Chem. Int. Ed.* **1999**, *38*, 3189. e) Molenveld, P.; Engbersen, J.F.J.; Reinhoudt, D.N. *Chem. Soc. Rev.* **2000**, *29*, 75.

33) Mancin, F.; Rampazzo, E.; Tecilla, P.; Tonellato, U. *Eur. J. Org. Chem*. **2003**, 281.

34) a) Neverov, A.A.; McDonald, T.; Gibson, G.; Brown, R.S. *Can. J. Chem.* **2001**, *79*, 1704. b) Neverov, A.A.; Gibson, G.; Brown, R.S. *Inorg. Chem.* **2003**, *42*, 228. c) Neverov, A.A.; Sunderland, N.E.; Brown, R.S. *Org. Biomol. Chem.* **2005**, *3*, 65.

35) a) Neverov, A.A.; Brown, R.S. *Can. J. Chem.* **2000**, *78*, 1247. b) Neverov, A.A.; Montoya-Pelaez, P.J.; Brown, R.S. *J. Chem. Chem. Soc.* **2001**, *123*, 210.

36) a) Tsang, J.S.; Neverov, A.A.; Brown, R.S. *J. Am. Chem. Soc.* **2003**, *125*, 7602. b) Liu, T.; Neverov, A.A.; Tsang, J.S.W.; Brown, R.S. *Org. Biomol. Chem.* **2005**, *3*, 1525.

37) a) Lewis, R.E.; Neverov, A.A.; Brown, R.S. *Org. Biomol. Chem.* **2005**, *3*, 4082. b)Melnychuk, S.A.; Neverov, A.A.; Brown, R.S. *Angew. Chem.* **2006**, *118*, 1799.

38) Tsang, J.S.W.; Neverov, A.A.; Brown, R.S. *Org. Biomol. Chem.* **2004**, *2*, 3457.

39) a) Desloges, W.; Neverov, A.A.; Brown, R.S. *Inorg. Chem.* **2004**, *43*, 6752. b) Neverov, A.A.; Brown, R.S. *Org. Biomol. Chem.* **2004**, *2*, 2245. c) Lu, Z.-L.; Neverov, A.A.; Brown, R.S. *Org. Biomol. Chem.* **2005**, *3*, 3379.

40) a) Gibson, G.; Neverov, A.A.; Brown, R.S. *Can. J. Chem.* **2003**, *81*, 495. b) Gibson, G.T.T.; Mohamed, M.F.; Neverov, A.A.; Brown, R.S. *Inorg. Chem.* **2006**, 45, 7891.

41) Neverov, A.A.; Lu, Z.-L.; Maxwell, C.I.; Mohamed, M.F.; White, C.J.; Tsang, J.S.W.; Brown, R.S. *J. Am. Chem. Soc.* **2006**, *128*, 16398.

42) Kim, J.; Lim, H. *Bull. Korean Chem. Soc.* **1999**, *4*, 491.

43) Bunn, S.E.; Liu, C.T.; Neverov, A.A.; Brown, R.S. *J. Am. Chem. Soc.* **2007**, *129*, 16238.

44) Liu, C.T.; Melnychuk, S.A.; Liu, C.; Neverov, A.A.; Brown, R.S. *Can. J. Chem.* **2009**, *87*, 640.

45) Koelle, G.B.; Gilman, A. *Pharmacol. Rev.* **1949**, *1*, 166.

46) Fest, C.; Schmidt, K.-J. *The Chemistry of Organophosphorus Pesticides: Reactivity, Synthesis, Mode of Action, Toxicology.* Springer-Verlag: New York, 1973.

47) a) Yang, Y.-C.; Baker, J.A.; Ward, J.R. *Chem. Rev.* **1992**, *92*, 1729. b) Yang, Y.-C. *Acc. Chem. Res.* **1999**, *32*, 109. c) Morales-Rojas, H.; Moss, R.A. *Chem. Rev.* **2002**, *102*, 2497. d) Smith, B.M. *Chem. Soc. Rev.* **2008**, *37*, 470.

48) Quin, L.D. *A Guide to Organophosphorus Chemistry.* Wiley-Interscience: New York, 2000; p. 369.

49) Gianessi, L.; Reigner, N. *Pesticide Use in U.S. Crop Production: 2002. Insecticides & Other Pesticides.* CropLife Foundation: Washington, DC, 2006.

50) Menger, F.M.; Tsuno, T. *J. Am. Chem. Soc.* **1989**, *111*, 4903.

51) Wagner-Jauregg, T.; Hackley, Jr. B.E.; Lies, T.A.; Owens, O.O.; Proper, R. *J. Am. Chem. Soc.* **1955**, *77*, 922.

52) Epstein, J.; Bauer, V.E.; Saxe, M.; Demek, M.M. *J. Am. Chem. Soc.* **1956**, *78*, 4068.

53) Courtney, R.C.; Gustafson, R.L.; Westerback, S.J.; Hyytiainen, H.; Chaberek, Jr. S.C.; Martell, A.E. *J. Am. Chem. Soc.* **1957**, *79*, 3030.

54) Gustafson, R.L.; Martell, A.E. *J. Am. Chem. Soc.* **1962**, *84*, 2309.

55) Ward, J.R.; Yang, Y.-C.; Wilson, Jr. R.B.; Burrows, W.D.; Ackerman, L.L. *Bioorg. Chem.* **1988**, *16*, 12.

56) a) Yang, Y.-C.; Szafraniec, L.L.; Beadury, W.T.; Bunton, C.A. *J. Org. Chem.* **1993**, *58*, 6964. b) Yang, Y.-C.; Berg, F.J.; Szafraniec, L.L.; Beadry, W.T.; Bunton, C.A.; Kumar, A. *J. Chem. Soc., Perkin Trans. 2.* **1997**, 607.

57) a) Berg, F.J.; Moss, R.A.; Yang, Y.-C.; Zhang, H. *Langmuir.* **1995**, *11*, 411. b) Moss, R.A.; Morales-Rojas, H.; Zhang, H.; Park, B.-D. *Langmuir.* **1999**, *15*, 2738.

58) a) Heath, D.F. *J. Chem. Soc.* **1956**, 3796. b) Cook, R.D.; Farah, S.; Ghawi, L.; Itani, A.; Rahil, J. *Can. J. Chem.* **1986**, *64*, 1630.

59) Kuo, L.Y.; Perrera, N.M. *Inorg. Chem.* **2000**, *39*, 2103.

60) Smolen, J.M.; Stone, A.T. *Environ. Sci. Technol.* **1997**, *31*, 1664.

61) a) Kazankov, G.M.; Sergeeva, V.S.; Efremenko, E.N.; Alexandrova, L.; Varfolomeev, S.D.; Ryabov, A.D. *Angew. Chem. Int. Ed.* **2000**, *39*, 3117. b) Kazankov, G.M.; Sergeeva, V.S.; Borisenko, A.A.; Zatsman, A.I.; Ryabov, A.D. *Russ. Chem. Bull. Int. Ed.* **2001**, *50*, 1844.

62) Kim, M.; Gabbaï, F.P. *Dalton Trans.* **2004**, 3403.

63) a) Kim, M.; Liu, Q.; Gabbaï, F.P. *Organometallics.* **2004**, *23*, 5560. b) Kim, M.; Picot, A.; Gabbaï, F.P. *Inorg. Chem.* **2006**, *45*, 5600.

64) Merrifield, R.B. *J. Am. Chem. Soc.* **1963**, *85*, 2149.

65) a) Crowley, J.I; Rapaport, H. *Acc. Chem. Res.* **1976**, *9*, 135. b) Akelah, A.; Sherrington, D.C. *Chem. Rev.* **1981**, *81*, 557. c) Kobayashi, S. *Chem. Soc. Rev.* 1998, *28*,1. d)Ley, S.V.; Baxendale, I.R.; Bream, R.N.; Jackson, P.S.; Leach, A.G.;

Longbottomg, D.A.; Nesi, M.; Scott, J.S.; Storer, R.I.; Taylor, S.J. *J. Chem. Soc., Perkin Trans. 1.* **2000**, 3815.

66) a) Senkan, S. *Angew, Chem., Int. Ed.* **2001**, *40*, 312. b) Reetz, M. *Angew, Chem., Int. Ed.* **2001**, *40*, 284. c) Leadbeater, N.E.; Marco, M. *Chem. Rev.* **2002**, *102*, 3217.

67) Guyot, A.; Bartholin, M. *Prog. Polym. Sci.* **1982**, *8*, 277.

68) Crudden, C.M.; Sateesh, M.; Lewis, R. *J. Am. Chem. Soc.* **2005**, *127*, 10045 (and references therein)

69) Chauvin, Y.; Commereuc, D.; Dawans, F. *Prog. Polym. Sci.* **1977**, *5*, 95.

70) Sherrington, D.C. *Chem. Commun.* **1998**, 2275.

71) Sherrington, D.C.; Kybett, A.P. *Supported Catalysts and Their Applications.* Royal Society of Chemistry: Cambridge, 2001; p.125.

72) a) Hoffmann, F.; Cornelius, M.; Morell, J.; Fröba, M. *Angew. Chem. Int. Ed.* **2006**, *45*, 3216. b) Wight, A.P.; Davis, M.E. *Chem. Rev.* **2002**, *102*, 3589.

73) Menger, F.M.; Tsuno, T. *J. Am. Chem. Soc.* **1989**, *111*, 4903.

74) Ward, J.R.; Yang, Y.-C.; Wilson, Jr. R.B.; Burrows, W.D.; Ackerman, L.L. *Bioorg. Chem.* **1988**, *16*, 12.

75) Lu, Q.; Singh, A.; Deschamps, J.R.; Chang, E.L. *Inorg.Chim. Acta.* **2000**, *309*, 82.

76) Hartshorn, C.M.; Singh, A.; Chang, E.L. *J. Mater. Chem.* **2002**, *12*, 602.

77) a) Burstyn, J. N.; Deal, K. A. *Inorg. Chem.* **1993**, *32*, 3585-3586. b) Deal, K. A.; Burstyn, J. N. *Inorg. Chem.* **1996**, *35*, 2792-2798. c) Deal, K. A.; Hengge, A. C.; Burstyn, J. N. *J. Am. Chem. Soc.* **1996**, *118*, 1713-1718. d) Hegg, E.L.; Burstyn, J.N. *Inorg. Chem.* **1996**, 35, 7474. e) Hegg, E.L.; Mortimore, S.H.; Cheung, C.L.; Huyett, J.E.; Powell, D.R.; Burstyn, J.N. *Inorg. Chem.* **1999**, 38, 2961.

78) a) Vichard, C.; Kaden, T.A. *Inorg. Chim. Acta.* **2002**, 337, 173. b) Arca, M.; Berni, E.; Caltagirone, C.; Devillanova, F.A.; Isaia, F.; Garau, A.; Giorgi, C.; Lippolis, V.; Perra, A.; Tei, L.; Valtancoli, B. *Inorg. Chem.* **2003**, *42*, 6929.

79) Hartshorn, C.M.; Deschamps, J.R.; Singh, A.; Chang, E.L *React. Funct. Polym.* **2003**, *55*, 219.

80) Lykourinou-Tibbs, V.; Ercan, A.; Ming, L.-J. *Catal. Commun.* **2003**, *4*, 549.

81) Wagner, G.W.; Bartram, P.W. *Langmuir*. **1999**, *15*, 8113.

82) Beaudry, W.T.; Wagner, G.W.; Ward, J.R. *J. Mol. Catal.* **1994**, *93*, 221.

83) a) Saltzman, S.; Mingelgrin, U.; Yaron, B. *J. Agric. Food Chem.* **1976**, *24*, 739. b) El-Amamy, M.M.; Mill, T. *Clays Clay. Miner.* **1984**, *32*, 67.

84) Moss, R.A.; Bolikal, D.; Durst, H.D.; Hovanec, J.W. *Tetrahedron Lett.* **1988**, *29*, 2433.

85) Moss, R.A.; Chatterjee, S.; Wilk, B. *J. Org. Chem.* **1986**, *51*, 4303.

86) Moss, R.A.; Chung, Y.-C.; Durst, H.D.; Hovanec, J.W. *J. Chem. Soc., Perkin Trans. 1*. **1989**, 1350.

87) Moss, R.A.; Chung, Y.-C. *Langmuir*. **1990**, *6*, 1614.

88) Moss, R.A.; Chung, Y.-C. *J. Org. Chem.* **1990**, *55*, 2046.

89) Morrow, J. *Comments Inorg. Chem.* **2008**, *29*, 169.

90) a) Feng, G.; Natale, D.; Prabaharan, R.; Marque-Rivas, J.C.; Williams, N.H. *Angew. Chem. Int. Ed.* **2006**, *45*, 7056. b) Feng, G.; Marque-Rivas, J.C.; Williams, N.H. *Chem. Commun.* **2006**, 1845.

91) a) Aït-Haddou, H.; Sumaoka, J.; Wiskur, S.L.; Folmer-Anderson, J.F.; Anslyn, E.V. Angew. Chem. Int. Ed. **2002**, *41*, 4014. b) Livieri, M.; Mancin, F.; Tonellato, U.; Chin, J.

Chem. Commun. **2004**, 2862. c) Feng, G.; Marque-Rivas, J.C.; Torres Martin de Rosales, R.; Williams, N.H. *J. Am. Chem. Soc.* **2005**, *127*, 13470. d) Lombardo, V.; Bonomi, R.; Sissi, C.; Mancin, F. *Tetrahedron*, **2010**, *66*, 2189. e) Bonomi, R.; Saielli, G.; Tonellato, U.; Scrimin, P.; Mancin, F. *J. Am. Chem. Soc.*, **2009**, *131*, 11278. f) Bonomi, R.; Selvestrel, F.; Lombardo, V.; Sissi, C.; Polizzi, S.; Mancin, F.; Tonellato, U.; Scrimin, P. *J. Am. Chem. Soc.*, **2008**, *130*, 15744. g) Livieri, M.; Mancin, F.; Saielli, G.; Chin, J.; Tonellato, U. *Chem. – Eur. J.*, **2007**, *13*, 2246.

Chapter 2 - Investigation of the Effect of Oxy Bridging Groups in Dinuclear Zn(II) Complexes that Catalyze the Cleavage of a Simple Phosphate Diester RNA Analog.

2.1 – Preface

With minor formatting changes and the addition of Scheme 2-2, this chapter is largely as it was published in *Inorganic Chemistry* (Mohamed, M.F.; Neverov, A.A.; Brown, R.S. *Inorg. Chem.* **2009**, *48*, 11425). Section 2.7 – Chapter 2 postscript was added after publication of the original article. All experiments (including synthesis, kinetics, and analytical data collection) were performed by Mark Mohamed. The manuscript was written by Mark Mohamed and Dr. R. Stan Brown. The published article is copyrighted by the American Chemical Society.

2.2 – Introduction

The phosphodiester linkage is exceptionally stable towards solvolytic cleavage and widely present throughout Nature as the chemically robust linker that gives great stability to DNA and RNA polymers. Many of the enzymes that facilitate the cleavage of these stable phosphate esters contain two or more metal ions (notably Zn(II) but in some cases Ca(II), Mg(II), Fe(III), and Mn(II)) in their active sites which act cooperatively, giving rate enhancements for P-O cleavage of up to 10^{17}-fold.[1] The impressive rate accelerations offered by metal ion containing phosphodiesterases have elicited considerable interest in the design of small molecule mono- and dinuclear metal complexes that catalyze the

cleavage of phosphate diesters.[2] The study of such biomimetic catalysts has provided important insights into the origin of the catalysis afforded by enzymes but, at the present time, few actually approach the accelerations achieved by the naturally occurring systems. Virtually all of the catalytic systems have been investigated in aqueous media where it appears that dinuclear complexes are generally more active than their mononuclear counterparts[3,4,5,6,7,8] although this is not always so.[9,10] This might suggest that cooperative effects between two metal ions are not easily realized in water, but there are some standout cases where: 1) a $Zn(II)_2$ complex of 1,3-*bis*-N_1-(1,3,7-triazacyclononanyl)propan-2-ol (**2.1**) is 120-fold more active towards the hydrolysis of an RNA model 2-hydroxypropyl-*p*-nitrophenyl phosphate (HPNPP, **2.2**) than is the mono-Zn(II) complex of 1,4,7-triazacyclononane;[6b] and 2) the dinuclear catalyst **2.3** is ~600-fold more active towards the hydrolysis of HPNPP than the corresponding mononuclear species.[4]

A common structural motif among dinuclear catalysts such as **2.1** and **2.3** that show metal ion cooperativity in water is the presence of a bridging alkoxy group in the linker unit connecting the two metal centers.[2,11] An oxyanion bridging group seems to be essential for cooperative catalytic activity[6b] since it serves to shield the cationic metal centers from one another and allows them to achieve a close proximity and act cooperatively.[12] Attempts to study systems lacking the bridging alkoxy group have proven difficult in water as these do not generally exhibit a catalysis that is greater than the sum of the parts, perhaps because they do not cleanly bind two metal ions due to strong electrostatic repulsions, but rather tend to form so-called “sandwich complexes”

under the kinetic conditions in which both ligand groups are complexed to one metal ion.[13]

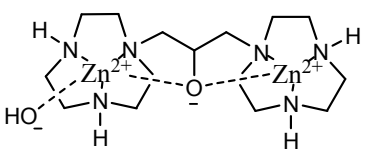

2.1

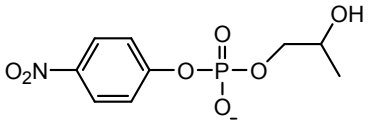

2.2

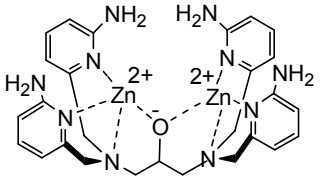

2.3

Work in this laboratory has found that the situation in the light alcohols (methanol and ethanol) is different from what one observes in water.[14] We have recently shown that the cleavage of HPNPP is accelerated by 10^{12}-fold relative to the background reactions in methanol and ethanol in the presence of the dinuclear Zn(II) complex **2.4**:$Zn(II)_2$:($^-$OR).[15,16,17] Notably, this catalyst in methanol is 10^8-fold more reactive than CH_3O^- alone and 1.5 x 10^4 times more active for cleavage of **2.2** than the corresponding mononuclear complex, **2.5**:Zn(II):($^-$OR), indicating strong metal ion cooperativity in the dinuclear system.[15,16] The large increase in activity seems to be attributable to a medium effect imbued by the alcohol since the $Zn(II)_2$ complex of **2.4** is reported to be no more reactive toward the cleavage of a phosphate diester in water than its mononuclear counterpart.[18] Since highly active dinuclear complexes of **2.4** form in alcohol solution in the absence of a bridging oxyanion in the linker, we wished to make comparisons of the catalytic activity of $Zn(II)_2$ systems with and without that bridging group, bearing in mind that the presence of a permanent oxyanionic group is expected to alter not only the coordination number of the metal ions, but their Lewis acidity and ability to acidify coordinated $HOCH_3$ to form the catalytically active mono-methoxy forms. This chapter describes a kinetic study of the cleavage of **2.2** in methanol (proceeding via the pathway given in

Scheme 2-1) catalyzed by the dinuclear Zn(II) complexes **2.6**:$Zn(II)_2$ and **2.7**:$Zn(II)_2$, which illustrates that the inclusion of a bridging phenoxide in the linker unit decreases the activity of the catalyst by a factor of 160. We also report a kinetic study of complex **2.8**:$Zn(II)_2$, which is 3.7 x 10^4 times less active than **2.4**:$Zn(II)_2$:($^-OCH_3$). These results indicate not only that the inclusion of the permanently fixed bridging alkoxy group is not essential for metal ion cooperativity in alcohol, but that this bridging group is in fact a significant detriment to the catalytic efficiency.

Scheme 2-1. Catalytic pathway for the catalytic cleavage of **2.2**. Charges on Zn omitted for simplicity; OAr = *p*-nitrophenoxy

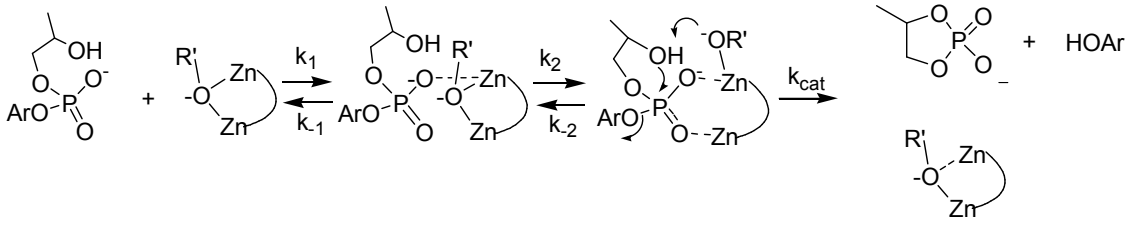

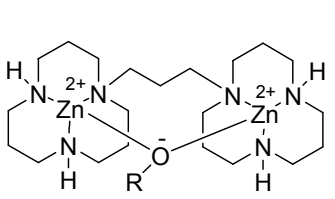

2.4:Zn_2:($^-$OR)

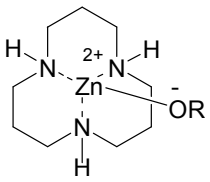

2.5:Zn:($^-$OR)

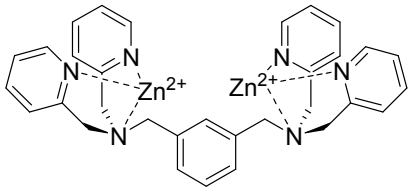

2.6:Zn_2

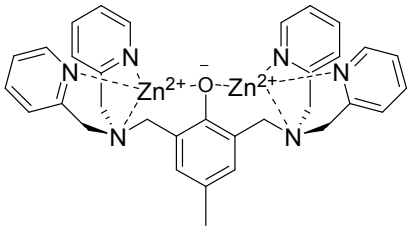

2.7:Zn_2

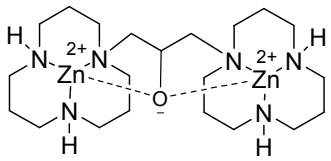

2.8:Zn_2

2.3 – Experimental

2.3.1 – Materials

Methanol (99.8%, anhydrous), $Zn(OTf)_2$ (98%), sodium methoxide (0.50 M solution in methanol, titrated against N/50 certified standard aqueous HCl solution and found to be 0.49 M), triethylamine (99%), 2-picoline (98%), 2,6-lutidine (99%), 2,2,6,6-tetramethylpiperidine (99%), di(2-picolyl)amine (97%), α,α-dibromo-*m*-xylene (97%), di-*tert*-butyl dicarbonate (1.0M in THF), trifluoromethanesulfonic acid, and 1,3-dibromo-2-propanol (95% technical grade) were purchased from Aldrich and used without further purification. 2,4,6-Collidine was purchased from BDH Chemicals. $HClO_4$ (70% aqueous solution, titrated to be 11.40 M) was purchased from Acros Organics and used as supplied. THF and Acetonitrile were purchased from Fisher Scientific and dried prior to use on an Innovative Technology, Inc. PureSolv solvent purification system. Silica gel for chromatography (ultra pure, 230-400 mesh) was purchased from Silicycle.

2.3.2 - Synthesis

The syntheses of *bis*(di-(2-pyridylmethyl)amino)-*m*-xylene **(2.6)**[19] and 2,6-*bis*(di-(2-pyridylmethyl)amino)-4-methylphenol (**2.7**) [20] were done as previously reported.

Synthesis of 1,3-*bis*-N_1-(1,5,9-triazacyclododecyl)-propan-2-ol (2.8)

The title compound was prepared by a modification of the published procedure for the synthesis of ligand **2.1**[6b] according to the procedure reported for ligand synthesis[21] to obtain the x-ray structure of the $Zn(II)_2$ complex of **2.8.**[22]

Scheme 2-2. Synthesis of ligand **2.8**.

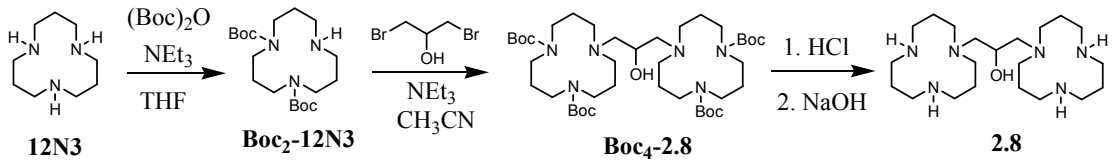

***N*, *N'*-*Bis*(*tert*-butoxycarbonyl)-1,5,9-triazacyclododecane (Boc_2-12N3)**

1,5,9-Triazacyclododecane (12N3)[23] (1.04 g, 6.1 mmol) was dissolved in 40 mL of dry THF with stirring and 1.7 mL (12 mmol, 2 eq) triethylamine was added. The stirring mixture was cooled in an ice bath under N_2 after which 12.1 mL of a 1.0 M solution of di-*tert*-butyl dicarbonate in THF (12 mmol, 2 eq) was slowly added via a dropping funnel over ~10 mins followed by an additional 10 mL dry THF to wash the funnel. The reaction mixture was allowed to stir under N_2 and slowly warm to room temperature. After stirring 72 hours, the solvent was removed under vacuum leaving a pale yellow viscous oil. The crude product was purified by flash chromatography on a silica column eluting with 6:1 $CHCl_3$:$HOCH_3$ (R_f = 0.43). Yield: 2.02 g (90%). ^{1}H NMR (300 MHz, $CDCl_3$): δ 3.29 (q, 8H, J = 6 Hz), δ 2.65 (t, 4H, J = 6 Hz), δ 1.88 (t, 2H, J = 6 Hz), δ 1.76 (m, 4H), δ 1.44 (s, 18H).

1,3-*Bis*(5,9-di(*tert*-butoxycarbonyl)-1,5,9-triazacyclododecyl)-propan-2-ol (Boc_4-2.8)

Boc_2-12N3 (1.99 g, 5.4 mmol), 1,3-dibromo-2-propanol (2.59 g, 2.7 mmol) and triethylamine (0.71g, 7 mmol) were dissolved in 50 mL of dry acetonitrile with stirring under N_2. The reaction flask was equipped with a condenser and heated to reflux under N_2 for 72 hr. The solvent was evaporated under vacuum to afford a thick oily residue

which was suspended in 60 mL of 3M NaOH and transferred to a separatory funnel. The aqueous mixture was extracted with 3 x 40 mL $CHCl_3$ and the combined organic layers were washed with 30 mL of water followed by drying over Na_2SO_4 and the solvent evaporated to yield a pale yellow oil which was purified by flash chromatography on a silica column eluting with 8:1 $CHCl_3$:$HOCH_3$ (R_f = 0.75). Yield: 1.46g (68%). ^{1}H NMR (300MHz, $CDCl_3$): δ 3.77 (m, 1H), δ 3.39 (m, 17H), δ 2.64-2.33 (m, 11H), δ 1.92-1.76 (m, 12H), δ 1.47 (s, 36H).

1,3-*Bis*-N_1-(1,5,9-triazacyclododecyl)-propan-2-ol (2.8)

Boc_4-**2.8** (1.46 g, 1.83 mmol) was dissolved in 25 mL of concentrated aqueous HCl (12 M) and allowed to stir at room temperature for 36 hours. The solvent was evaporated under vacuum to give an off-white solid which was then stirred in 50 mL of ethanol for 1 hour prior to filtering to give an off-white crystalline powder (the HCl salt of **2.8**). The hydrochloride salt (0.82 g, 1.3 mmol) was dissolved in 15 mL of 10 M aqueous NaOH and stirred for two hours during which an orange oily residue developed on the surface of the aqueous solution. The aqueous mixture was extracted with 4 x 20 mL $CHCl_3$ and dried over Na_2SO_4. The solvent was removed under reduced pressure to afford a viscous orange oil that was dried under high vacuum with gentle heating overnight. Yield 0.50g (96%). ^{1}H NMR (600 MHz, CD_3OD): δ4.06 (m, 1H), δ2.81 (m, 21H), δ2.56 (m, 2H), δ2.42 (m, 3H), δ2.08 (m, 2H), δ1.85 (m, 3H), δ1.75 (m, 3H), δ1.66 (m, 6H). ^{13}C NMR (100 MHz, $CDCl_3$): δ65.60, 59.10, 55.65, 48.90, 48.57, 47.88, 24.96. HRMS (ESI-TOF): calcd for $C_{21}H_{47}N_6O$ ($M\text{-}H^+$): 399.3805; found 399.3790.

2.3.3 - Methods

Potentiometric Titrations: Potentiometric titrations were performed[24a] in duplicate using an autotitrator equipped with an Accumet Accu-pHast combination electrode. The typical saturated KCl solution was removed from the outer jacket of the electrode, and then filled with a 1 M $LiClO_4$ solution in methanol. Solutions were titrated in a jacketed glass cell thermostatted at 25 °C while being sparged with N_2. The sodium methoxide titrant was standardized by titrating against an aqueous solution of Fisher-certified HCl (N/50). Aliquots of stock solutions were transferred into the titration cell via a glass pipette and the total volume was brought to 20.0 mL by adding anhydrous methanol. Subsequent ${}^{s}_{w}pH$ meter readings in methanol were converted to the ${}^{s}_{s}pH$ values by subtracting the δ correction factor of -2.24.[24b]

The $CH_3OH_2^+$ concentrations for the various kinetic runs were determined potentiometrically using a combination glass electrode (Radiometer model no. XC100-111-120-161) calibrated with certified standard aqueous buffers (pH = 4.00 and 10.00).

UV-Visible Kinetics in Methanol: The rates of catalyzed cleavage of **2.2** (0.05 mM) were monitored spectrophotometrically using a UV-vis spectrophotometer thermostatted at 25.0 ± 0.1 ˚C. Reaction rates were determined from the rate of appearance of *p*-nitrophenol at 320 nm or *p*-nitrophenolate at 400 nm. All kinetic experiments were performed with catalyst formed *in situ* through sequential addition of stock solutions (typically 25 mM) of sodium methoxide, ligand and $Zn(OTf)_2$ to anhydrous methanol such that $[^-OCH_3]$:[**2.6**]:$[Zn(OTf)_2]$ = 1:1:2 to make a total volume of 2.5 mL in quartz cuvettes and kinetic experiments were conducted over the range 0.05 mM < [**2.6**:$Zn(II)_2$]

< 1.0 mM. Formulation of the catalyst in this way gave solutions with ${}^{s}_{s}\text{pH}$ in the range of 9.0 ± 0.3. Kinetic studies involving **2.7**:$Zn(II)_2$ were performed under buffered conditions ($[buffer]_{total}$ = 25 mM) using mixtures of amine (2-picoline, ${}^{s}_{s}pK_a$ = 6.50; 2,6-lutidine, ${}^{s}_{s}pK_a$ = 7.30; *i*-Pr-morpholine, ${}^{s}_{s}pK_a$ = 8.80; triethylamine, ${}^{s}_{s}pK_a$ = 11.04; 2,2,6,6-tetramethylpiperidine, ${}^{s}_{s}pK_a$ = 12.02) and $HClO_4$ in methanol to adjust the ${}^{s}_{s}\text{pH}$ of the solution. Experiments were conducted over the range 0.075 mM < [**2.7**:$Zn(II)_2$] < 0.75 mM. Kinetic experiments with catalyst **2.8**:$Zn(II)_2$ were conducted under similar buffered conditions, but using HOTf to prepare the buffer. Examination of the catalytic activity of **2.8**:$Zn(II)_2$ as a function of the time after mixing of the catalyst components showed a levelling off of the activity after 20 min indicating that full formation of the catalyst required some time. The reported values of the pseudo-first order rate constants (k_{obs}) for the production of *p*-nitrophenol(phenolate) are the averages of duplicate runs.

2.4 – Results

2.4.1 – 2.6:$Zn(II)_2$ promoted cleavage of HPNPP

The formation of an active 2:1 dinuclear complex between ligand **2.6** and Zn(II) was confirmed through kinetic titration of the ligand with $Zn(OTf)_2$ where the k_{obs} for cleavage of **2.2** was monitored under buffered conditions at varying [$Zn(OTf)_2$]/[**2.6**] ratios at a constant [**2.6**] of 0.25 mM. The plot shown in Figure 2-1 indicates catalytic activity maximizes at [$Zn(OTf)_2$]/[**2.6**] = 2.0, and plateaus at higher ratios.

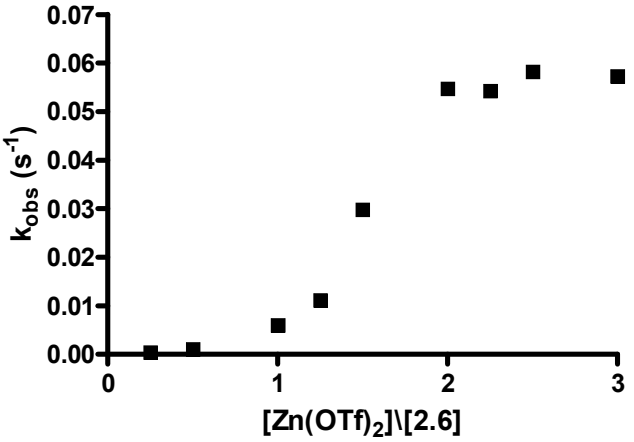

Figure 2-1. Dependence of the rate of methanolysis of HPNPP (0.05 mM) on the $[Zn(OTf)_2]/[\mathbf{2.6}]$ ratio at constant [**2.6**] (0.25 mM) in 25 mM *i*-Pr-morpholine buffer ($^{s}_{s}$pH = 9.1) at T = 25.0 ± 0.1 ˚C.

This kinetic titration supports the findings of an ^{1}H NMR titration that showed that addition of one equivalent of $Zn(OTf)_2$ to a 5 mM solution of **2.6** containing one equivalent of $NaOCD_3$ in CD_3OD, transformed the simple spectrum of the ligand to a complex spectrum, but addition of a second eq. of $Zn(OTf)_2$ gave a simplified spectrum with significant broadening. Addition of a third equivalent of $Zn(OTf)_2$ left the ^{1}H spectrum unchanged.

The plot of k_{obs} against increasing [**2.6**:$Zn(II)_2$:($^{-}OCH_3$)] (Figure 2-2) is indicative of the formation of a substrate-catalyst Michaelis complex. As is the case for all our previous studies with **2.4**:$Zn(II)_2$:($^{-}OCH_3$) in methanol,[15,16] triflate anion is also an inhibitor of the catalysis exhibited by **2.6**:$Zn(II)_2$:($^{-}OCH_3$) as evidenced by a downward curving plot of the k_{obs} for the cleavage of **2.2** at constant [**2.6**:$Zn(II)_2$:($^{-}OCH_3$)] vs increasing [tetrabutylammonium triflate]. These data were analyzed according to equation 1 (where k_{cat}^{0} is the rate constant at zero triflate concentration, K_i is the inhibition constant, and k_{inf}

is the rate constant at infinite triflate concentration) to give a triflate inhibition constant of 29.3 mM. For a more detailed discussion of the correction of experimental data for the inhibitory effect of the triflate anion, see references 15 and 17.

$$k_{obs} = \frac{k^{0}_{cat} K_i}{K_i + [OTf]_{total}} + k_{inf} \quad (1) \qquad k_{corr} = \frac{k_{obs}(K_i + [OTf])}{K_i} \quad (2)$$

Corrected pseudo first-order rate constants were determined on the basis of equation 2 (where k_{corr} is the corrected pseudo first-order rate constant, k_{obs} is the experimentally determined pseudo first-order rate constant, and K_i is the triflate inhibition constant) and the corrected k_{obs} vs [**2.6**:$Zn(II)_2$:($^{-}OCH_3$)] data were fit to universal binding equation (3)[25], giving a k_{cat}^{max} of 0.097 ± 0.003 s^{-1} and K_m of (1.1 ± 0.1) x 10^{-5} M where k_{cat}^{max} is the maximum observed rate constant, and K_m is the [**2.6**:$Zn(II)_2$:**2.2**] dissociation constant (taken as the reciprocal of the binding constant, K_B, from equation 3). The second-order rate constant for the cleavage of **2.2** catalyzed by **2.6**:$Zn(II)_2$ at $^{s}_{s}$pH 9.1 (defined as k_{cat}^{max}/K_m) is k_2 = 8.8 x 10^3 $M^{-1}s^{-1}$.

$$k_{obs} = k_{cat}(1 + K_B \times [S] + [Cat] \times K_B - X)/(2K_B)/[S] \quad (3)$$

where:

$$X = (1 + 2K_B \times [S] + 2 \times [Cat] \times K_B + K_B^2 \times [S]^2 - 2 \times K_B^2 \times [Cat][S] + [Cat]^2 \times K_B^2)^{0.5}$$

The $^{s}_{s}$pH-rate profile in Figure 2-3 for the **2.6**:$Zn(II)_2$ promoted cleavage of 0.5 mM **2.2** (conditions under which the catalyst-substrate complex is fully formed) was generated by

adding additional $NaOCH_3$ or $HClO_4$ in 0.25 equivalent portions to a catalyst formulated *in situ* by mixing two equivalents of $Zn(OTf)_2$ with one equivalent of **2.6** and one equivalent of $NaOCH_3$.

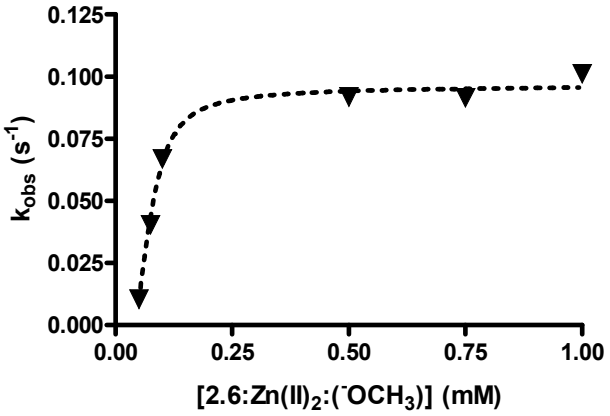

Figure 2-2. Plot of k_{obs} vs [**2.6**:$Zn(II)_2$] for cleavage of HPNPP (**2.2**) (5×10^{-5} M) determined from the rate of appearance of *p*-nitrophenol at 320 nm, ${}^{s}_{s}pH = 9.1$ and T = 25.0 ± 0.1 °C. Data are corrected for triflate inhibition and fitting to equation 3 gives $k_{cat}^{max} = 0.097 \pm 0.003$ s^{-1} and $K_m = (1.1 \pm 0.1) \times 10^{-5}$ M.

The log k_{obs} vs ${}^{s}_{s}pH$ kinetic data were fit to equation 4, derived for the process given in Scheme 2-3 where the active catalyst has a single methoxide, to give the constants ${}^{s}_{s}pK_a^1$ = 7.4 ± 0.1, ${}^{s}_{s}pK_a^2$ = 11.3 ± 0.1 and k_{cat}^{max} of 0.10 ± 0.01 s^{-1}. From these data and those contained in Figure 2-2, one can compute the second order rate constant for catalysis of the cyclization of **2.2** as $k_2^{cat} = k_{cat}^{max}/K_m = 9100$ $M^{-1}s^{-1}$.

Scheme 2-3. Postulated ${}^{s}_{s}pH$ dependent process for the cleavage of **2.2** mediated by **2.6**:$Zn(II)_2$. (Note: **Cat** = **2.6**:$Zn(II)_2$)

$$\textbf{Cat:}(HOCH_3)_2 \overset{{}^{s}_{s}K_a^{1}}{\rightleftharpoons} \textbf{Cat:}(^{-}OCH_3)(HOCH_3) + H^+ \overset{{}^{s}_{s}K_a^{2}}{\rightleftharpoons} \textbf{Cat:}(^{-}OCH_3)_2 + H^+$$

$$\textbf{2.2} \downarrow k_{cat}^{max}$$

$$P$$

$$k_{obs} = \left(\frac{k_{obs}^{max}\, {}^{s}_{s}K_a^{1}[H^+]}{[H^+]^2 + [H^+]\,{}^{s}_{s}K_a^{1} + {}^{s}_{s}K_a^{1}\,{}^{s}_{s}K_a^{2}} \right) \qquad (4)$$

Potentiometric titration of **2.6** (1.0 mM) with $NaOCH_3$ in methanol in the presence of 2.0 eq $Zn(OTf)_2$ and 1.0 eq. diphenyl phosphate (Na^+ form) shows two ionization events which, when fit using the Hyperquad 2000 NT computer program,[26] give apparent ${}^{s}_{s}pK_a$ values of 7.02 ± 0.04 and 10.82 ± 0.03 which can be compared with first and second kinetic ${}^{s}_{s}pK_a$ values of 7.4 and 11.3 respectively found for the data in Figure 2-3.

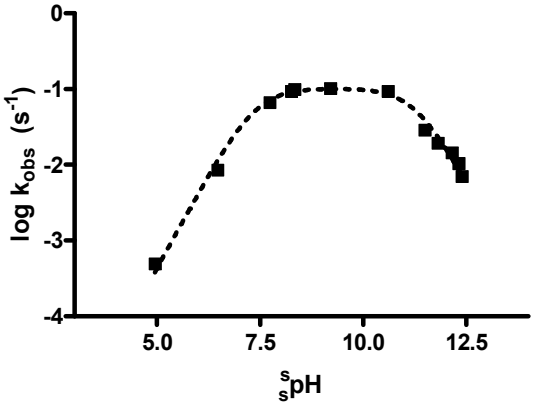

Figure 2-3. Plot of log k_{obs} vs ${}^{s}_{s}pH$ for the methanolysis of HPNPP (5 x 10^{-5} M) catalyzed by **2.6**:$Zn(II)_2$ (5 x 10^{-4} M). The best fit dashed line through the data points is calculated on the basis of equation 4 where ${}^{s}_{s}pK_a^{1} = 7.4 \pm 0.1$, ${}^{s}_{s}pK_a^{2} = 11.3 \pm 0.1$ and $k_{cat}^{max} = 0.10 \pm 0.01\ s^{-1}$.

2.4.2 – 2.7:Zn(II)$_2$ promoted cleavage of HPNPP.

As with **2.6**, the formation of a 2:1 complex between Zn(II) and ligand **2.7** was confirmed through a kinetic titration showing that the rate constant for cleavage of **2.2** (0.05mM) maximizes at [Zn(OTf)$_2$]/[**2.7**] = 2.0 at a constant [**2.7**] of 0.4 mM. This is consistent with ^{1}H NMR data which shows that upon addition of one equivalent of Zn(OTf)$_2$ to a 5 mM solution of **2.7**, a complex spectrum results which greatly simplifies on addition of a second equivalent of Zn(OTf)$_2$, indicative of a symmetric 2:1 complex.

Contrary to what was observed in studies with **2.6**:Zn(II)$_2$, the $^{s}_{s}$pH of solutions of **2.7**:Zn(II)$_2$ could not be held constant simply through addition of one equivalent of NaOCH$_3$, so the kinetic experiments with this complex were conducted under buffered conditions. The appearance of the plots of k_{obs} vs. [**2.7**:Zn(II)$_2$] for the cleavage of **2.2** (0.05mM) were $^{s}_{s}$pH-dependent with those determined between $^{s}_{s}$pH 6.5 and 11.5 exhibiting downward curvature suggestive of saturation binding, while those determined at $^{s}_{s}$pH > 12.0 were linear. The extent of buffer inhibition/catalysis was determined for all buffers by measuring the rate of cleavage of **2.2** at constant [**2.7**:Zn(II)$_2$] at varying [buffer] and where buffer inhibition was observed, plots of k_{obs} vs. [buffer]$_{total}$ were linear with a downward slope. The plots of k_{obs} vs. [**2.7**:Zn(II)$_2$] thus employed the rate constants that were extrapolated to zero buffer concentration. Second-order rate constants (k_2^{cat}) between $^{s}_{s}$pH = 6.5 and 11.5 were assigned as k_{cat}/K_m, the individual constants being obtained from fitting the k_{obs} vs. [**2.7**:Zn(II)$_2$] data to equation 3, while for experiments at $^{s}_{s}$pH > 12.0, the k_2^{cat} constants were taken as the gradients of the k_{obs} vs. [**2.7**:Zn(II)$_2$] plots. Kinetic constants (k_{cat} and K_m) and second-order rate constants are

summarized in Table 2-1. A plot of log k_2^{cat} vs. ${}^{s}_{s}pH$ for the cleavage of **2.2** catalyzed by **2.7**:Zn_2 is given in Figure 2-4, from which a kinetic ${}^{s}_{s}pK_a$ of 7.9 and k_2^{max} of 55.8 $M^{-1}s^{-1}$ are obtained by fitting the data in Table 2-1 to equation 5.

$$k_2^{cat} = \left(\frac{k_2^{max}\,{}^{s}_{s}K_a}{{}^{s}_{s}K_a + [H^+]} \right) \qquad (5)$$

Table 2-1. Kinetic constants (k_{cat} and K_m) and second-order rate constants for the cleavage of **2.2** (0.05 mM) catalyzed by **2.7**:$Zn(II)_2$ (0.075 – 0.75 mM) at T=25.0 ± 0.1˚C.[a]

Buffer	${}^{s}_{s}pH$	k_{cat} (s^{-1})	K_m (mM)	k_2^{cat} ($M^{-1}s^{-1}$)
2-picoline	6.50	(4.3 ± 0.2) x 10^{-5}	0.03 ± 0.01	1.4 ± 0.5
2,6-lutidine	7.30	(1.0 ± 0.01) x 10^{-4}	0.0055 ± 0.0008	18 ± 3
i-Pr-morpholine	8.80	(3.6 ± 0.2) x 10^{-3}	0.11 ± 0.04	32 ± 11
Triethylamine	11.04	0.078 ± 0.01	1.4 ± 0.3	56 ± 13
TMPP	12.02	[b]	[b]	51 ± 1
TMPP	12.33	[b]	[b]	81 ± 2

[a] Data corrected for buffer inhibition but not for triflate inhibition which is negligibly small.

[b] At these two ${}^{s}_{s}pH$ values, k_2^{cat} is determined as the gradient of the linear k_{obs} vs. [**2.7**:$Zn(II)_2$] plots.

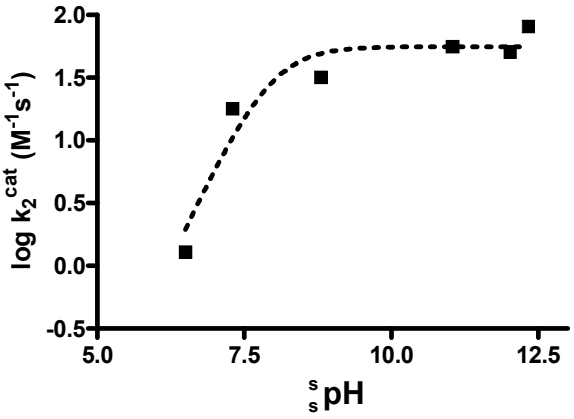

Figure 2-4. Plot of log k_2^{cat} vs $^{s}_{s}$pH for the cleavage of **2.2** (5 x 10^{-5} M) catalyzed by **2.7**:$Zn(II)_2$. The dashed line through the data points is calculated from the NLLSQ fit to equation 5 with $^{s}_{s}pK_a$ = 7.9 ± 0.2 and k_2^{cat} = 55.8 ± 12.9 $M^{-1}s^{-1}$.

2.4.3 – 2.8:$Zn(II)_2$ promoted cleavage of HPNPP.

Both the kinetic and ^{1}H NMR titration of ligand **2.8** with $Zn(OTf)_2$ confirm the formation of an active dinuclear **2.8:**$Zn(II)_2$ complex. A plot of observed rate constant for the cleavage of **2.2** versus the [$Zn(OTf)_2$]/[**2.8**] ratio at constant [**2.8**] maximizes at 2.0. Kinetic experiments with **2.8**:$Zn(II)_2$ were conducted under buffered conditions and at all $^{s}_{s}$pH values, plots of k_{obs} vs. [**2.8**:$Zn(II)_2$] for the cleavage of **2.2** were linear over the [catalyst] range employed. Buffer inhibition was examined by monitoring the rate of cleavage of **2.2** with constant [**2.8**:$Zn(II)_2$] at varying [buffer]. No significant inhibition was detected for 2,4,6-collidine or tetramethylpiperidine buffers, however the *i*-Pr-morpholine and triethylamine buffers exhibited weak inhibition. In the case of triethylamine the plot of k_{obs} vs. $[buffer]_{total}$ was linear with a downward slope from which a theoretical rate constant at zero buffer concentration was determined and used to correct the plot of k_{obs} vs. [**2.8**:$Zn(II)_2$]. With *i*-Pr-morpholine the k_{obs} vs. $[buffer]_{total}$ plot

exhibited downward curvature which, when fit to equation 1, gave an inhibition constant of K_i = 76.4 mM. The k_{obs} vs. [**2.8**:$Zn(II)_2$] plot was corrected for the buffer inhibition based on equation 2.

Second-order rate constants (Table 2-2) for the cleavage of **2.2** catalyzed by **2.8**:$Zn(II)_2$ were determined as the slope of the linear portions of the plots of k_{obs} vs. [**2.8**:$Zn(II)_2$]. Between ${}^{s}_{s}pH$ 7.8 and 8.3 these plots are upward curving which we attribute to dissociation of at least one metal ion from the dinuclear catalyst at low concentration giving a far less reactive or inactive mononuclear complex. Similar upward curvatures of the k_{obs} vs [catalyst] plots have been observed for the $Cd(II)_2$ complex of **2.1**[6c] and also for the $Zn(II)_2$ complex of **2.4**[15,16] and rationalized in terms of incomplete formation of the active dinuclear species at low concentrations. The plot of the log k_2^{cat} vs. ${}^{s}_{s}pH$ data from Table 2-2 is shown in Figure 2-5 which, when fit to equation 5, gave a kinetic ${}^{s}_{s}pK_a$ of 9.65 and k_2^{max} of 7.6 $M^{-1}s^{-1}$.

Table 2-2. Second-order rate constants for the cleavage of 0.05 mM **2.2** catalyzed by **2.8**:$Zn(II)_2$ (0.075 – 0.75 mM) at T = 25.0 ± 0.1 ˚C.[a]

Buffer	${}^{s}_{s}pH$	k_2^{cat} ($M^{-1}s^{-1}$)
2,4,6-collidine	7.8	0.08 ± 0.003
i-Pr-morpholine	8.3	0.4 ± 0.03
i-Pr-morpholine	8.8	1.1 ± 0.1
i-Pr-morpholine	9.3	2.7 ± 0.1
triethylamine	10.8	7.3 ± 0.1
TMPP	11.9	7.1 ± 0.2

[a] Data are corrected for buffer effects by extrapolating to zero [buffer], but are not corrected for triflate ion inhibition which is negligibly small.

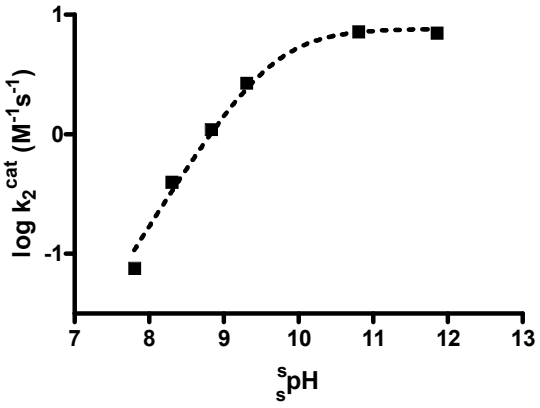

Figure 2-5. Plot of log k_2^{cat} vs $^{s}_{s}$pH for the methanolysis of 0.05 mM **2.2** catalyzed by **2.8**:$Zn(II)_2$. The dashed line through the data points is calculated from the fit of the data to eq. (3) which gives a $^{s}_{s}pK_a$ of 9.65 ± 0.09 and $k_2^{max} = 7.6 \pm 1.1$ $M^{-1}s^{-1}$.

2.5 – Discussion

To assess the consequences of a bridging oxyanion group in the linker we compared two sets of **L**:$Zn(II)_2$ systems by investigating their catalysis of the cleavage of **2.2**. The presence of this linker reduces the net positive charge of the dinuclear core by one unit such that one might anticipate a detrimental effect on catalysis of the cyclization of **2.2** *via* a pathway where the dianionic phosphate formed from deprotonation of the cyclizing 2-hydroxypropyl group and its dianionic transition state for cleavage as in Scheme 2-1. Nevertheless, the presence of such a linker seems to be a requirement to form active complexes in water where its presence acts as an electrostatic buffer to reduce the Zn(II)---Zn(II) repulsion. It has been stated[12a], on the basis of analysis of the activities of several systems[6b,12b,2], that "for Zn(II) complexes, a bridging linker is a necessity for cooperative catalysis. Zn(II) complexes that lack this linker are barely more active than their mononuclear analogs." Among the most effective linkers in this regard are the

calixarenes[2c] and 2-propoxy ones.[2a,4,6] While such linker systems with bridging anions that bind to both metal ions may well be beneficial in water, the summary of the kinetic data in Table 2-3 that compares the activities of **2.4**:$Zn(II)_2$ with **2.8**:$Zn(II)_2$ and **2.6**:$Zn(II)_2$ with **2.7**:$Zn(II)_2$ in methanol show that, in less polar solvents that more closely resemble the effective dielectric constants of the interiors of enzymes,[27] the presence of bridging oxyanion groups is detrimental to activity. It is also notable in the present case that, while many of the studies of dinuclear Zn(II) catalysts report on the *hydrolysis* of RNA analogues in water, the reactions monitored and their immediate products are not hydrolytic ones, but ones that result from intramolecular transesterifications as in Scheme 2-1 where the solvent nature, being water or alcohol, is not pertinent to the observed cleavage.

Table 2-3. Constants for the various catalysts used to calculate the $\Delta\Delta G^{\ddagger}_{stab}$ for **L**:$Zn(II)_2$ binding to the transition state of the presumed methoxide reaction for cyclization of **2.2**.

Catalyst	${}^{s}_{s}pK^{1}_{a}$	${}^{s}_{s}K^{1}_{a} / K_{auto}$ [a]	k_2^{-OMe} [b] ($M^{-1}s^{-1}$)	$k_2^{\mathbf{L}:Zn2:(-OMe)}$ ($M^{-1}s^{-1}$)	$\Delta\Delta G^{\ddagger}_{stab}$ [e] (kcal/mol)
2.4:$Zn(II)_2$:($^{-}OCH_3$)	9.3	2.95×10^{7}	2.6×10^{-3}	275,000 [c]	-21.1
2.8:$Zn(II)_2$:($^{-}OCH_3$)	9.65	1.17×10^{7}	2.6×10^{-3}	7.6[d]	-14.3
2.6:$Zn(II)_2$:($^{-}OCH_3$)	7.4	2.34×10^{9}	2.6×10^{-3}	9.1×10^{3} [d]	-21.7
2.7:$Zn(II)_2$:($^{-}OCH_3$)	7.9	7.41×10^{8}	2.6×10^{-3}	55.8 [d]	-18.0

[a] Determined from the kinetic or titrimetric ${}^{s}_{s}pK^{1}_{a}$ value for the complex and the autoprotolysis constant of methanol ($10^{-16.77}$ M^2).
[b] From ref. 28.
[c] From ref. 15.
[d] This work.
[e] Computed from equation 6 at standard state of 1 M.

2.5.1 - Comparison of the rates of cleavage of HPNPP promoted by 2.6:Zn(II)$_2$:($^-$OCH$_3$) and 2.7:Zn(II)$_2$:($^-$OCH$_3$)

The ${}^{s}_{s}pH$-rate profiles presented in Figures 2-3 and 2-4 indicate that the active catalysts in both systems are generated by ionizations having respective kinetic ${}^{s}_{s}pK_a$ values of 7.4 and 7.9 that result from the deprotonation of bound methanol to form a methoxide coordinated to one or both metal ions. For the two systems that contain the oxyanion linker (**2.7**:Zn(II)$_2$ and **2.8**:Zn(II)$_2$) the ionization of the oxyanion linker is not observed in any of our kinetic studies, but the associated ${}^{s}_{s}pK_a$ values should be lower than 7 by analogy with other systems investigated in water where the pK_a for ionization of the linker is lower than any ionization stemming from a metal-bound HOH.[6] The kinetic ${}^{s}_{s}pK^{1}_{a}$ determined for **2.6**:Zn(II)$_2$ is close to the titrimetric ${}^{s}_{s}pK_a$ of 7.02 found for the complex when bound to a non-reactive diphenyl phosphate anion which supports the assertion that the kinetically active form is a ternary complex between the Zn(II)$_2$ complex and bound substrate **2.2** or its kinetic equivalent **2.2**$^-$ (where the 2-hydroxypropyl group is deprotonated).

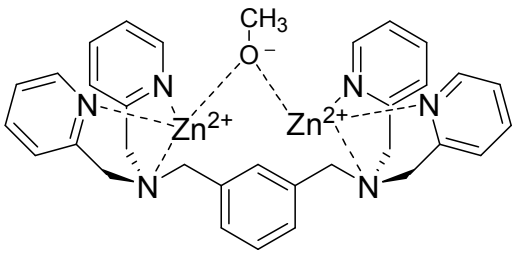

2.6: Zn$_2$:($^-$OCH$_3$)

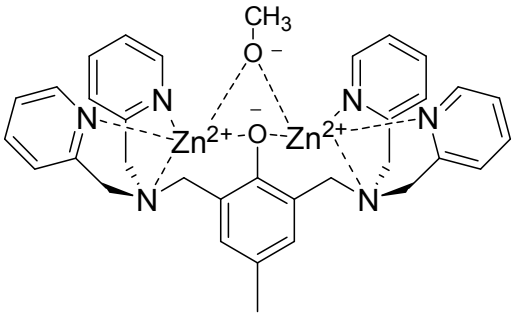

2.7: Zn$_2$:($^-$OCH$_3$)

Importantly, the potentiometric titration of **2.7**:$Zn(II)_2$ in the presence of equimolar diphenyl phosphate (Na^+ form) shows a well-defined ionization with a ${}^{s}_{s}pK_a$ of less than 4 which we attribute to the bridging phenoxy group. Unfortunately, the same potentiometric titrations of **2.7**:$Zn(II)_2$ along with equimolar diphenyl phosphate do not give information concerning the ${}^{s}_{s}pK_a$ values for Zn(II)-bound methanols because of the apparent displacement of phosphate from the complex that occurs at increasing [methoxide], likely as a result of the weaker binding between the phosphate and catalyst complex (which already has a bridging aryloxy anion present so that the net positive charge is reduced by one unit relative to the situation with **2.6**:$Zn(II)_2$). This interpretation is consistent with results of kinetic experiments showing that binding between substrate and **2.7**:$Zn(II)_2$ became weaker as ${}^{s}_{s}pH$ increased, as evidenced by the progression from saturation kinetics to linear kinetics at higher ${}^{s}_{s}pH$. For convenience, we represent the active forms of **2.6**:$Zn(II)_2$:($^{-}OCH_3$) and **2.7**:$Zn(II)_2$:($^{-}OCH_3$) as having bridging methoxides, although it is possible that this is only bound to one of the Zn(II) ions in **2.7**:$Zn(II)_2$:($^{-}OCH_3$).

Compared to the methoxide promoted reaction with $k_2^{OMe} = 2.6 \times 10^{-3}$ $M^{-1}s^{-1}$,[28] both **2.6**:$Zn(II)_2$:($^{-}OCH_3$) and **2.7**:$Zn(II)_2$:($^{-}OCH_3$) give significant rate accelerations for cleavage of **2.2**. At ${}^{s}_{s}pH = 9.1$, the centre of the bell-shaped pH-rate profile of Figure 2-3, the observed rate constant of $k_{cat}^{max} = 0.10$ s^{-1} for the **2.6**:$Zn(II)_2$:($^{-}OCH_3$)-catalyzed reaction is 1.7×10^9 greater than what is computed for the methoxide reaction at that ${}^{s}_{s}pH$. In terms of its apparent second-order rate constant, $k_{cat}^{max}/K_m = k_2^{cat} = 0.1$ $s^{-1}/1.1 \times$

10^{-5} M = 9100 $M^{-1}s^{-1}$, **2.6**:$Zn(II)_2$:($^{-}OCH_3$) is 5.2 x 10^6 more effective than methoxide. Similarly, above $^{s}_{s}pH$ = 8.8 where **2.7**:$Zn(II)_2$:($^{-}OCH_3$) is fully formed, its k_2^{cat} of 55.8 $M^{-1}s^{-1}$ is ~21,000 times larger than that of methoxide but ~160 times less reactive than **2.6**:$Zn(II)_2$:($^{-}OCH_3$) due to the presence of the bridging oxyanion.

2.5.2 - Comparison of the cleavage of HPNPP promoted by and 2.4:$Zn(II)_2$:($^{-}OCH_3$) and 2.8:$Zn(II)_2$:($^{-}OCH_3$)

NLLSQ fitting of the $^{s}_{s}pH$-rate constant data shown in Figure 2-5 for the **2.8**:$Zn(II)_2$ promoted cleavage of **2.2** to equation 5 gives a kinetic $^{s}_{s}pK_a$ of 9.65 and a k_2^{max} = 7.6 $M^{-1}s^{-1}$. Furthermore, a plot of k_{obs} vs added methoxide (not shown) indicates that maximal catalytic activity is attained at a methoxide/$Zn(II)_2$ ratio of 1.0 with a sharp drop in rate constant when the ratio is <1.0. Taken together, these data indicate that two methoxides per catalyst are required for activity: one to generate the bridging propoxy anion which is fully bound to the two metal ions below $^{s}_{s}pH$ 7 as a structural component, and a second added to the complex as $^{-}OCH_3$ or as a kinetic equivalent such as a deprotonated 2-oxypropyl substrate (**2.2**$^{-}$). Since none of the plots of k_{obs} vs. [**2.8**:$Zn(II)_2$] reveals evidence of saturation substrate binding at any $^{s}_{s}pH$, the k_2 values reported in Table 2-2 are simply given as the gradients of the lines.

Our previous[15,16] and more recent[29] work with **2.4**:$Zn(II)_2$ and 2-hydroxypropyl aryl phosphates (including **2.2**) gave kinetic values of $^{s}_{s}pK_a^1$ = 9.3 and $^{s}_{s}pK_a^2$ = 11.2. While the cleavage of 2-hydroxypropyl aryl phosphates having poor leaving groups gave saturation kinetic profiles, that with **2.2**, having a good *p*-nitrophenoxy leaving group,

was linear with a gradient of k_2 = 275,000 $M^{-1}s^{-1}$ which is about 10^8 larger than the k_2^{OMe} value for the methoxide reaction.[16] Mechanistic investigations led to the proposal that the catalyzed reaction follows a multi-step pathway consistent with a minimal process given in Scheme 2-1 with a bimolecular binding step of catalyst plus phosphate, followed by intramolecular rearrangement to form a catalytically competent complex where the phosphate is activated by binding to two metal ions. This is followed by one or more chemical steps that produce the observed phenol leaving group and the cyclic 5-membered phosphate. For catalyzed cleavage of substrates with good leaving groups like *p*-nitrophenoxy, the k_{cat} term in Scheme 2-1 is larger than k_{-2} so the rate limiting step is formation of the activated phosphate complex which leads to the linear form of the k_{obs} vs [catalyst] plot. With substrates having poor leaving groups, the k_{cat} term in Scheme 2-1 is smaller than k_{-2}, so saturation behaviour is observed.

The linear appearance of the k_{obs} vs. [**2.8**:$Zn(II)_2$] plots with **2.8**:$Zn(II)_2$:($^-OCH_3$) may involve a similar sort of two step binding process, although a more likely explanation is that the substrate binding is simply weaker due to the fact that the net positive charge on **2.8**:$Zn(II)_2$ is less than that on **2.4**:$Zn(II)_2$ or because the coordination number of the metal ions is higher in **2.8**:$Zn(II)_2$. In terms of k_2^{cat} values presented in Table 2-3, the activity of **2.8**:$Zn(II)_2$:($^-OCH_3$) is 37,000 times less than that of **2.4**:$Zn(II)_2$:($^-OCH_3$).

2.5.3 - Energetics calculations

Analysis of the energetic factors which govern the catalysis by the $Zn(II)_2$ complexes of **2.4**, and **2.6-2.8** compares the free energy of binding of the catalyst to the transition state

of the presumed lyoxide-promoted reaction.[30,31,32,6d] In Scheme 2-4 is a thermodynamic cycle that allows a quantitative assessment of the ΔG for binding the catalyst to a hypothetical TS involving methoxide plus substrate (or its kinetic equivalent of a TS involving the 2-oxypropyl aryl phosphate dianion). The $\Delta\Delta G^{\ddagger}_{stab}$ for this is given in equation 6 where ΔG_{Bind} is the free energy of binding $^{-}OCH_3$ to **L**:Zn(II)$_2$ (mathematically equivalent to the first ionization constant of the **L**:Zn(II)$_2$ complex divided by the $K_{autoprotolysis}$ of methanol ($10^{-16.77}$)), $\Delta G^{\ddagger}_{cat}{}^{\mathbf{L}:Zn(II)2:(-OMe)}$ and $\Delta G^{\ddagger}_{Non}$ are the activation free energies of the catalyzed and methoxide reactions calculable from their second-order rate constants give in Table 2-3. The units of the term in square brackets in equation 6 are M^{-1} signifying that this is formally an association constant of the catalyst and the TS.[30,31]

Scheme 2-4. Thermodynamic cycle comparing **L**:Zn(II)$_2$:($^{-}OCH_3$) and $^{-}OCH_3$ promoted cyclization reactions of **2.2**.

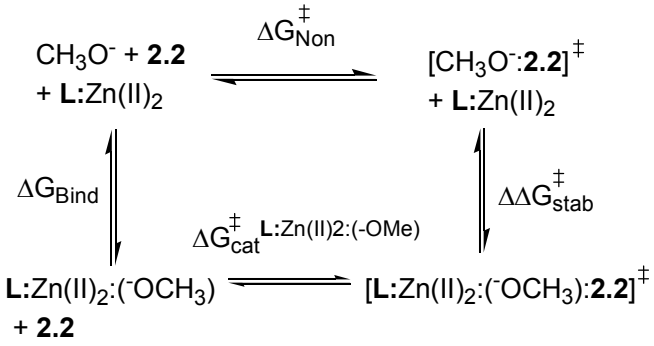

$$\Delta\Delta G^{\neq}_{stab} = (\Delta G_{Bind} + \Delta G_{cat}{}^{L:Zn(II)_2:(-OMe)}) - \Delta G^{\neq}_{Non} = -RT\ln\left[\frac{(k_2^{cat})(K_a / K_{auto})}{k_2^{-OMe}}\right] \quad (6)$$

Given in Table 2-3 are values for the various rate and equilibrium constants used for the calculations of the $\Delta\Delta G^{\ddagger}_{stab}$ at standard state. The data clearly indicate that free energy for

binding of the catalyst to the transition state consisting of CH_3O^- + **2.2**, or its kinetic equivalent of **2.2**$^-$, is more negative for the complexes without the bridging oxyanions. The origins of the effect can be gleaned from the graphical representations given in Figures 2-6 and 2-7 of the ΔG values of the three main components (ΔG_{Bind}, $\Delta G^{\ddagger}_{cat}$ $^{\mathbf{L}:Zn(II)2:(-OMe)}$ and $\Delta G^{\ddagger}_{Non}$) contributing to the $\Delta\Delta G^{\ddagger}_{stab}$ in eq. (6).

Figure 2-6 shows that binding of **2.6**:$Zn(II)_2$ or **2.7**:$Zn(II)_2$ with $^-OCH_3$ is exergonic by 12.8 and 12.2 kcal/mol respectively, and that the $\Delta G^{\ddagger}$ for the reaction of **L**:$Zn(II)_2$:($^-OCH_3$) with **2.2**[33] is endergonic by 12.1 and 15.1 kcal/mol respectively. Thus, while the affinity of each complex for methoxide is nearly the same because the $^{s}_{s}pK^{1}_{a}$ values are close, the activation energies are quite different with **2.7**:$Zn(II)_2$:($^-OCH_3$) being about 3 kcal/mol larger probably due to the fact that the apparent binding constant of **2.2** with the catalyst is smaller for the form having the oxyanion bridge. The $\Delta G^{\ddagger}$ for the methoxide reaction in all cases is computed to be 21.0 kcal/mol. Values of $\Delta\Delta G^{\ddagger}$ = 21.7 and 18.0 kcal/mol are calculated for the transition state stabilization afforded by **2.6**:$Zn(II)_2$ and **2.7**:$Zn(II)_2$.

Figure 2-7 shows analogous free energy plot for the process involving **2.4**:$Zn(II)_2$ and **2.8**:$Zn(II)_2$. Once again, the binding of methoxide to each complex is about the same at 10.0 and 9.7 kcal/mol respectively meaning that the presence of the oxyanion linker does not greatly perturb the $^{s}_{s}pK^{1}_{a}$. However the $\Delta G^{\ddagger}$ values for the k_2^{cat} for the catalyzed reactions are quite different at 10 and 16.2 kcal/ mol, with the complex with the bridging alkoxy group (**2.8**:$Zn(II)_2$:($^-OCH_3$)) being larger.

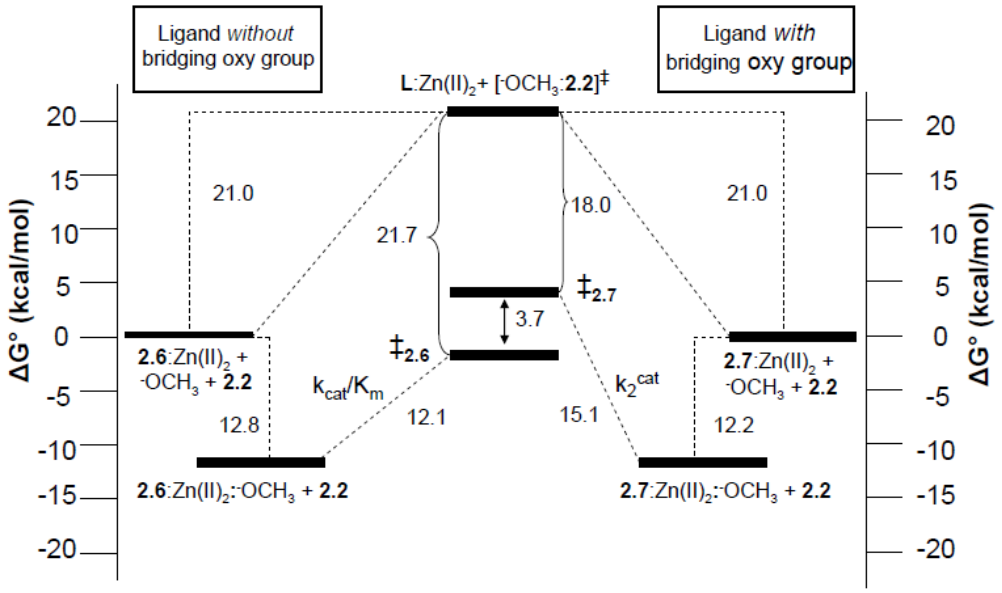

Figure 2-6. A free energy diagram comparing the reactions of CH_3O^-, **2.6**:$Zn(II)_2$:($^-OCH_3$) and **2.7**:$Zn(II)_2$:($^-OCH_3$) with **2.2** at standard state of 1.0 M and T=25 ^oC showing the computed ΔG values for CH_3O^- binding to **L**:$Zn(II)_2$ and the $\Delta G^‡$ for k_{cat}/K_m, k_2^{cat} and k_2^{-OMe} derived from the experimental rate and equilibrium constants.

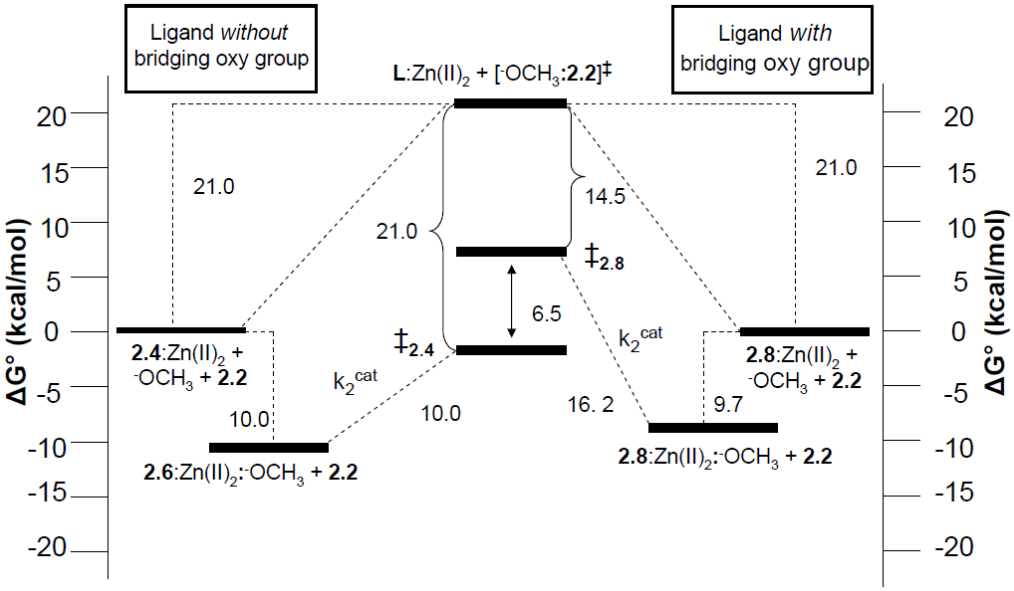

Figure 2-7. A free energy diagram comparing the reactions of CH_3O^-, **2.4**:$Zn(II)_2$:($^-OCH_3$) and **2.8**:$Zn(II)_2$:($^-OCH_3$) with **2.2** at standard state of 1.0 M and T=25 ^oC showing the computed ΔG values for CH_3O^- binding to **L**:$Zn(II)_2$ and the $\Delta G^‡$ for k_2^{cat} and k_2^{-OMe} derived from the experimental rate and equilibrium constants.

The representations in Figures 2-6 and 2-7 indicate that poorer catalysis for the oxyanion containing complexes originates in their smaller second-order rate constants (k_2^{cat} or k_{cat}/K_m values). These constants are made up of a pre-equilibrium binding of the substrate and catalyst, as well as the kinetic term for the intramolecular cleavage. The oxyanion could disfavour either or both of these by decreasing the Lewis acidity of the $Zn(II)_2$ complex due to reducing the net positive charge by one unit, thereby reducing the substrate binding. In addition, since strong electrostatic interactions are an important catalytic feature of reactions between positively charged catalysts and negatively charged substrates, any decrease in the net positive charge of the catalyst should reduce the electrostatic charge neutralization in the transition state and raise the activation energy of the chemical transformations. Finally, the bridging oxyanion occupies a coordination site on each Zn(II) ion, leaving fewer coordination sites available for binding of the substrate in the Michaelis complex and transition state.

2.6 – Conclusions

The observation that a bridging group such as an oxyanion is an essential component of the ligand to engender cooperativity in dinuclear catalysts in water dictates the design of the majority of the newer synthetic metallonucleases that have been investigated under aqueous conditions. It is generally observed that dinucleating ligands without such bridging groups cannot form dinuclear catalysts with activities much greater than the sum of their parts,[2,12] and in many, if not most, cases they are unable to form dinuclear complexes at all unless there is an electrostatic buffer that insulates the charge repulsion of the two metal ions and fixes them in place through binding. Thus, in aqueous solution

it has been a difficult task to investigate how such a linker influences the kinetics of cleavage of phosphates in comparison with systems that lack a bridging oxyanion group. The medium effect afforded by the light alcohols such as methanol and ethanol allows us to directly examine the effect of an anionic linker on the catalytic activity by comparing two sets of dinuclear Zn(II) complexes. The data clearly indicate that the inclusion of the propoxide and phenoxide in **2.8**:$Zn(II)_2$ and **2.7**:$Zn(II)_2$ makes them inferior in terms of rate acceleration when compared to the analogous complexes lacking the oxyanion bridge (**2.4**:$Zn(II)_2$ and **2.6**:$Zn(II)_2$). The presence of the phenoxide of **2.7**:$Zn(II)_2$ leads to a 3.7 kcal/mol loss in transition state stabilization compared to **2.6**:$Zn(II)_2$ which is manifested in a 160-fold decrease in k_2^{cat} for the cleavage of **2.2**. The substitution of the propoxy group for the propyl linker of **2.4**:$Zn(II)_2$ to produce **2.8**:$Zn(II)_2$ leads to a 3.7 x 10^4-fold drop in k_2^{cat} that results from a 6.5 kcal/mol decrease in transition state stabilization. The kinetic analysis described here demonstrates that the inclusion of a bridging oxyanion between the metal centers in a dinuclear complex is not only unnecessary for catalyzed cleavage of **2.2** in methanol, but in fact quite counterproductive in terms of rate. It seems likely that the requirement for an anionic bridging group for these sorts of dinuclear catalysts in water is a necessary, but not optimal, compromise to ameliorate unfavourable electrostatic interactions and heavier solvation of the metal ions leading to poorer binding with the ligand and poorer catalysis.

2.7 - Chapter 2 postscript

As discussed in section 2.5.2, the appearance of linear kinetics for the methanolysis of **2.2** catalyzed by **2.8**:$Zn(II)_2$ could be the result of the two-step process in Scheme 2-1 (where

$k_{-2} < k_{cat}$) or due to poor binding of the substrate. Following publication of this work, we were interested to further explore these possibilities. In the case of **2.4**:$Zn(II)_2$, the k_{cat} term in Scheme 2-1 is larger than k_{-2} so the rate limiting step is formation of the activated phosphate complex which leads to the linear form of the k_{obs} vs [catalyst] plot. In addition to the compromised Lewis acidity and higher coordination number, we wondered if the dramatic drop in activity upon introduction of the oxyanion bridge in **2.8**:$Zn(II)_2$ may be the result of the anion impeding the rearrangement step. To test this hypothesis, we first examined the inhibition of the methanolysis of **2.2** by the non-reactive phosphate diester dibenzyl phosphate. We reasoned that if we observed inhibition due to binding of the inhibitor, then the linear form of the kinetics for **2.8**:$Zn(II)_2$ could not be due to poor substrate binding. Mr. Scott Strum, an undergraduate student working under my direct supervision performed the inhibition experiment. Figure 2-8 shows the plot of k_{obs} for the methanolysis of **2.2** catalyzed by constant [**2.8**:$Zn(II)_2$] = 0.75mM vs. [dibenzyl phosphate] in methanol buffered at ${}^{s}_{s}pH$ = 11.9 (TMPP buffer). The inhibition data were fit to equation 1 to obtain an inhibition constant of $K_i = (1.4 \pm 0.4) \times 10^{-3}$ M.

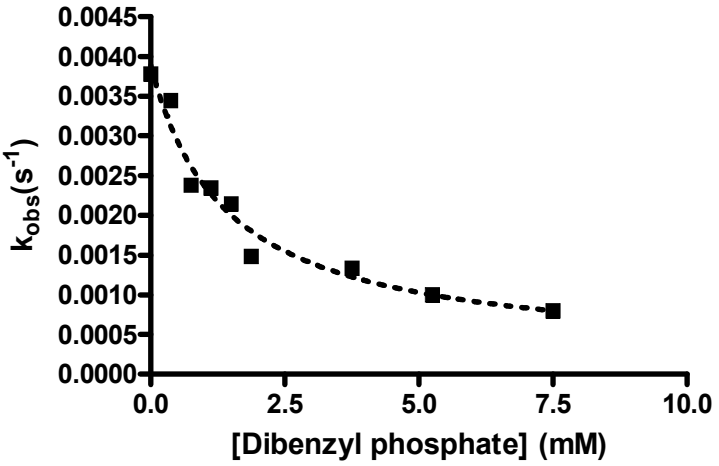

Figure 2-8. Plot of k_{obs} for the methanolysis of **2.2** (5 x 10^{-5} M) catalyzed by constant [**2.8**:$Zn(II)_2$] = 0.75mM vs. [dibenzyl phosphate] in methanol buffered at ${}^{s}_{s}pH$ = 11.9 (TMPP buffer), T = 25 °C.

Given that our kinetic studies with **2.8**:$Zn(II)_2$ were conducted in the concentration range of 0.1 mM < [**2.8**:$Zn(II)_2$] < 0.75 mM, the relatively weak inhibition constant determined for dibenzyl phosphate means that under these conditions we would not have reached concentrations where saturation binding would be evident. We therefore determined to expand the concentration range over which we studied **2.8**:$Zn(II)_2$. The plot of k_{obs} vs. [**2.8**:$Zn(II)_2$] for the methanolysis of **2.2** in methanol buffered at ${}^{s}_{s}pH$ = 8.6 is shown in Figure 2-9 (experiments performed by Mr. Scott Strum under my supervision). Figure 2-9 demonstrates that at high concentrations of catalyst (> 1.5 mM), there is evidence for saturation binding with substrate **2.2**. Fitting of the kinetic data to equation 3 gave kinetic parameters of k_{cat} = (7.7 ± 1.2) x 10^{-4} s^{-1} and K_m = (2.4 ± 0.9) x 10^{-3} M. The data are not corrected for buffer inhibition, but this is not expected to change the shape of the graph or the magnitude of the binding constant.

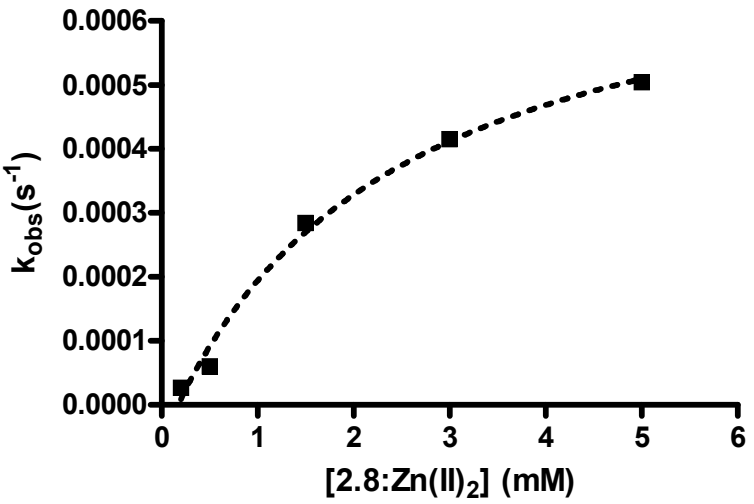

Figure 2-9. Plot of k_{obs} vs [**2.8**:Zn(II)$_2$] for cleavage of HPNPP (**2.2**) (5 x 10^{-5} M) in methanol buffered at ${}^{s}_{s}$pH = 8.6 and T=25 °C.

The substrate binding constant determined in this way coincides well with the binding constant determined for inhibition by dibenzyl phosphate (K_i = (1.4 ± 0.4) x 10^{-3} M). It should be noted that the inhibition experiment in Figure 2-8 were conducted at ${}^{s}_{s}$pH = 11.9 while the experiments in Figure 2-9 were at ${}^{s}_{s}$pH = 8.6. We were unable to explore high concentrations of **2.8**:Zn(II)$_2$ at high ${}^{s}_{s}$pH due to insolubility of the catalyst above [**2.8**:Zn(II)$_2$] = 2.0 mM.

These additional experiments have demonstrated that the linear kinetics that we observed originally were the result of working in a limited concentration range. The observation of saturation kinetics implies that for **2.8**:Zn(II)$_2$ the k_{cat} step of Scheme 2-1 is rate limiting. Given that **2.4**:Zn(II)$_2$ exhibited linear kinetics for the methanolysis of **2.2** (where k_2 in Scheme 2-1 is rate limiting), the inclusion of the oxy anion bridge in **2.8**:Zn(II)$_2$ appears to have the overall effect of reducing k_{cat} relative to k_{-2}. This is consistent with our

original proposal that the effect of the oxy anion is to reduce the Lewis acidity and compromise the catalyst's ability to stabilize the negative charge build-up in the transition state.

2.7 - References and notes

1) Schroeder, G. K.; Lad, C.; Wyman, P.; Williams, N. H.; Wolfenden, R. *Proc. Nat. Acad. Sci. U.S.A.* **2006**, *103*, 4052.

2) For a representative list of references on various metal containing complexes, see: a) Mancin, F.; Tecillia, P. *New J. Chem.* **2007**, *31*, 800. b) Weston, J. *Chem. Rev.* **2005**, *105*, 2151. c) Molenveld, P.; Engbertsen, J. F. J.; Reinhoudt, D. N. *Chem. Soc. Rev.* **2000**, *29*, 75. d) Williams,N. H.; Takasaki, B.; Wall, M.; Chin, J. *Acc. Chem. Res.* **1999**, *32*,485. e) Mancin, F.; Scrimin, P.; Tecilla, P.; Tonellato, U. *Chem. Commun.* **2006**, 2540. f) Morrow, J. R.; Iranzo, O. *Curr. Opin. Chem.Biol.* **2004**, *8*, 192.

3) a) Yamada, K.; Takahashi, Y.-i.; Yamamura, H.; Araki, A.; Saito, K.; Kawai, M. *Chem. Commun.* **2000**, 1315. b) Subat, M.; Woinaroschy, K.; Gerstl, C.; Sarkar, B.; Kaim, W.; König, B. *Inorg. Chem.* **2008**, *47*, 4661.

4) a) Feng, G.; Mareque-Rivas, J. C.; Williams, N. H. *Chem. Commun.* **2006**, 1845; b) Feng, G.; Natale, D.; Prabaharan, R.; Mareque-Rivas, J. C.; Williams, N. H. *Angew. Chem. Int. Ed.* **2006**, *45*, 7056.

5) Mancin, F.; Rampazzo, E; Tecilla, P.; Tonellato, U. *Chem. Eur. J.* **2004,** 281.

6) a) Yang, M.-Y.; Iranzo, O.; Richard, J. P.; Morrow, J. R. *J. Am. Chem. Soc.* **2005,** *127*, 1064. b) Iranzo, O.; Elmer, T.; Richard, J. P.; Morrow, J. R. *Inorg. Chem.* **2003**, *42,*

7737. c) Iranzo, O.; Richard, J. P.; Morrow, J. R. *Inorg. Chem.* **2004**, *43,* 1743. d) Iranzo, O.; Kovalevsky, A. Y.; Morrow, J. R.; Richard, J. P. *J. Am. Chem. Soc.* **2003**, *125*, 1988.

7) Linjalahti, H.; Feng, G.; Mareque-Rivas, J. C.; Mikkola, S.; Williams N. H. *J. Am. Chem. Soc*. **2008**, *130***,** 4232.

8) Humphrey, T.; Iyer, S.; Iranzo, O.; Morrow, J. R.; Richard, J. P; Paneth, P.; Hengge, A. C. *J. Am. Chem. Soc.* **2008**, *130*, 17858.

9) Bauer-Sienbenlist, B.; Meyer, F.; Farkas, E.; Vidovic, D.; Cuesta-Seijo, J. A.; Herbst-Irmer, R.; Pritzkow, H. *Inorg. Chem.* **2004**, *43*, 4189.

10) Arca, M.; Bencini, A.; Berni, E.; Caltagiirone, C.; Devillanova, F. A.; Isaia, F.; Garau, A.; Giorgi, C.; Lippolis, V.; Perra, A.; Tei, L.; Valtancoli, B. *Inorg. Chem.* **2003**, *42,* 6929.

11) Gadja, T.; Krämer, R.; Jancsó, A. *Eur. J. Inorg. Chem.* **2000**, 1635.

12) a) Morrow, J. *Comments on Inorganic Chemistry.* **2008**, *29*, 169. b) Koike, T.; Inoue, M.; Kimura, E.; Shiro, M. J. Am. Chem. Soc. **1996**, *118*, 3091.

13) a) McCue, K.P.; Morrow, J.R. *Inorg. Chem*. **1999**, *38*, 6136. b) DasGupta, B.; Haidar, R.; Hsieh, W.-Y.; Zompa, L.J. *Inorg. Chim. Acta.* **2000**, *306*, 78.

14) Brown, R. S.; Lu, Z.-L. Liu, C. T.; Tsang, W. Y.; Edwards, D. R.; Neverov, A. A. *J. Phys. Org. Chem.* **2009**, *23*, 1.

15) Neverov, A. A.; Lu, Z.-L.; Maxwell, C. I.; Mohamed, M. F.; White, C. J.; Tsang, J. S. W.; Brown, R. S. *J. Am. Chem. Soc.* **2006**, *128*, 16398.

16) Bunn, S. E.; Liu, C. T.; Lu, Z.-L.;Neverov, A. A.; Brown, R. S. *J. Am. Chem. Soc.* **2007**, *129*, 16238.

17) Liu, C. T.; Neverov, A. A.; Brown, R. S. *J. Am. Chem. Soc.* **2008**, *130*, 16711.

18) Kim, J.; Lim, H. *Bull. Korean Chem. Soc.* **1999**, 20, 491.

19) Gultneh, Y.; Ahvazi, B.; Khan, A.R.; Butcher, R.J.; Tuchagues, J.P. *Inorg. Chem.* **1995**, 34, 3633.

20) Borovik, A.S.; Papaefthymiou, V.; Taylor, L.F.; Anderson, O.P.; Que, L., Jr. *J. Am. Chem. Soc.* **1989**, *111*, 6183.

21) Weisman, G. R.; Vachon, D. J.; Johnson, V. B..; Gronbeck, D. A. *J. Chem. Soc. Chem. Commun.* **1987,** 886.

22) Kim, Y.; Han, S.; Jang, y.; Kim, J. *X-ray Structure Analysis Online* **2005**, *21*, 201.

23) Alder, R.W.; Mowlam, R.W.; Vachon, D.J.; Weisman, G.R. *J. Chem. Soc. Chem. Commun.* **1992**, 507.

24) a.) Gibson, G.; Neverov, A. A.; Brown, R. S. *Can. J. Chem*. **2003**, *81*,495. b) For the designation of pH in non-aqueous solvents we use the nomenclature recommended by the IUPAC, *Compendium of Analytical Nomenclature. Definitive Rules 1997* 3rd ed., Blackwell, Oxford, U. K. 1998. The pH meter reading for an aqueous solution determined with an electrode calibrated with aqueous buffers is designated as ${}^{w}_{w}\mathrm{pH}$; if the electrode is calibrated in water and the 'pH' of the neat buffered methanol solution then measured, the term ${}^{s}_{w}\mathrm{pH}$ is used; and if the electrode is calibrated in the same solvent and the 'pH' reading is made, then the term ${}^{s}_{s}\mathrm{pH}$ is used. In methanol ${}^{s}_{w}\mathrm{pH}$ -(-2.24) = ${}^{s}_{s}\mathrm{pH}$, and since the autoprotolysis constant of methanol is $10^{-16.77}$, neutral ${}^{s}_{s}\mathrm{pH}$ is 8.4.

25) Eq. (3) was obtained from the equations for equilibrium binding and for conservation of mass by using the commercially available MAPLE software, *Maple 9.00*, June 13,

2003, Build ID 13164, Maplesoft, a division of Waterloo Maple Inc. 1981-2003, Waterloo, Ontario, Canada.

26) Gans, P.; Sabatini, A.; Vacca, A. *Talanta* **1996**, *43*, 1739.

27) a) Richard, J. P.; Ames, T. L. *Bioorg. Chem.* **2004**, *32*, 354. b) Cleland, W. W.; Frey, P. A.; Gerlt, J. A. *J. Biol. Chem.* **1998**, *273*,25529. c) Czerwinski, R. M.; Harris, T. K.; Massiah, M. A.; Mildvan, A.S.; Whitman, C. P. *Biochemistry* **2001**, *40*, 1984. d) Plow, F.; Kowlessur,D. Malthouse, J. P. G.; Mellor, G. W.; Hartshorn, M. J.; Pinitglang, H. P.;Topham, C. M.; Thomas, E. W.; Verma, C.; Brocklehurst, K. *J. Mol. Biol.* **1996**, *257*, 1088. e) Cachau, R. E.; Garcia-Moreno, E. B. *J. Mol. Biol.***1996**, *255*, 340. f) Kanski, R.; Murray, C. J. *Tetrahedron Lett.* **1993**, 2263.

28) Tsang, J. S.; Neverov, A. A.; Brown, R. S. *J. Am. Chem. Soc.* **2003**, *125*, 1559.

29) R. S. Brown and C. T. Liu, unpublished results. By way of comparison, the first $^{s}_{s}pK_a$ for formation of **2.4**:$Zn(II)_2$:($^{-}OCH_3$) determined by half-neutralization, is 9.41 (ref. 16).

30) Wolfenden, R. *Nature*, **1969**, *223*, 704.

31) For applications of this energetic treatment to phosphate cleavage and other reactions see Yatsimirsky, A. K. *Coord. Chem. Rev*. **2005**, *249*, 1997 and references therein.

32) Yang, M.-Y.; Morrow, J. R.; Richard, J. P. *Bioorg. Chem.* **2007**, *35*, 366.

33) $\Delta G^{\ddagger}$ for the complex or methoxide promoted reactions calculated from the Eyring equation as $\Delta G^{\ddagger}$= -RTln($k_2^{\mathbf{L}:Zn(II)2:(-OMe)}/(kT/h)$) or -RTln($k_2^{-OMe}/(kT/h)$) where kT/h = 6 x 10^{12} s^{-1} at 298 K.

Chapter 3 – Cleavage of an RNA Model Catalyzed by Dinuclear Zn(II) Complexes Containing Rate Accelerating Pendants. Comparison of the Catalytic Benefits of H-Bonding and Hydrophobic Substituents.

3.1 – Preface

With minor formatting changes and an expanded introduction, this chapter is largely as it is currently in press in the *Journal of Organic Chemistry*. All experiments (including synthesis, kinetics, and analytical data collection) were performed by Mark Mohamed. The manuscript was written by Mark Mohamed and Dr. R. Stan Brown. The published article is copyrighted by the American Chemical Society.

3.2 – Introduction

In many natural metalloenzymes, the catalytic role of the metal ions is enhanced by contributions from strategically oriented amino acid residues in the active site.[1,2] Many examples exist of positively charged amino acid residues (particularly those of arginine, lysine, and histidine) serving to stabilize the transition state of phosphoryl transfer via hydrogen-bonding and electrostatic interactions.[3] Particular examples of catalytic amino acids in metalloenzymes include alkaline phosphatase (AP), where the positively charged guanidinium of Arginine-166 plays an important role in substrate binding through hydrogen-bonding with the non-bridging oxygen atoms of the phosphate (Figure 3-1 A).[4] Work by Herschlag demonstrated that replacement of Arg-166 with serine affected only the monoesterase activity of AP but not the diesterase activity,[5] indicating that the residue is an important contributor to the enzyme's specificity as a phosphomonoesterase. The

importance of hydrogen-bonding by cationic guanidinium groups was also observed in Staphylococcal Nuclease (SNase), a Ca(II) dependent DNA cleaving enzyme (Figure 3-1 B).[6] It was found that both the Ca(II) cation and two arginine residues were essential for catalysis. Replacement of both of the arginine residues resulted in a decrease of 35000-fold in terms of the k_{cat} for the hydrolysis of DNA. Aside from direct catalytic participation, the amino acid residues in the enzyme active site determine the local chemical environment of the metal-ion cofactors. The outer coordination sphere surrounding a metal ion has been shown to play a major role in biologically relevant metal promoted reactions.[7]

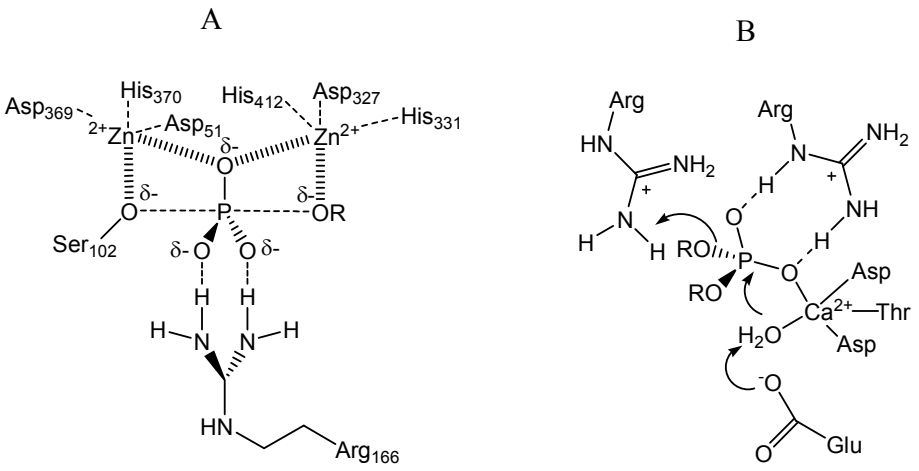

Figure 3-1. Representations of the active sites of (A) Alkaline Phosphatase (adapted diagram from Reference 5) and (B) Staphylococcal Nuclease (B, adapted diagram from Reference 2) showing the roles of arginine as a hydrogen-bond donor.

The study of synthetic compounds which mimic phosphate cleaving enzymes has been an area of intense interest for many years. While much attention has focused on mimicking the metal-ion cofactors present in many phosphatase enzymes,[8,9] comparatively little work has been directed at simulating the cooperative effects of metal ions and amino acid residues.[10] Owing to the prevalence of hydrogen-bonding as a mode of activation in

enzyme catalysis,[7a] a recent trend in the design of transition metal complexes which catalyze the cleavage of phosphate esters has been the incorporation of ancillary hydrogen-bonding substituents which are postulated to enhance catalysis through favourable hydrogen-bonding interactions in the reaction transition state.[11] The majority of these catalysts have been based on the *bis*(2-amino-pyridinyl-6-methyl)amine unit (**3.1**) which incorporates a primary amino group at the 2-position of each pyridyl ring.

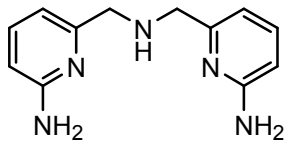

3.1

Some years ago, Chin and Mancin[11d] showed that the mononuclear Zn(II) complex **3.2** (n = 2) was 230-fold more reactive towards the hydrolysis of *bis*(*p*-nitrophenyl) phosphate than the corresponding complex without the NH_2 groups. Soon after, Williams *et al.*[11b] demonstrated that the mononuclear Zn(II) complex **3.2** (n = 1) was just as effective at catalyzing the cleavage of the RNA model 2-hydroxypropyl-*p*-nitrophenyl phosphate (HPNPP, **3.6**) as was the dinuclear complex **3.3**. These results suggested that in terms of catalytic enhancement, the hydrogen-bond donors are just as effective as a second metal ion.

Finally, by combining the cooperativity of two metal ions with the effects of hydrogen-bond donors, Williams prepared catalyst **3.4** and found it to be a very effective catalyst for the cleavage of **3.6** in water.[11a] At pH = 7.4 in water, catalyst **3.4** showed saturation kinetics (catalyst **3.4** is one of only a few examples of synthetic nucleases which show saturation in water) and was found to have a second-order rate constant of k_{cat}/K_m = 53 $M^{-1}s^{-1}$ which is 725-fold greater than the second-order rate constant for catalyst **3.3**.

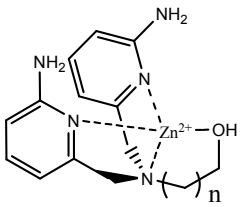

3.2

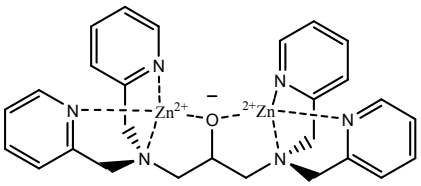

3.3

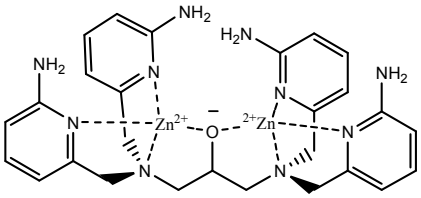

3.4

The fact that complexes bearing hydrogen-bond donating groups are generally more active than the corresponding unsubstituted complexes is evidence that catalyst activity can be modulated by strategically incorporating additional functionality.

Work from this laboratory has been directed towards the cleavage of simple RNA and DNA model compounds catalyzed by dinuclear Zn(II) complexes in the light alcohols (methanol and ethanol). We have demonstrated that the cleavage of phosphate diesters is accelerated by $10^{11\text{-}13}$-fold relative to the background reactions in the presence of a catalytic system comprising an alcohol medium and the dinuclear complex **3.5**:$Zn(II)_2$,[12,13,14] a catalytic system which far outperforms any synthetic nuclease models reported that operate in water. The remarkable rate enhancements observed upon moving from aqueous solution into lower dielectric constant alcohols points to an important medium effect which has, until recently, been underappreciated. One of the major contributors to the rate enhancements observed in alcohol is the fact that ionic and electrostatic interactions are strengthened in low dielectric constant media (due to reduced solvation of ions and increased Coulombic interactions). Inspired by the recent reports of the benefits of incorporation of hydrogen-bonding substituents, we reasoned that the enhanced electrostatic interactions in methanol relative to water might augment any hydrogen-bonding interactions in passing from water to alcohol and hence even

greater catalysis might be achieved. In addition, building on the catalytic acceleration that results from media of greater hydrophobicity than water, we wondered if the addition of simple hydrophobic groups proximal to the dinuclear core might create an extended hydrophobic pocket and enhance catalysis through interactions similar to the hydrophobic effects observed in aqueous media.[15]

In this chapter is described a kinetic study of the cleavage of the simple RNA analog, 2-hydroxypropyl-*p*-nitrophenyl phosphate (**3.6**, HPNPP) in methanol catalyzed by a series of dinuclear Zn(II) complexes with alkyl substituents (**3.8:**$Zn(II)_2$, **3.9:**$Zn(II)_2$ and **3.13:**$Zn(II)_2$) comparing their activities with the non-functionalized parent complexes, (**3.7:**$Zn(II)_2$ and **3.12**:$Zn(II)_2$). The studies show that the rate of the catalyzed cleavage of substrate **3.6** can be enhanced by up to three orders of magnitude by modification of a dinuclear Zn(II) catalyst with simple alkyl substituents. We have also studied a pair of dinuclear catalysts which are functionalized with H-bonding groups, **3.10:**$Zn(II)_2$ and **3.11:**$Zn(II)_2$. The data indicate that both H-bond donating substituents and alkyl substituents enhance catalysis relative to the unsubstituted complex, but surprisingly, the H-bond donating substituents are no better than alkyl substituents in accelerating the cyclization of **3.6** in methanol.

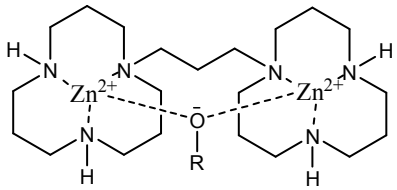

3.5:$Zn(II)_2$

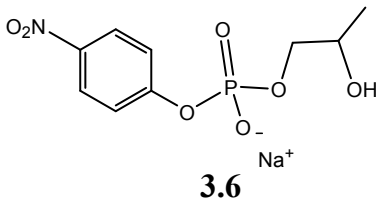

3.6

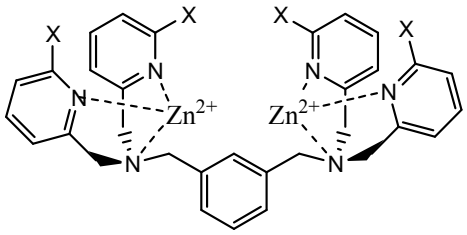

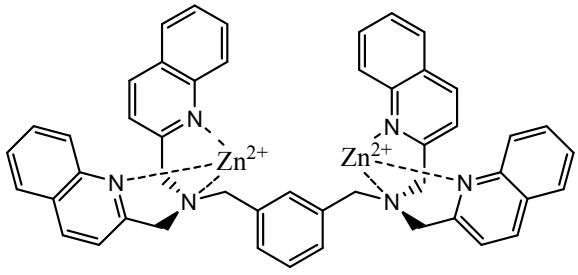

3.7:$Zn(II)_2$. X = H
3.8:$Zn(II)_2$. X = CH_3
3.10:$Zn(II)_2$. X = NH_2
3.11:$Zn(II)_2$. X = $NH(C{=}O)CH_3$

3.9:$Zn(II)_2$

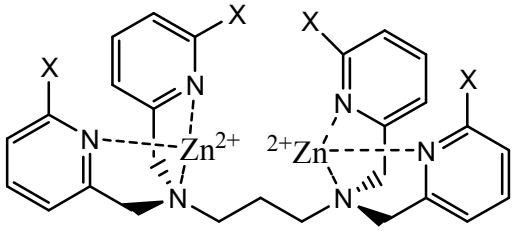

3.12:$Zn(II)_2$. X = H
3.13:$Zn(II)_2$. X = CH_3

3.3 - Experimental

3.3.1 – Materials

Methanol (DriSolv) was purchased from EMD Chemicals. $Zn(OTf)_2$ (98%), sodium methoxide (0.50 M solution in methanol, titrated against N/50 certified standard aqueous HCl solution and found to be 0.49 M), triethylamine (99%), 2-picoline (98%), 2,6-lutidine (99%), 2,2,6,6-tetramethylpiperidine (99%), 1,3-diaminopropane (99%), m-xylylenediamine (99%), and trifluoromethanesulfonic acid were purchased from Aldrich and used without further purification. Silica gel for chromatography (ultra pure, 230-400 mesh) was purchased from Silicycle.

3.3.2 – Synthesis

The syntheses of *bis*(di-(2-pyridylmethyl)amino)-*m*-xylene (**3.7**)[16], and 1,3-*bis*(di-(2-pyridylmethyl)amino)propane (**3.12**)[17] were done as previously reported.

Bis(*bis*-(methylpyridylmethyl)amine)-*m*-xylene (3.8)

To a suspension of 2-bromomethyl-6-methylpyridine[18] (3.6 g, 19.3 mmol) in 20 mL of water was added *m*-xylylenediamine (0.54 mL, 0.57 g, 4.2 mmol) followed by solid NaOH (2.0 g, 50.0 mmol). The dark red mixture was stirred vigorously and heated to reflux for 24 hours. The aqueous mixture was cooled to room temperature, 50 mL of $CHCl_3$ was added and the layers were separated. The aqueous phase was extracted with an additional 50 mL $CHCl_3$. The combined organic layers were washed once with 50 mL saturated brine and dried over Na_2SO_4. Evaporation of the solvent gave a dark brown viscous oil. The oily residue was suspended in 50 mL hexanes which immediately precipitated a brown powder that was removed by filtration. The filtrate was evaporated to yield an orange oil which was taken up in a minimum amount of hot hexanes. Cooling of the solution in an ice bath caused a sticky orange residue to deposit on the walls of the flask, leaving behind a golden yellow solution. The yellow solution was decanted and placed in the freezer. After several hours, a white powder precipitated which was collected by vacuum filtration. Yield: 1.0 g (43%). m.p. = 59 – 61 °C. ^{1}H NMR (300 MHz, $CDCl_3$): δ2.49 (s, 12H), δ3.69 (s, 4H), δ3.80 (s, 8H), δ6.97 (d, 4H, J = 9 Hz), δ7.27 (m, 3H), δ7.41-7.52 (m, 9H). ^{13}C NMR (75 MHz, $CDCl_3$): δ24.28, 58.44, 59.86, 119.45, 121.45, 127.63, 128.24, 129.20, 136.78, 138.82, 157.38, 158.78. HRMS (EI-TOF):

calcd. for $C_{36}H_{40}N_6$ (M^+): 556.3314; found 556.3328. Anal. Cald. for $C_{36}H_{40}N_6$: C, 77.64; H, 7.24; N, 15.10; Found: C, 77.52; H, 7.32; N, 15.21.

***Bis*(*bis*-(2-quinolylmethyl)amine)-*m*-xylene (3.9)**

To a suspension of 2-bromomethylquinoline[19] (1.8 g, 8.2 mmol) in 20 mL of water was added *m*-xylylenediamine (0.23 mL, 0.24 g, 1.8 mmol) followed by solid NaOH (0.96 g, 24.0 mmol). The biphasic mixture was stirred vigorously and heated to reflux for 24 hours. The aqueous mixture was cooled to room temperature, 50 mL of $CHCl_3$ was added and the layers were separated. The aqueous phase was extracted with an additional 50 mL $CHCl_3$. The combined organic layers were washed once with 50 mL saturated brine and dried over Na_2SO_4. Evaporation of the solvent gave a dark orange viscous oil. The crude product was purified by flash silica gel chromatography on a Biotage SP1 purification system eluting with 10:0.75 $CHCl_3$:$HOCH_3$. The fractions containing the product were combined and the solvent evaporated to give a viscous orange oil. The oil was taken up in a minimum amount of hot hexanes. Upon cooling in an ice bath, a sticky orange residue separated from a golden yellow solution. The solution was decanted and placed in the freezer overnight during which an off-white powder precipitated which was collected by filtration. Yield: 0.6 (48%). m.p. = 73 – 76 °C. ^{1}H NMR (300 MHz, $CDCl_3$): δ3.75 (s, 4H), δ4.02 (s, 8H), δ7.29 (m, 2H), δ7.46 (t, 4H, J = 6 Hz), δ7.58 – 7.75 (m, 14H), δ8.0 (dd, 8H, J = 9 Hz, 21 Hz). ^{13}C NMR (75 MHz, $CDCl_3$): δ58.96, 61.08, 121.08, 126.29, 127.46, 127.63, 128.14, 128.42, 129.17, 129.55, 129.80, 136.47, 139.17, 147.67, 160.56. HRMS (ESI-TOF): calcd. for $C_{48}H_{41}N_6$ ($M\text{-}H^+$): 701.3392; found 701.3364. Anal. Cald. for $C_{48}H_{40}N_6$: C, 82.26; H, 5.75; N, 11.99; Found: C, 82.57; H, 5.89; N, 11.74.[20]

***Bis*(*bis*-(2-aminopyridylmethyl)amine)-*m*-xylene (3.10)**

To a mixture of 2-pivaloylamino-6-bromomethylpyridine[21] (2.07 g, 7.6 mmol) and K_2CO_3 (0.68 g, 4.9 mmol) in 50 mL anhydrous acetonitrile was added m-xylylenediamine (0.247 mL, 0.26 g, 1.91 mmol). The stirring mixture was heated to reflux under N_2 atmosphere overnight. The reaction mixture was cooled to room temperature and filtered to remove the insoluble inorganic salts which were washed with an additional 10 mL acetonitrile. The filtrate was evaporated to yield *bis*(*bis*-(2-pivaloylaminopyridylmethyl)amine)-*m*-xylene as an orange foam (1.66 g, 97%) which was carried on to the next step without further purification.

^{1}H NMR (300 MHz, CD_3OD): δ1.30 (s, 36H), δ3.70 (s, 12H), δ7.30 (m, 7H), δ7.48 (s, 1H), δ7.70 (t, 4H, J = 6 Hz), δ7.96 (d, 4H, J = 6 Hz). ^{13}C NMR (100 MHz, CD_3OD): δ23.20, 27.62, 40.79, 59.95, 60.67, 113.87, 120.05, 129.19, 129.37, 130.70, 140.02, 152.44, 159.27, 179.51. HRMS (ESI-TOF): calcd. for $C_{52}H_{69}N_{10}O_4$ ($M\text{-}H^+$): 897.5503; found 897.5455.

To a solution of *bis*(*bis*-(2-pivaloylaminopyridylmethyl)amine)-*m*-xylene (1.66 g, 1.85 mmol) in 100 mL of ethanol was added 100 mL of 10 M aqueous NaOH. The mixture was heated to reflux overnight with vigorous stirring. The volume of the solution was reduced to ~100 mL by rotary evaporation and the resulting mixture was diluted with an additional 50 mL of water. The aqueous mixture was extracted with 3x100 mL $CHCl_3$ and the combined organic extracts were dried over Na_2SO_4. The solvent was evaporated under vacuum to give a yellow foam. The foam was re-crystallized from THF to give a crystalline material which became a white powder upon drying. Yield: 0.8 g (77%). m.p.

= 150 – 154°C. ^{1}H NMR (400 MHz, CD_3OD): δ3.52 (s, 8H), δ3.62 (s, 4H), δ6.41 (d, 4H, J = 8 Hz), δ6.91 (d, 4H, J = 8 Hz), δ7.22 (s, 2H), δ7.23 (s, 1H), δ7.38 (t, 3H, J = 8 Hz), δ 7.58 (s, 1H). ^{13}C NMR (100 MHz, CD_3OD): δ59.66, 60.64, 108.33, 112.47, 128.75, 129.20, 129.90, 139.71, 140.51, 158.73, 160.45. HRMS (ESI-TOF): calcd. for $C_{32}H_{37}N_{10}$ ($M\text{-}H^+$): 561.3202; found 561.3214. The spectral data match those recently reported by Gunning *et. al*[22] who prepared the title compound by an alternate synthetic route.

***Bis*(*bis*-(2-acetylaminopyridylmethyl)amine)-*m*-xylene (3.11)**

To a mixture of 2-acetylamino-6-bromomethylpyridine[11d] (1.5 g, 6. mmol) and K_2CO_3 (0.6 g, 4.4 mmol) in 20 mL anhydrous acetonitrile was added *m*-xylylenediamine (0.22 mL, 0.23 g, 1.6 mmol). The stirring mixture was heated to reflux under N_2 atmosphere overnight. The reaction mixture was cooled to room temperature and filtered to remove the insoluble inorganic salts which were washed with an additional 10mL acetonitrile. The filtrate was evaporated to yield an orange foamy residue which was purified by flash silica gel chromatography on a Biotage SP1 purification system using CH_2Cl_2: $HOCH_3$: NH_4OH (10:0.75:0.1) as the eluent (R_f = 0.18). The yellow solid obtained after chromatography was further purified by suspension in hot diethyl ether (20 mL) followed by filtration to yield a fluffy off-white solid. Yield: 1.0 g (84%). m.p. = 125 - 130ºC. ^{1}H NMR (400 MHz, CD_3OD): δ2.11 (s, 12H), δ3.65 (s, 12H), δ7.23-7.27 (m, 7H), δ7.51 (s, 1H), δ7.65 (t, 4H, J = 8 Hz), δ7.91 (d, 4H, J = 8 Hz). ^{13}C NMR (100 MHz, CD_3OD): δ23.97, 59.63, 60.62, 113.55, 119.89, 129.02, 129.23, 130.59, 136.67, 140.31, 152.35, 159.60, 171.99. HRMS (ESI-TOF): calcd. for $C_{40}H_{45}N_{10}O_4$ ($M\text{-}H^+$): 729.3625; found

729.3618. The spectral data match those recently reported by Gunning *et. al*[22] who prepared the title compound by an alternate synthetic route.

1,3-*bis*(*bis*-(methylpyridylmethyl)amine)propane (3.13)

To a suspension of 2-bromomethyl-6-methylpyridine[18] (5.7 g, 31.0 mmol) in 20 mL of water was added 1,3-diaminopropane (0.55 mL, 0.49 g, 6.6 mmol) followed by solid NaOH (3.2 g, 80.0 mmol). The dark red mixture was stirred vigorously and heated to reflux for 24 hours. The aqueous mixture was cooled to room temperature, 50 mL of CH_2Cl_2 was added and the layers were separated. The aqueous phase was extracted with an additional 40 mL CH_2Cl_2 and the combined organic layers were dried over Na_2SO_4. Evaporation of the solvent gave a dark brown viscous oil. The crude product was chromatographed on a silica gel column, eluting with 10:1 CH_2Cl_2:$HOCH_3$ to afford a pale orange oil. The oil was taken up in a minimum amount of hot hexanes which, upon cooling in the freezer overnight, yielded a white powder which was collected by filtration. Yield: 0.54 g (17%). m.p. = 78 - 81°C. ^{1}H NMR (400 MHz, $CDCl_3$): δ1.80 (s, 2H), δ2.49 (s, 12H), δ2.55 (m, 4H), δ3.73 (s, 8H), δ6.96 (d, 4H, J = 8 Hz), δ7.26 (d, 4H, J = 8 Hz), δ7.47 (t, 4H, J = 8 Hz). ^{13}C NMR (75 MHz, $CDCl_3$): δ25.09, 53.07, 61.18, 120.06, 121.88, 137.19, 158.03, 159.95. HRMS (EI-TOF): calcd. for $C_{31}H_{38}N_6$ (M^+): 494.3158; found 494.3177.

3.3.3 – Methods

Kinetics in Methanol using UV-Visible spectroscopy: The rates of catalyzed cleavage of **3.6** (0.05 mM) were monitored by UV-vis spectrophotometry at 25.0 ± 0.1 °C by

observing the rate of appearance of *p*-nitrophenol at 320 nm or *p*-nitrophenolate at 400 nm. All kinetic experiments were performed with catalyst formed *in situ* through sequential addition of stock solutions (typically 100 - 200 mM) of ligand and $Zn(OTf)_2$ to buffered methanol solutions ([buffer] = 50 mM) to make a total volume of 2.5 mL in quartz cuvettes. Reactions were initiated by the addition of 25 μL of 5 mM substrate to the catalyst solution. Buffer solutions were prepared using mixtures of amines and HOTf in methanol to adjust the ${}^{s}_{s}pH$[23] of the solution (2-picoline, ${}^{s}_{s}pH$= 6.20 - 6.40; 2,6-lutidine, ${}^{s}_{s}pH$= 6.90 - 7.30; *i*-Pr-morpholine, ${}^{s}_{s}pH$= 8.00 – 9.50; triethylamine, ${}^{s}_{s}pH$= 10.85 - 11.25; 2,2,6,6-tetramethylpiperidine, ${}^{s}_{s}pH$= 12.00 – 12.10). Where buffer inhibition was observed, plots of k_{obs} vs. [buffer] (typically 10 mM ≤ [buffer] ≤ 50 mM) were linear with a downward slope. Extrapolation of the plot of k_{obs} vs. [buffer] to [buffer] = 0 gave a theoretical rate constant in the absence of buffer that was used to correct the original experimental data. For all catalysts, a correction constant was determined for each buffer as the ratio k_0/k_{50} (where k_0 is the theoretical rate constant in the absence of buffer and k_{50} is the rate constant in 50 mM buffer) and the original pseudo first-order rate constants were multiplied by this constant. The reported values of the pseudo first-order rate constants (k_{obs}) for the production of *p*-nitrophenol(phenolate) are the averages of duplicate runs.

The kinetics of the reactions with half-life times less than ~5 s were determined using a stopped-flow reaction analyzer thermostatted at 25.0 °C. Catalyst complexes were formed *in situ* in 4-dram vials, transferred to glass syringes and loaded onto the stopped-flow reaction analyzer. Reaction rates were determined from the rate of appearance of *p*-nitrophenol at 320 nm or *p*-nitrophenolate at 400 nm. At least four replicate experiments

were performed at each catalyst concentration and the reported values of pseudo first-order rate constants (k_{obs}) are the averages.

The $CH_3OH_2^+$ concentrations for the various kinetic runs were determined potentiometrically using a combination glass electrode (Radiometer model no. XC100-111-120-161) calibrated with certified standard aqueous buffers (pH = 4.00 and 10.00). The measured ${}^{s}_{w}pH$ meter readings in methanol were converted to the ${}^{s}_{s}pH$ values by subtracting the δ correction factor of -2.24.[23]

3.4 - Results

The catalyzed cleavage of **3.6** was studied in buffered methanol solution with all catalyst complexes with the exception of **3.11:**$Zn(II)_2$, and in all cases the kinetic data were corrected for the effect of buffer (as described in the Experimental section). Kinetic experiments with **3.11:**$Zn(II)_2$, were conducted in the absence of buffer due to strong buffer inhibition. The catalyst was formed *in situ* through sequential addition of stock solutions of sodium methoxide, ligand and $Zn(OTf)_2$ to anhydrous methanol such that [$^-OCH_3$]:[**3.11**]:[$Zn(OTf)_2$] = 1:1:2. Formulation of the catalyst in this way gave solutions with ${}^{s}_{s}pH$ = 9.9 ± 0.4. The data for **3.11:**$Zn(II)_2$ were corrected for the effect of the triflate counterion by plotting k_{obs} for the cleavage of **3.6** at constant [**3.11:**$Zn(II)_2$:$^-OCH_3$] vs increasing [tetrabutylammonium triflate]. The inhibition data were analyzed according to equation 1 to give a triflate inhibition constant of 5.8 mM. The kinetic data were corrected to reflect the concentration of catalyst free from triflate inhibition ($[Cat]_{free}$) according to equation 2.

$$k_{obs} = \frac{k^0_{cat} K_i}{K_i + [OTf]_{total}} + k_{inf} \quad (1) \qquad [Cat]_{free} = \frac{[Cat]_{Total} K_i}{K_i + [OTf]_{total}} \quad (2)$$

The plots of k_{obs} vs [catalyst] for the cleavage of **3.6** catalyzed by **3.7:**$Zn(II)_2$ - **3.10:**$Zn(II)_2$ and **3.13:**$Zn(II)_2$ were ${}^{s}_{s}pH$-dependent, with all catalyst complexes showing both linear behaviour (Figure 1A) and saturation binding (Figure 1B), indicative of a change in the strength of binding between the catalyst complex and the substrate as a function of ${}^{s}_{s}pH$. In all cases, a significant x-intercept was observed, similar to the behaviour of most other dinuclear Zn(II) complexes in methanol that we have reported,[12,13,14,24] consistent with dissociation of a Zn(II) ion from the complex at low concentration that leads to an inactive or severely less active mono-nuclear form. Complex **3.12:**$Zn(II)_2$ was found to exhibit linear kinetics over the ${}^{s}_{s}pH$ range studied. The second-order rate constants (k_2^{cat}) were determined as the slope of the plots of k_{obs} vs [catalyst] from the linear kinetics plots.

The observation of saturation kinetics is indicative of formation of a catalyst:substrate complex followed by a chemical step leading to the spectroscopically observed product (Scheme 3-1). Where saturation kinetics were observed, the data were fit to the universal binding equation, eq. (3)[25] to obtain values of k_{cat} (the maximum observed rate constant) and K_M (the [**L:**$Zn(II)_2$:**3.6**] dissociation constant, taken as the reciprocal of the binding constant, K_B, from eq. (3)). In these cases, the apparent second-order catalytic rate constant is given as $k_{cat}/K_M = k_2^{cat}$.

Scheme 3-1. Proposed pathway for the cleavage of **3.6** promoted by **L**:Zn(II)$_2$.

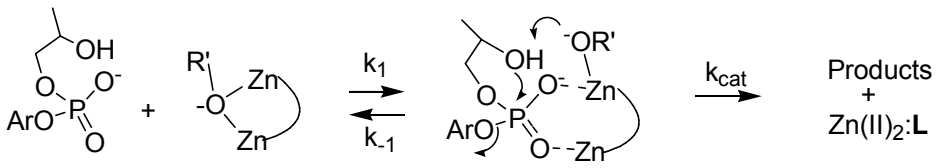

$$k_{obs} = k_{cat}(1 + K_B \times [S] + [Cat] \times K_B - X)/(2K_B)/[S] \qquad (3)$$

where:

$$X = (1 + 2K_B \times [S] + 2 \times [Cat] \times K_B + K_B^2 \times [S]^2 - 2 \times K_B^2 \times [Cat][S] + [Cat]^2 \times K_B^2)^{0.5}$$

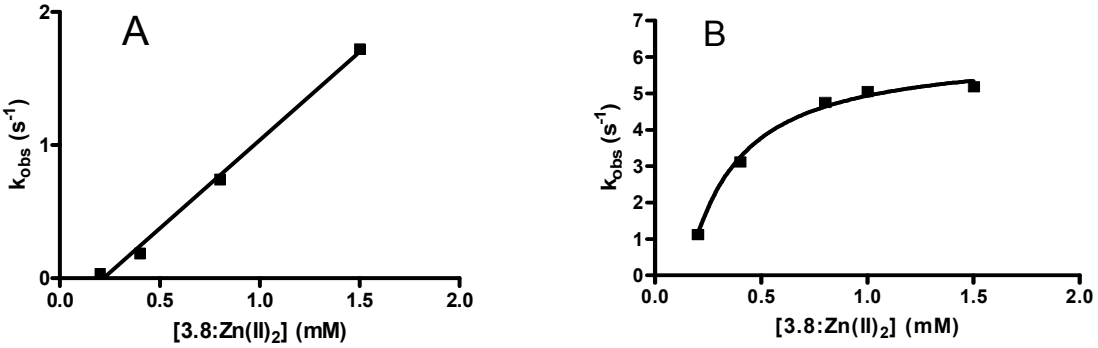

Figure 3-2. Plots of k_{obs} vs [**3.8**:Zn(II)$_2$] for the cleavage of HPNPP (**3.6**) (5 x 10^{-5} M) showing: A) a linear dependence at $^{s}_{s}$pH = 6.90 (k_2 = 1327 $M^{-1}s^{-1}$); and B) saturation kinetics at $^{s}_{s}$pH = 7.95 (k_{cat} = 6.2 s^{-1}, K_M = 0.21 mM, k_{cat}/K_M = 30,000 $M^{-1}s^{-1}$) determined from the rate of appearance of *p*-nitrophenol at 320 nm, T = 25.0 ± 0.1 °C. Data are corrected for the effect of buffer.

The k_{obs} vs [catalyst] plot obtained with **3.11:**Zn(II)$_2$ also showed curvature suggestive of the formation of a catalyst-substrate complex. Values of k_{cat} and K_M were determined by fitting the corrected kinetic data to eq. 3.

The log k_2^{cat} vs. ${}^{s}_{s}pH$ plots for all catalysts were bell shaped (see Figure 3-3) consistent with the formation of an active complex by the first acid dissociation from the complex, followed by a second deprotonation leading to loss of catalysis.

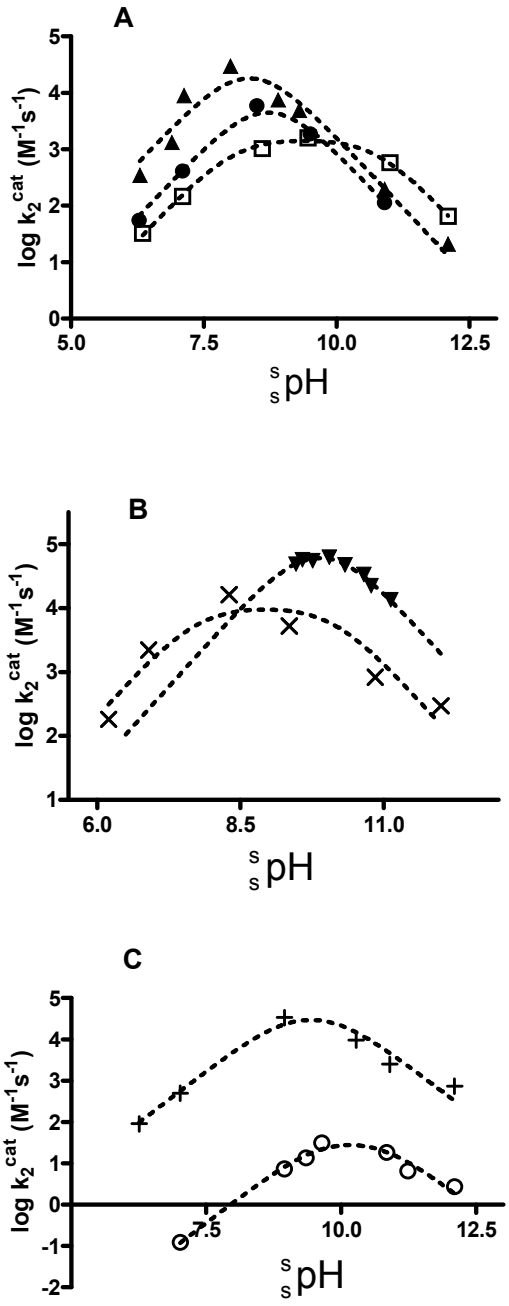

Figure 3-3. Plots of log k_2^{cat} vs. $^{s}_{s}$pH for (A) **3.7**:$Zn(II)_2$ (□), **3.8**:$Zn(II)_2$ (▲), and **3.9**:$Zn(II)_2$ (●); (B) **3.10**:$Zn(II)_2$ (X) and **3.11**:$Zn(II)_2$ (▼); (C) **3.12**:$Zn(II)_2$ (○) and **3.13**:$Zn(II)_2$ (+).

The log k_2^{cat} vs. ${}^{s}_{s}pH$ data were fit to eq. 4 (derived for an equilibrium involving two deprotonation events, Scheme 3-2) to give kinetic ${}^{s}_{s}pK_a$ values. In the case of **3.11:**$Zn(II)_2$, for ${}^{s}_{s}pH$ values below 9.5 and above 11.1, the absolute slope of the plot of log k_2^{cat} vs. ${}^{s}_{s}pH$ was much greater than unity which we interpret being due to an instability of the catalyst complex outside this ${}^{s}_{s}pH$ range. The data outside this ${}^{s}_{s}pH$ range were omitted from the non-linear fit.

$$k_2 = \left(\frac{k_2^{max}\, {}^{s}_{s}K_a^{1}[H^+]}{[H^+]^2 + [H^+]\,{}^{s}_{s}K_a^{1} + {}^{s}_{s}K_a^{1}\,{}^{s}_{s}K_a^{2}} \right) \qquad (4)$$

Scheme 3-2. ${}^{s}_{s}pH$ dependent process for the cleavage of **3.6** mediated by **L**:$Zn(II)_2$:($^-OCH_3$). (Note: **Cat** = **L**:$Zn(II)_2$)

$$\textbf{Cat:}(HOCH_3)_2 \overset{{}^{s}_{s}K_a^{1}}{\rightleftharpoons} \textbf{Cat:}(^-OCH_3)(HOCH_3) + H^+ \overset{{}^{s}_{s}K_a^{2}}{\rightleftharpoons} \textbf{Cat:}(^-OCH_3)_2 + H^+$$

$$\textbf{3.6} \downarrow k_2^{cat}$$

$$P$$

The various kinetic parameters and kinetic ${}^{s}_{s}pK_a$ values (k_{cat}, K_M, and $k_{cat}/K_M = k_2^{cat}$) for each catalyst complexes operating at their optimal ${}^{s}_{s}pH$ (defined as the ${}^{s}_{s}pH$ where the maximum catalytic rate for each complex is observed) are summarized in Table 3-1. With the exception of **3.12:**$Zn(II)_2$, for which all plots of k_{obs} vs [**3.12:**$Zn(II)_2$] were linear, the change in the shape of the plot of k_{obs} vs [**L:**$Zn(II)_2$] from linear to curved as a function of ${}^{s}_{s}pH$ suggests an increasing tightness of binding of the substrate and complex up to the

$^{s}_{s}$pH-rate maximum, above which the K_M value steadily increases (binding becomes weaker). In the case of **3.9:**$Zn(II)_2$, binding of the substrate to the catalyst complex was only observed at the $^{s}_{s}$pH-rate maximum ($^{s}_{s}$pH = 8.50) while plots of k_{obs} vs [**3.9:**$Zn(II)_2$] were linear at all other $^{s}_{s}$pH values. Since the active form of the catalysts is thought to be the monomethoxy form, we believe that the increase in the tightness of binding upon approaching the $^{s}_{s}$pH-rate maximum is attributed to the introduction of a transient methoxide bridge between the two Zn(II) ions that pre-organizes them into a configuration which is optimal for binding the anionic substrate in a bidentate fashion. The introduction of a second methoxide at higher $^{s}_{s}$pH has the dual effect of neutralizing the positive charge of the Zn(II) centres and possibly disrupting the configuration of the catalyst which weakens the binding between the catalyst and substrate.

Table 3-1. Kinetic constants (k_{cat}, K_M, and $k_{cat}/K_M = k_2$) for the cleavage of **3.6** (0.05 mM) catalyzed by the **L**:$Zn(II)_2$ complexes of ligands **3.7** – **3.13** under optimal $^{s}_{s}$pH conditions[a] in methanol at T = 25.0 ± 0.1˚C

Complex	$^{s}_{s}pK_a^1$	$^{s}_{s}pK_a^2$	k_{cat} (s^{-1})	K_M (M)	$k_{cat}/K_M = k_2^{cat}$ ($M^{-1}s^{-1}$)
3.7:$Zn(II)_2$	8.1 ± 0.1	10.8 ± 0.1	0.13 ± 0.01	(7.8 ± 3.5) x 10^{-5}	(1.6 ± 0.7) x 10^3
3.8:$Zn(II)_2$	≥ 8.4 [b]	≤ 8.3 [b]	6.2 ± 0.4	(2.1 ± 0.5) x 10^{-4}	(29.8 ± 7.0) x 10^3
3.9:$Zn(II)_2$	8.9 ± 0.4	8.5 ± 0.4	4.3 ± 0.8	(7.3 ± 3.2) x 10^{-4}	(5.9 ± 2.7) x 10^3
3.10:$Zn(II)_2$	7.7 ± 0.5	10.2 ± 0.5	3.89 ± 0.03	(2.4 ± 0.1) x 10^{-4}	(16 ± 1) x 10^3

3.11:$Zn(II)_2$	9.7 ± 0.5	10.1 ± 0.4	7.2 ± 0.3	(6.6 ± 0.9) x 10^{-5}	(109 ± 5) x 10^3
3.12:$Zn(II)_2$	9.6 ± 0.3	10.8 ± 0.3	NA	NA	(31 ± 1) [c]
3.13:$Zn(II)_2$	9.0 ± 0.7	9.9 ± 0.7	3.2 ± 0.1	(9.4 ± 2.2) x 10^{-5}	(33.9 ± 8.0) x 10^3

[a] Optimal ${}^{s}_{s}pH$ defined as highest experimental value for k_{cat} in the ${}^{s}_{s}pH$/rate constant profile.
[b] See reference 26
[c] The second-order rate constants are determined from the slope of the linear plot of k_{obs} vs [**L:**$Zn(II)_2$]

3.5 – Discussion

The 2-di-picolylamine ligand is useful for the study described here due to its well-demonstrated use as a platform for Zn(II) catalysts[11,27] and the easy access to substituted derivatives.[22] It also serves as an appropriate comparison of the results herein with those from past work since the *bis*(2-amino-pyridinyl-6-methyl)amine unit has been a commonly used ligand for the study of the effects of H-bonding substituents on the substrate binding characteristics of phosphates and catalysis of cleavage of certain substrates.[11,28]

3.5.1 - Cleavage of 2 catalyzed by complexes 3.7:$Zn(II)_2$, 3.8:$Zn(II)_2$, 3.10:$Zn(II)_2$, and 3.11:$Zn(II)_2$

It is a striking feature of the data in Table 3-1 that all the functionalized catalyst complexes (**3.8**, **3.9**, **3.10**, **3.11,** where X= CH_3, quinolyl, NH_2, $NH(C{=}O)CH_3$)) exhibit a greater activity than the parent complex (**3.7:**$Zn(II)_2$; where X=H). Since all of the $Zn(II)_2$ complexes of **3.7**, **3.8**, **3.10**, and **3.11** exhibit saturation kinetics, a direct comparison of

the effect of substituent can be made for both substrate binding (K_M) and catalytic rate constant (k_{cat}) once fully bound. All complexes show comparable affinity for substrate as judged by the K_M values in Table 3-1. While it is tempting at the outset to suggest that the H-bonding possible in **3.11:**$Zn(II)_2$[28] will lead to tighter substrate binding by this complex, its K_M is comparable to that of the parent complex **3.7:**$Zn(II)_2$ (7.8×10^{-5} M), suggesting that the putative H-bonding is not beneficial to stabilizing the Michaelis complex. Direct comparison of the K_M values of **3.8:**$Zn(II)_2$ ($X=CH_3$) and **3.10:**$Zn(II)_2$ ($X=NH_2$) indicates these are essentially the same at 2.1×10^{-4} M and 2.4×10^{-4} M respectively, indicating that the possible H-bonding amino group provides the same general effect that the non-H-bonding methyl group does. In fact, considering that the K_M value is related to the dissociation constant for the **L**:$Zn(II)_2$:($-OCH_3$):**3.6** complex, or its kinetic equivalent, **L**:$Zn(II)_2$:**3.6**$^-$ (where the 2-hydroxypropyl group of the bound substrate is deprotonated by the internal methoxide),[29] both of these complexes bind substrate more weakly than does the parent **3.7:**$Zn(II)_2$. The relative invariance of binding between the dinuclear complexes and phosphate diester **3.6** is surprising, but consistent with the recent findings of Gunning *et al*.[22] who found no remarkable differences in the binding constant between a series of phosphates (such as inorganic phosphate, Adenosine-5'-monophosphate, β-glycerophosphate, and *p*-nitrophenyl phosphate) and **3.7:**$Zn(II)_2$, **3.10:**$Zn(II)_2$, and **3.11:**$Zn(II)_2$ as determined by isothermal titration calorimetry.

The values of K_M reported in Table 3-1 refer to the binding constants determined from fitting of the data to eq. 3 at the optimal ${}^{s}_{s}pH$ for each catalyst complex under the assumption that all of the catalyst is capable of binding the substrate ([cat] = [ligand] =

½[Zn(II)]). However, at the ${}^{s}_{s}pH$ values obtained at the maxima of the various ${}^{s}_{s}pH$-rate profiles, the concentration of the active monomethoxy species (Scheme 3-2) is less than the total concentration of catalyst complex in solution (particularly so in the cases where ${}^{s}_{s}pK^{1}_{a}$ and ${}^{s}_{s}pK^{2}_{a}$ are similar, as in **3.8:**$Zn(II)_2$ and **3.9:**$Zn(II)_2$). Given this consideration, the values of K_M in Table 3-1 may be considered as upper limits.[30] This effect may also contribute to the absence of a clear trend in K_M values, but does not alter the interpretation of the k_{cat} values.

The major difference between the 2-substituted pyridyl complexes and the parent complexes studied here is observed in the k_{cat} terms given in Table 3-1. In all cases, the substituted complexes were found to have k_{cat} terms which are greater than the parent complex by over an order of magnitude, indicating that while all of the complexes are able to bind the substrate with similar affinity, the substituted complexes excel at promoting the cleavage of the bound substrate. It is interesting that the k_{cat} values for all of the substituted complexes fall within a very narrow range suggesting that the different substituents (be they amino, acetamido or alkyl) are all equally capable of stabilizing the transition state for the chemical cleavage step in Scheme 3-1 relative to what is provided by the parent complexes. It is also significant that the k_{cat} values for **3.10**:$Zn(II)_2$ and **3.11**:$Zn(II)_2$ differ by only a factor of two despite a large difference in the H-bond donating abilities of the NH_2 and $NH(C{=}O)CH_3$ groups. The Taft-Kamlet α-parameters (a measure of a protic solvent's hydrogen bond donating ability)[31] for aniline (0.26) and N-methylformamide (0.62)[32] give a rough estimate of the H-bond donating ability of the NH_2 and $NH(C{=}O)CH_3$ substituents, suggesting that N-H bond of the amide should be a significantly better hydrogen-bond donor than the N-H-bond of an aniline type amine. It

appears that the large difference in H-bond donating ability is subtly manifested in the strength of substrate binding (K_M differs by ~3.5) and the catalytic rate constant (factor of two) so that the overall difference in the k_{cat}/K_M terms is at most seven-fold for these two complexes. Furthermore the fact that the ordering of k_{cat} (and K_M) for **3.8**:$Zn(II)_2$, (where the CH_3 substituent is expected to have $\alpha = 0$[32]) **3.10**:$Zn(II)_2$ and **3.11**:$Zn(II)_2$ are 6.2, 3.9 and 7.2 s^{-1} respectively (30 x 10^{-3}, 16 x 10^{-3} and 109 x 10^{-3} $M^{-1}s^{-1}$ respectively) is evidence that H-bonding cannot be said to be significantly more effective than whatever the CH_3 group's effect is in improving catalysis relative to what is provided by the parent **3**:$Zn(II)_2$.

3.5.2 - Cleavage of 3.6 Catalyzed by 3.9:$Zn(II)_2$, 3.12:$Zn(II)_2$ and 3.13:$Zn(II)_2$

The beneficial effects of simple methyl substituents (as in **3.8**:$Zn(II)_2$) led us to wonder if an extension of the hydrophobic region around the metal-ions might confer even greater activity. We therefore prepared catalyst **3.9**:$Zn(II)_2$ where the pyridine rings are replaced with quinolyl rings to bury the metal ions within a deeper hydrocarbon cavity. The kinetic parameters for **3.9**:$Zn(II)_2$ are listed in Table 3-1 and at first glance it would appear that **3.9**:$Zn(II)_2$ is the least active of the functionalized catalysts, with a k_2^{cat} of only 5.9 x 10^3 $M^{-1}s^{-1}$ compared to 109 x 10^3 $M^{-1}s^{-1}$ for **3.11**:$Zn(II)_2$. Inspection of the individual kinetic parameters, k_{cat} and K_m, reveals that **3.9**:$Zn(II)_2$ has a saturating rate constant (k_{cat}) which is less than a factor of two less than that of **3.11**:$Zn(II)_2$ and is in fact larger than that of **3.10**:$Zn(II)_2$. The difference in second-order rate constants arises from weaker binding of the substrate to catalyst **3.9**:$Zn(II)_2$, over 10-fold weaker than the binding between the substrate and **3.11**:$Zn(II)_2$. The weaker binding may be attributable to the large quinolyl groups which prevent substrate binding by steric crowding. The fact

that the k_{cat} term for **3.9**:$Zn(II)_2$ is comparable to those of **3.8**:$Zn(II)_2$, **3.10**:$Zn(II)_2$, and **3.11**:$Zn(II)_2$ indicates that although it has lower affinity for the substrate, once bound to the substrate it will catalyze the conversion to products at the same rate as the other functionalized catalysts.

To give further evidence for the acceleratory properties of simple CH_3 substituents and to confirm that the catalysis observed with **3.8**:$Zn(II)_2$ is not unique for the xylyl structures, we investigated **3.12**:$Zn(II)_2$ and **3.13**:$Zn(II)_2$ where the two Zn(II)-complexing ligands are connected by a flexible propyl linker. The k_{obs} values for the cleavage of **3.6** promoted by **3.13**:$Zn(II)_2$ were much greater than those for **3.12**:$Zn(II)_2$ over the same concentration range. Because the k_{obs} vs [**3.12**:$Zn(II)_2$] plots are strictly linear, we can obtain only a second-order rate constant for the catalyzed reaction of $k_2^{cat} = 31\ M^{-1}s^{-1}$ from the slope of the plots. However, the k_{obs} vs [**3.13**:$Zn(II)_2$] plots show evidence of saturation binding so it is possible to obtain both the k_{cat} and K_M terms as well as a k_2^{cat} of $33 \times 10^3\ M^{-1}s^{-1}$ suggesting that **3.13**:$Zn(II)_2$ is ~ 10^3 more reactive than **3.12**:$Zn(II)_2$ under optimal $^{s}_{s}$pH conditions. The presence of the CH_3 groups in **3.13**:$Zn(II)_2$ affords far stronger substrate binding, comparable to what is seen in the best of the xylyl cases, as well as a k_{cat} term which is similar to what is seen for the xylyl complexes where X = alkyl, NH_2, or $NH(C{=}O)CH_3$.

3.6 – Conclusions

The above findings point out that caution should be exercised in rationalizing the accelerating effect of H-bond donating substituents on complexes cleaving phosphate

diesters such as **3.6**. Where such arguments are made, they are largely based on enhanced reaction rate compared to a complex without the H-bonding group, and x-ray diffraction evidence on bound substrates or surrogates.[11a,28] However, the latter structural evidence only confirms the possibility of H-bonding interactions in the ground state but do not necessarily mean that these interactions are maintained (and necessarily strengthened) in the transition state for the chemical reaction. Even so, an observed accelerating effect designated to a suitably placed H-bonding group may be difficult to ascribe uniquely without a more extensive set of comparisons.

We have shown that the cleavage of a phosphate diester, **3.6**, catalyzed by several $Zn(II)_2$ complexes based on the *bis*[*bis*(2-X-, 6-pyridylmethyl)amino] propyl and xylyl systems is accelerated by at least two, and perhaps more effects resulting from functionalization of the catalyst with X=CH_3, NH_2, $NH(C{=}O)CH_3$ and $(CH)_4$ groups. Functionalization of the catalyst with hydrophobic and sterically demanding CH_3 groups seems to be an effective strategy to enhance catalysis without invoking any H-bonding effects. The activities of the CH_3-substituted systems is comparable to the effects afforded by NH_2 and $NH(C{=}O)CH_3$ substituents. While the importance of H-bonding interactions in enzymatic reactions is well established,[1,2,7] the ability to mimic them with simple model systems has been less conclusively demonstrated, particularly since other effects such as steric, local polarity, and medium induced ones now seem to be as important in such systems as are presented here. Given that the 2-NH_2 group and 2-CH_3 groups are roughly iso-structural with similar steric demands, it is difficult to decide which of H-bonding or steric effects is the more important. While we can not unambiguously rule out H-bonding as a mode of activation, our findings suggest that the acceleratory effects of H-

bond donating substituents may be the result of a general, and perhaps more complex effect of substitution at the 2-position of the pyridyl rings of the *bis*[*bis*(2-X-6-pyridylmethyl)]amino metal receptors.

3.7 - References

1) a) Sträter, N.; Lipscomb, W.N.; Klabunde, R.; Krebs, B. *Angew. Chem. Int. Ed.* **1996**, *35*, 2024. b) Wilcox, D.E. *Chem. Rev.* **1996**, *96*, 2435.

2) Krämer, R. *Coord. Chem. Rev.* **1999**, *182*, 243.

3) Perreault, D.M.; Anslyn, E.V. *Angew. Chem. Int. Ed.* **1997**, *36*, 432.

4) a) Chaidaroglou, A.; Brezinski, D.J.; Middleton, S.A.; Kantrowitz, E.R. *Biochemistry*. **1988**, *27*, 8338. b) Coleman, J.E. *Annu. Rev. Biophys. Biomol. Struct.* **1992**, *21*, 441.

5) O'Brien, P.J.; Herschlag, D. *Biochemistry.* **2001**, *40*, 5691.

6) Serpersu, E.H.; Shortle, D.; Mildvan, A.S. *Biochemistry.* **1987**, *26*, 1289.

7) a) Borovik, A.S. *Acc. Chem. Res.* **2005**, *38*, 54 (and references therein) b) Marque Rivas, J.C. *Current Organic Chemistry.* **2007**, *11*, 1434 (and references therein)

8) a) Weston, J. *Chem. Rev.* **2005**, *105*, 2151. b) Parkin, G. *Chem. Rev.* **2004**, *104*, 699.

9) For a representative list of references on various metal containing complexes, see: a) Mancin, F.; Tecillia, P. *New J. Chem.* **2007**, *31*, 800; b) Weston, J. *Chem. Re*v. **2005**, *105*, 2151; c) Molenveld, P.; Engbertsen, J. F. J.; Reinhoudt, D. N. *Chem. Soc. Re*v. **2000**, *29*, 75; d) Williams, N. H.; Takasaki, B.; Wall, M.; Chin, J. *Acc. Chem. Res.* **1999**, *32*,485; e) Mancin, F.; Scrimin, P.; Tecilla, P.; Tonellato, U. *Chem. Commun.* **2005**, 2540; f) Morrow, J. R.; Iranzo, O. *Curr. Opin. Chem.Biol.* **2004**, *8*, 192.

10) Blaskó, A.; Bruice, T.C. *Acc. Chem. Res.* **1999**, *32*, 475.

11) For a representative example of studies on small molecule enzyme mimics utilizing hydrogen bond donors, see: a) Feng, G.; Natale, D.; Prabaharan, R.; Marque-Rivas, J.C.; Williams, N.H. *Angew. Chem. Int. Ed.* **2006**, *45*, 7056. b) Feng, G.; Marque-Rivas, J.C.; Williams, N.H. *Chem. Commun.* **2006,** 1845. c) Aït-Haddou, H.; Sumaoka, J.; Wiskur, S.L.; Folmer-Anderson, J.F.; Anslyn, E.V.. *Angew. Chem. Int. Ed.* **2002**, *41*, 4014. d) Livieri, M.; Mancin, F.; Tonellato, U.; Chin, J. *Chem. Commun.* **2004**, 2862. e) Feng, G.; Marque-Rivas, J.C.; Torres Martin de Rosales, R.; Williams, N.H. *J. Am. Chem. Soc.* **2005**, *127*, 13470. f) Lombardo, V.; Bonomi, R.; Sissi, C.; Mancin, F. *Tetrahedron*, **2010**, *66*, 2189. g) Bonomi, R.; Saielli, G.; Tonellato, U.; Scrimin, P.; Mancin, F. *J. Am. Chem. Soc.*, **2009**, *131*, 11278. h) Bonomi, R.; Selvestrel, F.; Lombardo, V.; Sissi, C.; Polizzi, S.; Mancin, F.; Tonellato, U.; Scrimin, P. *J. Am. Chem. Soc.*, **2008**, *130*, 15744. i) Livieri, M.; Mancin, F.; Saielli, G.; Chin, J.; Tonellato, U. *Chem. – Eur. J.*, **2007**, *13*, 2246.

12) Neverov, A. A.; Lu, Z.-L.; Maxwell, C. I.; Mohamed, M. F.; White, C. J.; Tsang, J. S. W.; Brown, R. S. *J. Am. Chem. Soc.* **2006**, *128*, 16398.

13) Bunn, S. E.; Liu, C. T.; Lu, Z.-L.; Neverov, A. A.; Brown, R. S. *J. Am. Chem. Soc.* **2007**, *129*, 16238

14) Liu, C. T.; Neverov, A. A.; Brown, R. S. *J. Am. Chem. Soc.* **2008**, *130*, 16711.

15 a) Blokzijl, W.; Engberts, J.B.F.N. *Angew. Chem. Int. Ed. Engl.,* **1993**, *32*, 1545. b) Otto, S.; Engberts, J.B.F.N. *Org. Biomol. Chem.* **2003**, *1*, 2809.

16) Gultneh, Y.; Ahvazi, B.; Khan, A.R.; Butcher, R.J.; Tuchagues, J.P. *Inorg. Chem.* **1995**, *34*, 3633.

17) Hofmann, A.; van Eldik, R. *Dalton Trans*., **2003**, 2979.

18) Zhang, J.; Leitus, G.; Ben-David, Y.; Milstein, D. *J. Am. Chem. Soc.* **2005**, *127*, 10840.

19) Zhao, Q.; Liu, S.; Li, Y.; Wang, Q. *J. Agric. Food Chem*. **2009**, *57*, 2849.

20) Elemental analysis measurements were obtained using a Thermo Scientific Flash 2000 Organic Elemental Analyzer (FlashEA 1112 series). It should be noted that using this instrument, we were required to analyze compound **3.9** several times to obtain a carbon content which was consistent with the calculated value. In combination with the elemental analysis results, the ^{1}H, ^{13}C, and HRMS data are all consistent with the desired compound.

21) Martinho, M.; Banse, F.; Sainton, J.; Philouze, C.; Guillot, R.; Blain, G.; Dorlet, P.; Lecomte, S.; Girerd, J.J. *Inorg. Chem.* **2007**, *46*, 1709.

22) Drewry, J.A.; Fletcher, S.; Hassan, H.; Gunning, P.T. *Org. Biomol. Chem.* **2009**, *7*, 5074.

23) a.) Gibson, G.; Neverov, A. A.; Brown, R. S. *Can. J. Chem*. **2003**, *81*, 495; b) For the designation of pH in non-aqueous solvents we use the nomenclature recommended by the IUPAC, *Compendium of Analytical Nomenclature. Definitive Rules 1997* 3rd ed., Blackwell, Oxford, U. K. 1998. The pH meter reading for an aqueous solution determined with an electrode calibrated with aqueous buffers is designated as ${}^{w}_{w}\mathrm{pH}$; if the electrode is calibrated in water and the 'pH' of the neat buffered methanol solution then measured, the term ${}^{s}_{w}\mathrm{pH}$ is used; and if the electrode is calibrated in the same solvent and the 'pH' reading is made, then the term ${}^{s}_{s}\mathrm{pH}$ is used. In methanol ${}^{s}_{w}\mathrm{pH}$ -(-

2.24) = ${}^{s}_{s}pH$, and since the autoprotolysis constant of methanol is $10^{-16.77}$, neutral ${}^{s}_{s}$pH is 8.4.

24) Mohamed, M.F.; Neverov, A.A.; Brown, R.S. *Inorg. Chem.* **2009**, *48*, 11425.

25) Eq. (3) was obtained from the equations for equilibrium binding and for conservation of mass by using the commercially available MAPLE software, *Maple 9.00*, June 13, 2003, Build ID 13164, Maplesoft, a division of Waterloo Maple Inc. 1981-2003, Waterloo, Ontario, Canada.

26) The computed values of ${}^{s}_{s}pK^{1}_{a}$ and ${}^{s}_{s}pK^{2}_{a}$ for **3.8**:Zn(II)$_2$ are very similar and heavily correlated to each other and with k_2^{cat}. This precludes an exact numerical determination of these parameters. The values listed in Table 3-1 are the lower and upper limits for ${}^{s}_{s}pK^{1}_{a}$ and ${}^{s}_{s}pK^{2}_{a}$ respectively.

27) Yashiro, M.; Kaneiwa, H.; Oneka, K.; Komiyama, M. *Dalton Trans.* **2004**, 605.

28) Lee, J.H.; Park, J.; Lah, M.S.; Chin, J.; Hong, J.-I. *Org. Lett.* **2007**, *9*, 3729.

29) a) Yang, M.-Y.; Iranzo, O.; Richard, J. P.; Morrow J. R. *J. Am. Chem. Soc.*, **2005**, *127*, 1064; b) Feng, G.; Mareque-Rivas, J. C.; Torres Martýn de Rosales, R.; Williams, N. H. *J. Am. Chem. Soc.* **2005**, *127*, 13470.

30) Computation of the amounts of the neutral, monomethoxy and dimethoxy forms of the catalyst (Scheme 3-2) from the various ${}^{s}_{s}pK^{1}_{a}$ and ${}^{s}_{s}pK^{2}_{a}$ values indicates that the amount of monomethoxy plus neutral forms of the catalyst (the ones most likely to bind the anionic substrate) range from 95% (for **3.7**:Zn(II)$_2$) to 62% (for **3.11**:Zn(II)$_2$). Under the assumption that these two forms are the ones responsible for substrate binding, the

actual K_M values would be 95 to 71% less than are in Table 3-1. However, the uncertainties in the various K_M and ${}^{s}_{s}pK_a$ values computed from fits of the experimental data to eq. (3) indicate that these kinds of corrections to the K_M values in Table 3-1 are unwarranted.

31) a) Taft, R.W.; Kamlet, M.J. *J. Am. Chem. Soc.* **1976**, *98*, 2886. b) Kamlet, M.J.; Abboud, J.-L. M.; Abraham, M.H.; Taft, R.W. *J. Org. Chem.* **1983**, *48*, 2877.

32) Marcus, Y. *J. Solution Chem.* **1991**, *20*, 929.

Chapter 4 – Methanolysis of Neutral Organophosphorus Esters Catalyzed by Zn(II) Complexes of 1,10-phenanthroline Immobilized on Polystyrene Polymer Supports.[1]

4.1 – Introduction

Neutral organophosphorus esters with at least one leaving group having a pK_a of less than 8 exhibit high levels of toxicity owing to their ability to inhibit acetylcholinesterase, an enzyme of crucial importance for normal neuronal function.[2] The toxicity of organophosphorus compounds has led to their widespread use as chemical warfare (CW) agents and pesticides, and as a result has necessitated the development of methodologies to rapidly and safely decompose these materials. Our research group's interest in metal-catalyzed alcoholysis reactions led us to explore the use of divalent metal ions to promote the cleavage of neutral phosphate esters in methanol as a decontamination strategy. Early on, we identified Zn(II) and Cu(II) as effective catalysts for the methanolysis of the CW agent simulant paraoxon (**4.1**) and the P=S pesticide fenitrothion (**4.2**).[3,4] It became clear that while the metal ions were effective catalysts, their speciation in solution is an important consideration. While the monomeric forms of the catalyst are most active, the more thermodynamically stable forms appear to be dimers and higher order aggregates, the latter particularly for transition metal ions in the absence of ligands. We believed that the addition of chelating ligands might help limit oligomerization and increase the concentration of catalytically active monomers in solution. To this end, we studied the effect of several nitrogen based ligands including 1,5,9-triazacyclododecane (**4.3**), 1,10-phenanthroline (**4.4**), and 2,9-dimethylphenanthroline (**4.5**). For the methanolysis of

paraoxon (**4.1**), the Zn(II) complex of **4.4** proved to be an effective catalyst but the complex was found to exist largely as a 2:2 dimer (two Zn(II) ions + two ligands) with only a small concentration of the catalytically active monomer.[3]

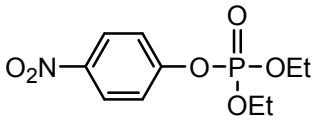

4.1

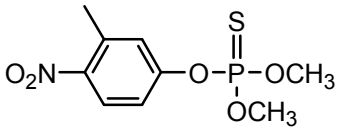

4.2

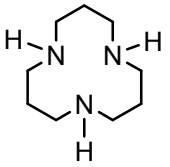

4.3

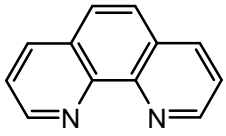

4.4

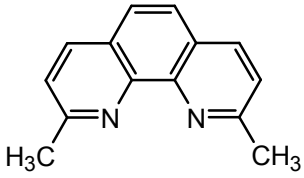

4.5

We were encouraged by the activity of the **4.4**:Zn(II) complex and wondered if immobilization of the complexes on a solid support might preclude dimerization by physically separating the complexes.

While several examples of polymer supported transition metal complexes for the hydrolysis of organophosphates exist,[5] there are no studies which have investigated alcoholysis reactions. Preliminary experiments from our group examining Zn(II) and Cu(II) complexes of di(2-picolyl)amine (DPA) immobilized on polystyrene and silica gel as catalyst for the methanolysis of **4.1** and **4.2** were promising.[6] Although the catalysis was modest compared to the homogeneous reaction, the complex of DPA:Cu(II) immobilized on an insoluble polystyrene-co-divinylbenzene copolymer gave a 7700-fold

rate enhancement for the methanolysis of **4.2** while the Zn(II) complex immobilized on the same polymer support gave a 300-fold acceleration for the methanolysis of **4.1**.

The noted catalytic activity of the monomeric form of **4.4**:Zn(II) inspired us to immobilize this species on a polymeric support and study its ability to catalyze the cleavage of neutral organophosphates. This chapter describes the immobilization of ligand **4.6** on various polystyrene based polymers and the formulation of the Zn(II) complex of the affixed ligand. We also describe the activity of these heterogeneous catalysts towards the cleavage of the G-agent simulant **4.7** and the V-agent simulant **4.8** under neutral conditions in methanol.

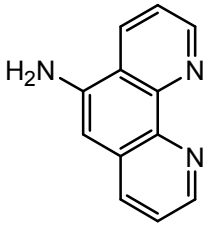

4.6

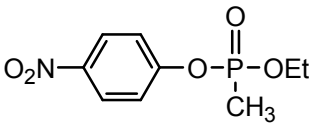

4.7

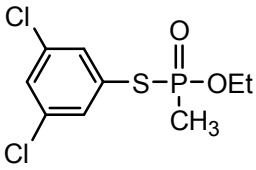

4.8

4.2 – Experimental

4.2.1 – Materials

Methanol (99.8% anhydrous), DMF (99.8%, anhydrous), sodium methoxide (0.5M solution in methanol), $HClO_4$ (70% aqueous solution), $Zn(CF_3SO_3)_2$, and 1,10-phenanthroline were purchased from Aldrich and used as supplied. 1,4-Dioxane (extra dry, with molecular sieves, water < 50 ppm) was purchased from Acros Organics and used without further purification. Pd/C catalyst (5%) was purchased from Fluka.

Macroporous Merrifield resin (Macro-Ald) (1.2 mmol Cl/g, 100-200 mesh) was purchased from Aldrich. Macroporous chloromethylated polystyrene (PL-CMS MP) resin (Macro-PL) (>12% of cross linking with divinylbenzene, 2.8 mmol Cl/g, porosity size 100 Å, particle size 150-300 μm) was purchased from Polymer Laboratories. Substrates **4.7** and **4.8** were synthesized according to the literature procedures.[7,8]

4.2.2 – Synthesis

Scheme 4-1. Synthesis of ligand **4.6**

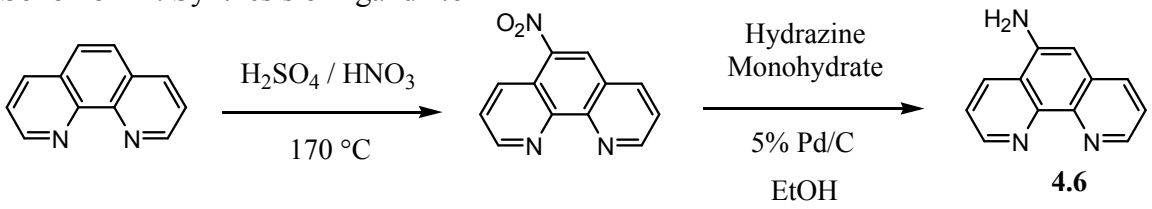

4.6

5-amino-1,10-phenanthroline (4.6)

5-Amino-1,10-phenanthroline was prepared via a modification of a previously published route.[9] 1,10 – Phenanthroline (10 g, 55.5 mmol) was added to 60 mL of concentrated sulfuric acid with stirring until the solid dissolved, and the solution was heated to 170 ˚C. To the stirred solution, 30 mL of fuming nitric acid (>90%) was added dropwise and the mixture was allowed to stir at 170 ˚C overnight. The hot reaction mixture was poured into 100 mL of ice water and the pH of the aqueous mixture was adjusted to ~3 with 50% aqueous NaOH. The resulting yellow precipitate was filtered and washed with a large excess of distilled water, followed by drying *in vacuo* to yield 7.1 g (57 %) of 5-nitro-1,10-phenanthroline. Mp = 198 – 200 ºC (lit. = 193 ºC). ^{1}H NMR (300 MHz, DMSO-d_6): δ7.96 (m, 2H), δ8.79 (d, 1H, J = 6 Hz), δ8.90 (d, 1H, J = 9 Hz), δ9.05 (s, 1H), δ9.25 (d,

1H, J = 3 Hz), δ9.28 (d, 1H, J = 3 Hz). ^{13}C NMR (75 MHz, DMSO-d_6): δ121.46, 125.58, 125.65, 126.66, 127.10, 133.17, 139.57, 146.56, 147.92, 152.27, 154.46.

Without further purification, the 5-nitro-1,10-phenanthroline (7.1 g, 31.6 mmol) was dissolved in 150 mL anhydrous ethanol. To the stirred solution was added 1.5 g of 5% Pd/C catalyst, the mixture was heated to 70 ˚C and the reaction flask was wrapped in aluminum foil to protect against light. A solution of hydrazine monohydrate (7.9 g, 0.16 mmol) in 150 mL anhydrous ethanol was prepared and slowly added dropwise to the heated reaction mixture. The reaction mixture was left to stir at 70 ˚C overnight.

The resulting mixture was filtered though Celite and the solvent was evaporated *in vacuo* to give the solid product. The yellow solid was recrystallized from a minimum amount of hot ethanol and dried *in vacuo*. 3.78 g (61 %). Mp = 252 – 253 ˚C (lit. = 253 – 254 ˚C).

^{1}H NMR (400 MHz, DMSO-d_6): δ6.14 (s, 2H), δ6.86 (s, 1H), δ7.50 (m, 1H), δ7.73 (m, 1H), δ8.04 (d, 1H, J = 8 Hz), δ8.68 (m, 2H), δ9.04 (d, 1H, J = 4 Hz). ^{13}C NMR (75 MHz, DMSO-d_6): δ102.93, 122.97, 123.19, 124.32, 131.71, 131.97, 133.85, 141.65, 143.83, 145.95, 147.33, 150.47. LRMS (EI-TOF): calc. for $C_{12}H_9N_3$ ($M\text{-}H^+$): 195.07; found 195.04.

4.2.3 - Example of modification of polymeric resins with 5-amino-1,10-phenanthroline (Macro-PL-4.6b)

Polymer-bound phenanthroline was prepared via a modification of a published route.[9] Commercial macroporous chloromethylated polystyrene (Macro-PL) (0.824 g, 2.31 mmol of Cl, 1 eq.) and solid 5-amino-1,10-phenanthroline (0.724 g, 3.71 mmol, 1.6 eq)

were added to a 100 mL round bottom flask equipped with a reflux condenser and a small magnetic stirbar. To the flask was added 50 mL of anhydrous DMF and the mixture was gently stirred to avoid crushing of the polymer and heated to reflux. After 1 hour of heating, triethylamine (520 μL, 3.7 mmol) was added to the reaction mixture and the mixture was maintained at reflux. An additional 230 μL (1.65 mmol) of triethylamine was added after 24 hours of heating and the two phase mixture was kept at reflux for another 48 hours. After cooling, the polymer was filtered and washed with 20 mL of DMF and 100 mL of methanol. The resin was left to stir gently in boiling DMF for three hours followed by filtration and rinsing with methanol. To remove any residual DMF, the polymer was boiled in acetone at 60˚C overnight, collected, filtered and washed with acetone and then methanol. The functionalized polymer was treated with a 20 mL solution of sodium methoxide (5 mM) in methanol for 15 hours to remove any traces of acid and residual exposed chloromethyl functionality.

4.2.4 - Metal complexation of polymer bound ligand

A 0.1 M solution of $Zn(OTf)_2$ was prepared in methanol and the polymer was immersed in this solution overnight after which it was separated by filtration, washed with methanol and dried in oven at 60 °C for 24 hours.

4.2.5 - Analysis of the Zn(II) loading

A known mass of the metal-loaded polymer (around 0.01 g) was immersed in 2 mL of nitric acid solution in methanol (5% v/v) for 30 minutes. The methanol solution was

carefully decanted away from the polymer and transferred to a 4-dram vial. The acid wash was repeated four times. The combined methanol washes were evaporated to ~0.2 mL which was diluted with water in a volumetric flask (25 or 50 mL). The concentration of Zn(II) in this solution was obtained by atomic absorption spectrometry using a Varian Spectra AA-20 Plus Spectrometer, calibrated with known [Zn(II)] solutions (0.1 to 0.5 ppm). Based on the concentration of Zn(II) in the solution and the initial mass of metal-loaded polymer, concentrations of Zn(II) on the polymer (expressed as mmol/g) were calculated.

4.2.6 – Kinetics

All kinetics experiments were conducted in 2.5 mL of a methanol solution buffered with *i*-Pr-morpholine (6.8 x 10^{-3} M) at $^{s}_{s}$pH = 8.8. The rates of methanolysis of **4.7** catalyzed by the heterogeneous catalysts was followed by monitoring the appearance of *p*-nitrophenol at 312 nm, or the disappearance of starting material at 264 nm, using a Cary 100 UV-vis spectrophotometer with the cell compartment thermostated at 25.0 ± 0.1 °C. The rates of methanolysis of **4.8** were followed by monitoring its disappearance at 253 nm. A solution of the substrate in 2.5 mL of buffered methanol was added to a quartz UV cell containing the solid catalyst and the cell was immediately placed in the spectrometer to gather a time-zero absorbance. The cell was removed from the spectrometer every minute and shaken manually for 13 seconds (~30 times) and replaced in the spectrometer for a short time to allow settling of the insoluble polymer before collecting a new absorbance spectrum from 200-400 nm. The reactions were run to completion and the

pseudo first-order rate constants (k_{obs}) were determined by fitting the absorbance vs. time traces to a standard exponential model. Kinetic experiments were performed in duplicate.

4.3 – Results and Discussion

4.3.1 – Polymer functionalization

Scheme 4-2. General approach to the modification of the polymer resins with **4.6**.

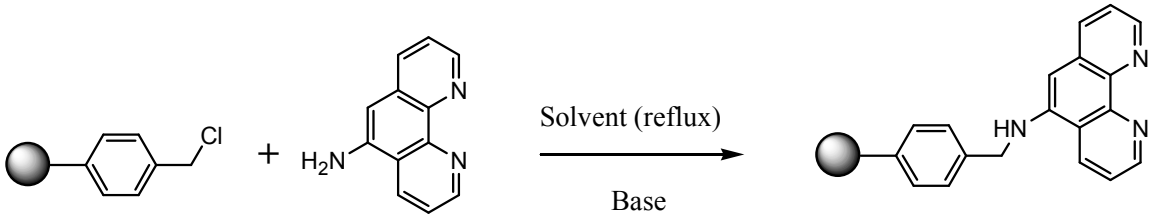

Over the course of this study, we examined three different polymers as scaffolds for the heterogeneous catalysts. We employed two commercially available macroporous chloromethylated polystyrene resins (Macro-Ald and Macro-PL) and one macroporous copolymer of styrene and 4-chloromethylstyrene crosslinked with divinylbenzene which was prepared in our laboratory by Dr. Benoît Didier. The general approach to the functionalization of the polystyrene polymer is outlined in Scheme 4-2. The functionalization conditions and final Zn(II)-loadings for all of the polymeric materials are listed in Table 4-1.

Our first attempts were with the macroporous Merrifield resin purchased from Aldrich (Macro-Ald). Based on the previous work of Binnemans *et al.*,[9] our initial efforts employed 1,4-dioxane as the functionalization solvent and triethylamine as the base. Heating the polymer to reflux in the presence of one equivalent of **4.6** (relative to the

total amount of chloride in the resin) for 4 days followed by soaking in a $Zn(OTf)_2$ solution gave a material (Macro-Ald-**4.6a**) with a metal loading of 0.034 mmol/g. Modification of this procedure with the addition of a second equivalent of **4.6** to the initial reaction mixture increased the final metal loading to 0.098 mmol/g (Macro-Ald-**4.6b**). The concentration of chloride in the commercial Merrifield resin was stated to be 1.2 mmol/g, in which case the metal-loadings that we obtained represent only 2.8% and 8.2% of the possible total. The Macro-Ald polymer proved to be an inconvenient material for our catalytic studies. The polymer was easily crushed during the functionalization process, resulting in a fine powder which was not amenable to the UV-visible kinetic experiments. We next turned to another commercial macroporous chloromethylated polystyrene, Macro-PL, which appeared to have physical properties that would be more conducive to our experiments such as robust spherical particles which were more resistant to mechanical degradation. Functionalization of Macro-PL in the presence of two equivalents of **4.6** and triethylamine in 1,4-dioxane at reflux, followed by metallation gave a material (Macro-PL-**4.6a**) with 0.035 mmol/g of Zn(II) (corresponding to 1.3% conversion of the initial 2.8 mmol/g chloride in the starting polymer). We found that replacement of 1,4-dioxane with dimethylformamide (DMF) as the functionalization solvent improved the final metal loading to 0.098 mmol/g (Macro-PL-**4.6b**) which corresponds to 3.5% conversion. To further improve the grafting of **4.6** onto the polymer, we increased the concentration of the reaction solution (from 0.035 M to 0.2 M) which further increased the loading of the material (Macro-PL-**4.6c**) to 0.14 mmol/g (5% conversion). Increasing the reaction temperature to 200 °C by using *N*-methyl-2-

pyrrolidone (NMP) as the solvent had no benefit and led to a material with 0.14 mmol/g Zn(II) (Macro-PL-**4.6d**).

Due to a limited supply of the macroporous styrene-co-4-chloromethylstyrene-co-divinylbenzene copolymer prepared in our laboratory (Macro-RSB), we were only able to attempt one grafting procedure. Heating Macro-RSB in 1,4-dioxane to reflux with triethylamine and **4.6** followed by introduction of $Zn(OTf)_2$ gave a 0.065 mmol/g metal loading (Macro-RSB-**4.6**). We were unable to analyze the chloride content of the initial copolymer and so we cannot determine the degree of functionalization.

Table 4-1. Reaction conditions and characteristics of polystyrene resins functionalized with the Zn(II)-complex of **4.6**

Name	**Polymer (chloride loading)**	**Solvent (Reflux Temp.)**	**Final Zn(II)-loading (% conversion)**
Macro-Ald-**4.6a**	Macro-Ald (1.2 mmol/g)	1,4-dioxane (101 °C)	0.034 mmol/g (2.8%)
Macro-Ald-**4.6b**	Macro-Ald (1.2 mmol/g)	1,4-dioxane (101 °C)	0.098 mmol/g (8.2%)
Macro-PL-**4.6a**	Macro-PL (2.8 mmol/g)	1,4-dioxane (101 °C)	0.035 mmol/g (1.3%)
Macro-PL-**4.6b**	Macro-PL (2.8 mmol/g)	DMF (153 °C)	0.098 mmol/g (3.5%)
Macro-PL-**4.6c**	Macro-PL (2.8 mmol/g)	DMF (153 °C)	0.14 mmol/g (5%)
Macro-PL-**4.6d**	Macro-PL (2.8 mmol/g)	NMP (200 °C)	0.14 mmol/g (5%)
Macro-RSB-**4.6**	Macro-RSB	1,4-dioxane (101 °C)	0.065 mmol/g

While we were able to increase the catalyst loading through manipulation of the reaction conditions, we have not rigorously optimized the polymer functionalization procedure.

However, as will be shown in the discussion to follow, Macro-PL-**4.6a-d** all show virtually the same catalytic activity which appears to indicate that there is no advantage to increasing the Zn(II)-loading beyond a certain point.

4.3.2 – Catalytic Studies

The catalytic activity of the heterogeneous catalysts was determined for the methanolysis of substrates **4.7** and **4.8**. The kinetic experiments were conducted by weighing a known amount of the polymeric material into a quartz UV cell (typically 0.05 g – 0.20 g) followed by addition of a solution of the substrate in methanol buffered with *i*-Pr-morpholine at ${}^{s}_{s}\mathrm{pH} = 8.8$ (near neutrality in methanol, ${}^{s}_{s}\mathrm{pH} = 8.4$). Manual agitation of the UV cell suspended the insoluble catalysts in the reaction solution and allowed contact between the catalytic sites and the substrate. We intentionally avoided stirring the mixture with a magnetic stir bar as this led to crushing of the polymer into a fine powder which interfered with the UV-visible beam of the spectrometer. The fine particles were also difficult to recover for repeated use. We found that this manual agitation procedure was reproducible and adequate for our studies.

Table 4-2 lists the pseudo first-order rate constants for the methanolysis of substrates **4.7** and **4.8** catalyzed by the solid catalysts at ${}^{s}_{s}\mathrm{pH} = 8.8$ and 25 ºC as well as the rate constants for the base promoted reactions at that ${}^{s}_{s}\mathrm{pH}$. All of the data have been normalized to reflect the rate constant for the reaction catalyzed by 0.10 g of polymer. Normalization of the rate data was done based on the observation that a plot of k_{obs} for the methanolysis of **4.7** catalyzed by Macro-PL-**4.6b** at ${}^{s}_{s}\mathrm{pH} = 8.8$ versus the weight of polymer (Figure 4-1) is linear with a slope of 1.3. The values of k_2 in Table 4-2 were

computed as k_{obs}/[Zn(II)] based on the metal-loading of the polymer as if the **4.6**:Zn(II) complex was fully dissolved in solution. Since we have no way of assessing how much of the immobilized Zn(II) is accessible to the reaction solution, the values of k_2 calculated in this way are lower limits.

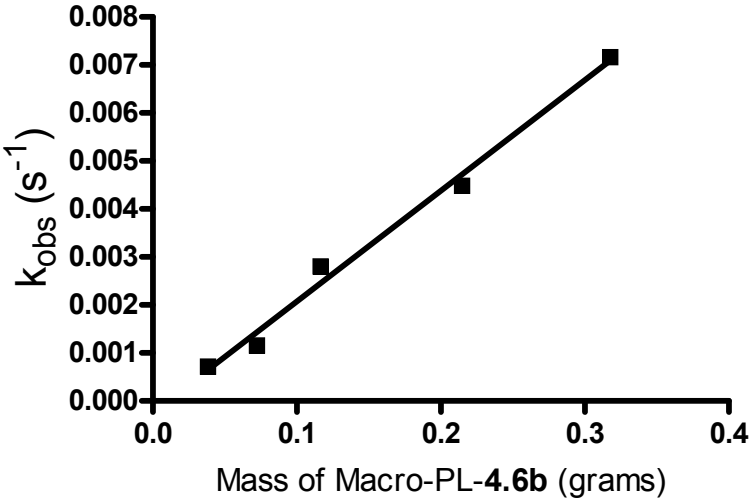

Figure 4-1. Pseudo first-order rate constant (k_{obs}) for the methanolysis of **4.7** catalyzed by Macro-PL-**4.6b** at $^{s}_{s}$pH = 8.8, T = 25 ºC, versus the weight of catalyst.

Table 4-2. Observed pseudo first-order rate constants (k_{obs}) and apparent second-order rate constants (k_2) for the methanolysis of **4.7** (3 x 10^{-5} M) and **4.8** (3 x 10^{-4} M) catalyzed by **4.6**:Zn(II) grafted onto polystyrene resins in 2.5 mL of *i*-Pr-morpholine buffered methanol ($^{s}_{s}$pH = 8.8, T = 25 °C). Data are normalized for 0.1 g of polymer.

Catalyst	$k_{obs}^{4.7}$ (s^{-1})	$k_2^{4.7}$ ($M^{-1}s^{-1}$)	$k_{obs}^{4.8}$ (s^{-1})	$k_2^{4.8}$ ($M^{-1}s^{-1}$)
$NaOCH_3$	2.83 x 10^{-8}	2.70	2.33 x 10^{-8}	2.17
Macro-Ald-**4.6a**	3.03 x 10^{-4}	0.18	1.89 x 10^{-4}	0.12
Macro-Ald-**4.6b**	3.03 x 10^{-4}	0.067	NA	NA
Macro-PL-**4.6a**	1.06 x 10^{-3}	0.75	1.57 x 10^{-3}	1.12
Macro-PL-**4.6b**	2.20 x 10^{-3}	0.56	4.58 x 10^{-3}	1.17

Macro-PL-**4.6c**	1.89×10^{-3}	0.34	NA	NA
Macro-PL-**4.6d**	1.79×10^{-3}	0.32	NA	NA
Macro-RSB-**4.6**	5.65×10^{-4}	0.22	1.28×10^{-3}	0.50

Note: Error limits considered to be ± 10 % based on uncertainties in duplicate rate measurements.

The observed rate constants (k_{obs}) given in Table 4-2 are those for the disappearance of the starting materials **4.7** and **4.8**. Over the course of the kinetic experiments, we monitored both the disappearance of the starting material as well as the release of the phenol/thiophenol product. In virtually all cases, the observed rate of disappearance of the starting material was greater than the rate of appearance of the product. We also observed that a reaction catalyzed by a fresh sample of catalyst showed full consumption of the starting material, but released a less than expected amount of product (as determined by the ΔAbs). Upon multiple uses of the same polymer catalyst, the release of product reached the expected level. These observations are consistent with a scenario in which the polymeric material absorbs the phenol product, but eventually becomes saturated.

The catalyzed reactions were run under conditions where the solutions were manually shaken in order to disperse the solid catalysts. Since heterogeneous reactions are sensitive to the speed of mixing, we examined the effect of the frequency of shaking the reaction solution. Table 4-3 gives the rate constants (k_{obs}) for the methanolysis of **4.7** catalyzed by 0.32 g of Macro-PL-**4.6b** with varying frequencies of shaking. In all cases, the duration of time over which the UV cell was agitated was constant (13 seconds) but the interval between agitations was varied. The data in Table 4-3 shows that both the rate of

disappearance of **4.7** as well as the appearance of *p*-nitrophenol increase with increased frequency of shaking. The data in Table 4-3 are subject to 10 % experimental error, but the trend in the observed rate constants with shaking frequency, coupled with the observation that there is no reaction without agitation of the reaction solution is consistent with a scenario in which the overall process is at least partially limited by mass transport phenomena (ie: penetration of the substrate into the polymer matrix and release of the phenol product out of the polymer into solution).

Table 4-3. Dependence of the pseudo first-order rate constants for the disappearance of **4.7** (3 x 10^{-5} M) and the appearance of *p*-nitrophenol catalyzed by Macro-PL-**4.6b** on the frequency of shaking.

Interval Between Agitations	**k_{obs} for the loss of 4.7 (s^{-1})**	**k_{obs} for the appearance of *p*-nitrophenol (s^{-1})**
30 seconds	0.011	0.0045
60 seconds	0.009	0.0038
120 seconds	0.007	0.0032

In terms of comparing the activities of the various immobilized catalysts, the data in Table 4-2 show that the complexes of **4.6**:Zn(II) grafted onto Macro-PL are the most active. In the best case, 0.1 g of Macro-PL-**4.6b** in *i*-Pr-morpholine buffered methanol at $^{s}_{s}$pH = 8.8 accelerates the methanolysis of **4.7** by a factor of 7.8 x 10^4-fold over the background reaction at the same $^{s}_{s}$pH and a factor of 2.0 x 10^5-fold for the methanolysis

of **4.8**. In fact, all of the solid catalysts enhance the rate of methanolysis of **4.7** by at least a factor of 10^4-fold relative to the base catalyzed reaction at the same ${}^{s}_{s}\mathrm{pH}$. In terms of the time taken to decompose the toxic materials, the half-life times for the decomposition of **4.7** and **4.8** in methanol at ${}^{s}_{s}\mathrm{pH} = 8.8$ have been reduced from 283 years and 344 years respectively for the base promoted reactions, to 5.25 minutes and 2.52 minutes respectively in the presence of Macro-PL-**4.6b**.

While we do not have data for the rate of methanolysis of **4.7** and **4.8** catalyzed by **4.4**:Zn(II) under homogeneous conditions, we can make a rough comparison with the data for the **4.4**:Zn(II) catalyzed methanolysis of **4.1**. In solution,[3] the monomeric form of **4.4**:Zn(II) catalyzes the cleavage **4.1** with a second-order rate constant of 2.1 $M^{-1}s^{-1}$, which is greater than the second-order rate constants obtained for all of the immobilized catalysts described here (Table 4-2). Considering that phosphonate **4.7** is 245-times more reactive towards methoxide than is **4.1** ($k_2^{OMe} = 2.70\ M^{-1}s^{-1}$ for **4.7** and $k_2^{OMe} = 0.011\ M^{-1}s^{-1}$ for **4.1**), then the second-order rate constant for the cleavage of **4.7** catalyzed by **4.4**:Zn is expected to be much greater than 2.1 $M^{-1}s^{-1}$ and hence significantly higher than any of the rates for the reactions catalyzed by solid supported catalysts. The fact that the reactions catalyzed by the solid-supported catalysts are slower than those in homogeneous solution is a common observation in heterogeneous catalysis.[10,11] The reduced rates under heterogeneous conditions generally arise from slow transport of the reaction solution and components into the polymer matrix to come into contact with the catalytic sites.

The enhanced activity of the Macro-PL grafted catalysts compared to Macro-Ald catalysts may be explained on the basis of the accessibility of the catalytic sites to the reaction solution. Experiments conducted by Dr. Benoît Didier examining the pore volume accessible to methanol of the various polymer supports (following the protocol of Chemin *et al.*)[12] found the pore volume of Macro-PL to be 0.48 mL/g compared to 0.31 mL/g for Macro-Ald.[1] Macro-RSB was found to have a pore volume of 0.49 mL/g in which case its reduced activity is the result of some other factor which may include the concentration of catalytic sites relative to the surface area, but this remains unclear at this time.

The data in Table 4-2 for the catalysts anchored on Macro-PL reveals an interesting feature of the heterogeneous systems, in that there appears to be a limit to the benefit of increasing the Zn(II)-loading. The 2.8-fold increase in the Zn(II)-loading in Macro-PL-**4.6b** relative to Macro-PL-**4.6a** results in only a two-fold increase in the rate of methanolysis of **4.7**, while the increase in metal loading on going to Macro-PL-**4.6c** and Macro-PL-**4.6d** does not give any additional activity at all. The apparent leveling off of the catalytic activity with additional metal loading suggests that at least some of the metal sites are buried in the polymer matrix beyond the reach of the reaction solution and these catalytic sites never come into contact with the substrate. The relative invariance of the rate with metal loading may also be explained on the basis of the rate being partially limited by penetration of the reaction solution into the polymer matrix (which is consistent with the observation of a dependence of the rate on the frequency of shaking). It is possible that at low catalyst loadings, the rate of methanolysis is limited by the chemical step involving cleavage of the leaving group from the substrate. At higher

Zn(II) loadings in the polymer, the chemical step becomes sufficiently fast that the overall rate is limited by mass transport processes which results in an apparent "saturation" of the rate.

4.3.3 – Catalyst Recycling

Perhaps the most important feature of an immobilized catalyst is its ability to be recovered and reused several times. Experiments conducted in collaboration with Dr. Benoît Didier of this laboratory found Macro-PL-**4.6b** to be highly stable over the course of several sequential reactions. Figure 4-2 shows the results of ten sequential reactions in which a 0.10 g sample of Macro-PL-**4.6b** was used to catalyze the methanolysis of **4.7** in *i*-Pr-morpholine buffered methanol at $^{s}_{s}$pH = 8.8. After each reaction, the reaction solution was carefully removed from the UV cell by pipette and a fresh substrate solution was added.

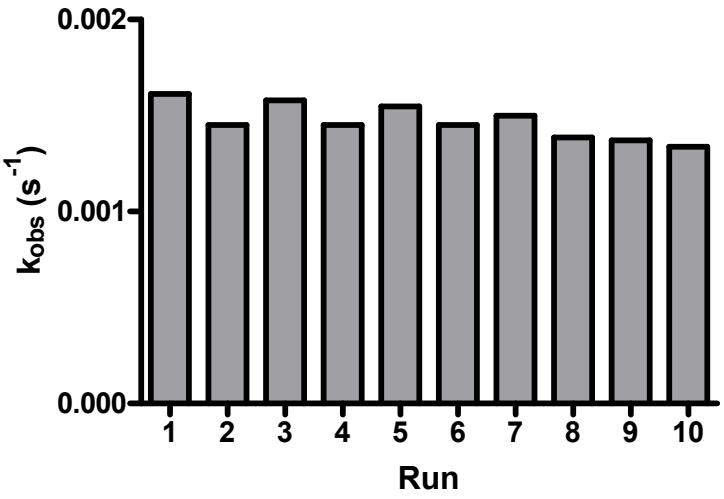

Figure 4-2. Pseudo first-order rate constants (k_{obs}) for the methanolysis of **4.7** (3 x 10^{-5} M) catalyzed by Macro-PL-**4.6b** (0.10 g) at $^{s}_{s}$pH = 8.8, T = 25 °C over ten sequential runs.

For polymer-supported catalyst systems which are intended for recovery and reuse, stability of the material upon storage and shelf-life are important considerations. In order to assess catalyst stability under different conditions, we also investigated the effect of catalyst storage. We compared a sample of Macro-PL-**4.6b** which was stored in N-*iso*-propylmorpholine buffer solution at $^{s}_{s}pH$ = 8.8 for 48 hours with one which was dried and stored in air. A 0.0947 g sample of Macro-PL-**4.6b** was weighed into a UV cell and suspended in 1.0 mL of buffer and left to sit for 48 hours. After 48 hours, 1.5 mL of 5 x 10^{-5} M **4.7** in buffered methanol was added to the UV cell (to give a final [**4.7**] = 3 x 10^{-5} M) and the reaction was followed using the normal shaking methodology. This reaction gave an observed rate constant which was the same (within experimental error) as that obtained for a reaction catalyzed by Macro-PL-**4.6b** which was dried and stored in air.

4.3.4 – Catalyst packed columns

Our experiments which showed the dependence of the observed rate constants on the shaking frequency (Table 4-3) illustrate an important consideration with regards to immobilized catalysts, namely that the reaction only takes place while the reaction solution is in fluxional contact with the catalyst. Our requirement to monitor the methanolysis reactions by UV-visible spectrophotometry precluded constant stirring of the catalyst in the reaction solution (as this would obstruct the beam passing through the UV-cell). An attractive alternative to stirring the insoluble catalyst in the reaction solution is to pack the catalyst into a column and pass the substrate solution through the column. This procedure would, in principle, increase the contact time between the

catalyst and the substrate solution and would allow for a continuous flow system to decontaminate large volumes of solution.

To test this hypothesis, we prepared an improvised continuous flow system as depicted in Figure 4-3 which comprises a variable-flow peristaltic pump connected (via Teflon tubing) to a small glass column (i.d. 3 mm, length 5 cm) which was packed with ~0.1 g of polymer, and an injection valve which allowed the introduction of the substrate solution into the system.

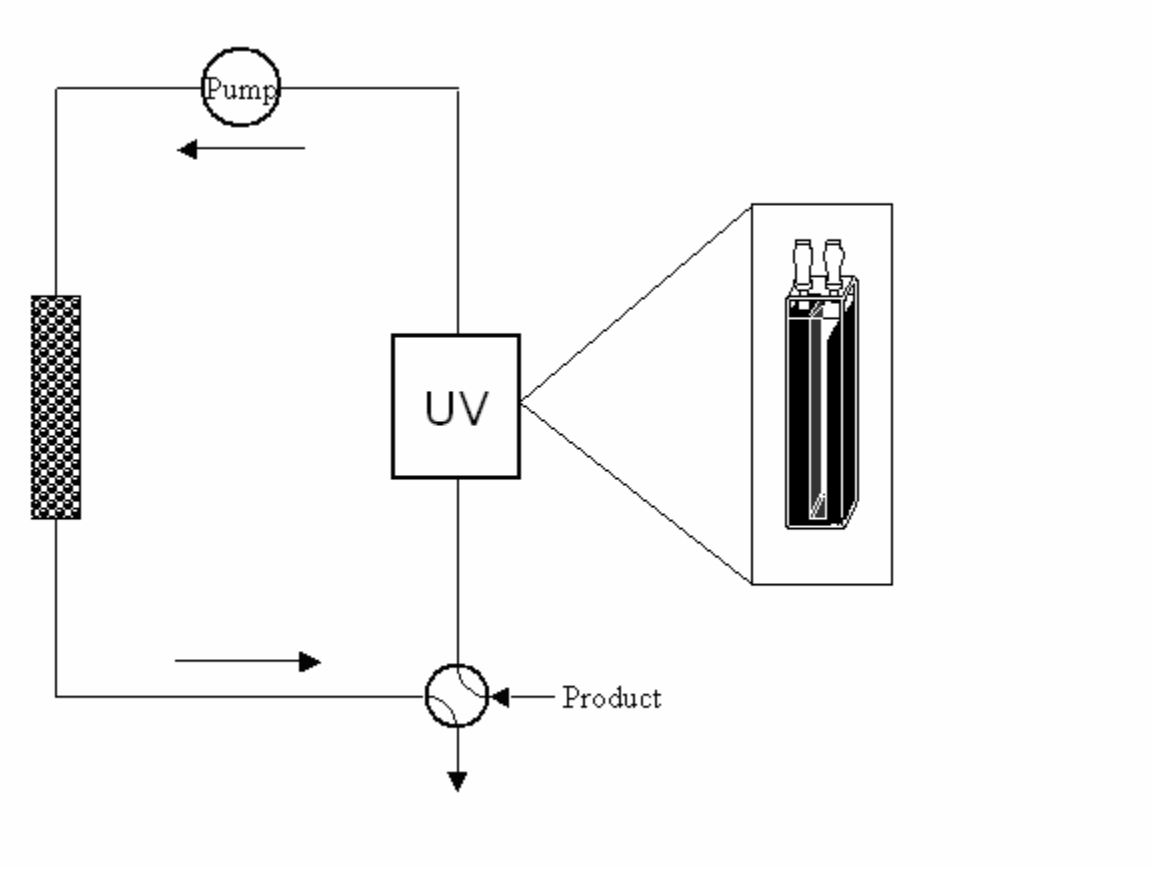

Figure 4-3. Continuous flow system with the polymer filled column shown as a shaded rectangle connected to a peristaltic pump, a flow-through UV cell inside a UV-visible spectrometer, and an injection valve. (flow cell diagram taken from www.sternacells.com)

Reactions were monitored using a quartz UV flow cell (see insert of Figure 4-3). Once the substrate solution was introduced into the system, the injection valve was closed to create a continuous loop.

In one example, 0.0924 g of Macro-PL-**4.6b** was packed into the glass column and a 3 x 10^{-4} M solution of **4.7** in methanol at $^{s}_{s}$pH = 8.8 was introduced into the system with a flow rate of ~ 1.0 mL/min. The solution was circulated for 20 minutes while the UV spectrum (from 250 – 350 nm) of the solution in the flow cell was collected every 15 seconds. The plot of absorbance vs. time (Figure 4-4) followed good first order behaviour for the disappearance of starting material and appearance of product. When fit to a first-order exponential, values of k_{obs} for the disappearance of **4.7** and the appearance of *p*-nitrophenol were calculated to be $k_{obs}^{dis.}$ = 2.64 x 10^{-3} s^{-1} and $k_{obs}^{app.}$ = 3.05 x 10^{-3} s^{-1}. Following the experiment, the catalyst was washed by circulating a fresh buffer solution through the polymer for 10 minutes, and then a new solution of **4.7** (3 x 10^{-4} M) was introduced. The second reaction was found to have $k_{obs}^{dis.}$ = 2.06 x 10^{-3} s^{-1} and $k_{obs}^{app.}$ = 2.18 x 10^{-3} s^{-1}. The difference between the rate of disappearance of **4.7** and the appearance of *p*-nitrophenol in the first reaction is interesting since, contrary to all other experiments, it is the rate of appearance of the product which exceeds the rate of disappearance of the substrate. The reason for this discrepancy is unclear at this time, however upon repeating the experiment, the large difference in rate constants is no longer observed.

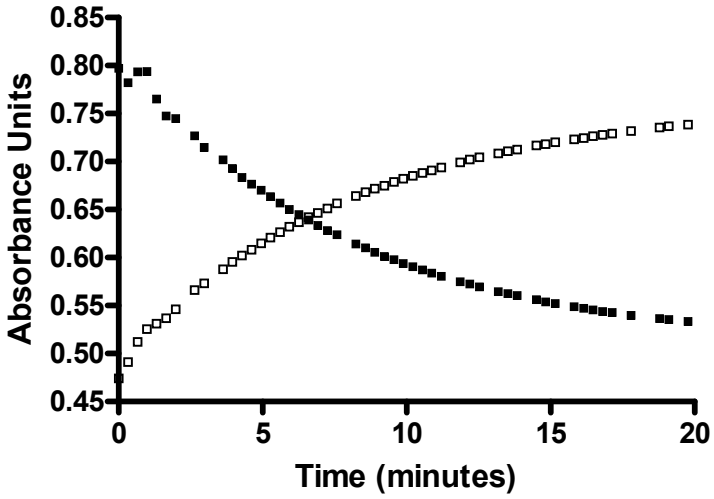

Figure 4-4. Absorbance vs. time traces for the disappearance of **4.7** (■, absorbance at 270 nm) and the appearance of 4-nitrophenol (□, absorbance at 310nm) catalyzed by 0.0924 g of Macro-PL-**4.6b** in a circulating system in *i*-Pr-morpholine buffered methanol ($^{s}_{s}$pH = 8.8) at T = 25 °C. Flow rate ~ 1.0 mL/min.

When normalized for 0.1 g polymer, the rate constants for the methanolysis of **4.7** catalyzed by Macro-PL-**4.6b** in the circulating system is about 40% greater than the rate constant obtained when manually shaking the UV cell containing the reaction mixture. The fact that the column system only gives a ~40% increase in rate is likely the result, in large part, to the fact that the ratio of column volume to total circulating volume is quite low. While the total volume of the system was determined to be ~1.5 mL, the volume of the glass column is only 0.35 mL and when packed with polymer the volume accessible to solvent is significantly less than this. Considering also that the flow rate of the pump was estimated at ~1.0 mL/min, the bulk of the solution in the system is not in contact with the catalyst at any given time. This suggests that a larger packed column with a low volume circulating system is optimal for fast decontaminations.

Although the rate constants for the duplicate reactions described above differ slightly, we believe that this is not due to a loss of catalytic activity. A separate experiment conducted with the assistance of Dr. Benoît Didier found that a 0.094 g sample of Macro-PL-**4.6b** loaded in the glass column was able to decompose substrate **4.8** over eight consecutive reactions without loss of activity (Figure 4-5). It should be noted that the decrease in the rate constants for the methanolysis of **4.8** catalyzed by Macro-PL-**4.6b** in the column system relative to the value reported in Table 4-2 is likely due to the very low flow rate (0.43 mL/min) used in the circulating experiments.

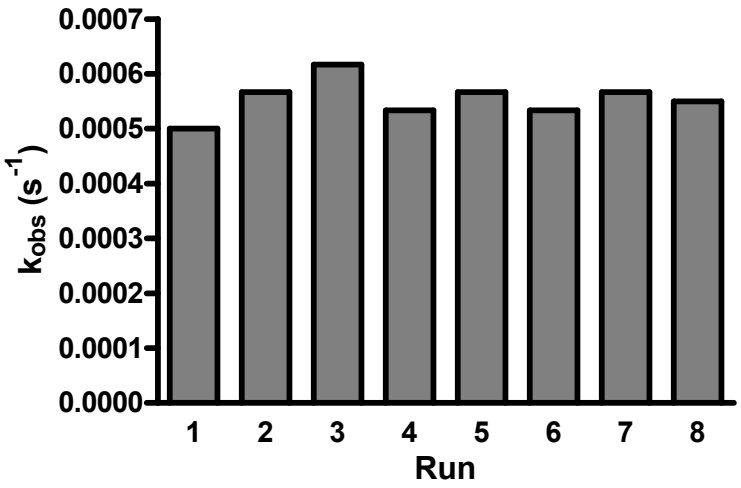

Figure 4-5. Pseudo first-order rate constants (k_{obs}) for the methanolysis of **4.8** (3 x 10^{-4} M) catalyzed by Macro-PL-**4.6b** (0.094 g) in a circulating system in *i*-Pr-morpholine buffered methanol ($^{s}_{s}$pH = 8.8) at T = 25 °C over eight sequential runs.

4.4 – Conclusions

In this work we have demonstrated that the active monomeric form of **4.4**:Zn(II) can be generated on a solid support through grafting of ligand **4.6** onto an appropriate

chloromethylated polystyrene resin, followed by soaking in a $Zn(OTf)_2$ solution. We have demonstrated this methodology using a series of solid supports including two commercially available resins and one synthetic resin prepared in our laboratory. The results show that these heterogeneous catalysts are effective towards the destruction of a G-agent simulant (**4.7**) and a V-agent simulant (**4.8**) in neutral methanol at room temperature, and offer significant rate enhancement over the background reactions. While there is a range of activities depending on the polymer support, all of the immobilized catalysts give at least 10^4-fold acceleration for the methanolysis of both substrates. In the best case, Macro-PL-**4.6c** gives nearly 8 x 10^4-fold acceleration for the methanolysis of **4.7** and 2 x 10^5-fold acceleration for the destruction of **4.8**. Furthermore, the catalysts are robust and show excellent stability upon recycling.

We have found that using our methodology, we are only able to achieve low catalyst loadings on the solid supports (typically 1 – 8 % conversion of the initial chloride content of the starting polymer); however, we have demonstrated that such low loadings are sufficient to give good catalysis. In fact, in the case of Macro-PL-**4.6**, metal loadings in excess of ~0.1 mmol/g (3.5% conversion) do not appear to give any additional catalytic benefit. This property of the immobilized catalysts may in fact be seen as desirable since it obviates the need to fully optimize the functionalization procedure and allows the catalyst to achieve maximum activity with relatively low metal loading.

Finally, we have demonstrated that the materials can be packed into columns and used in continuous flow systems. While the catalysts employed in this way are slightly more effective than when simply agitated in solution, the use of larger columns where the ratio

of column volume to total circulating volume is maximized will be necessary to achieve the full benefit of this system.

4.5 – References

1) Didier, B.; Mohamed, M.F.; Csaszar, E.; Colizza, K.G.; Neverov, A.A.; Brown, R.S. *Can. J. Chem.* **2008**, *86*, 91.

2) a) Yang, Y.-C.; Baker, J.A.; Ward, J.R. *Chem. Rev.* **1992**, *92*, 1729. b) Yang, Y.-C. *Acc. Chem. Res.* **1999**, *32*, 109. c) Morales-Rojas, H.; Moss, R.A. *Chem. Rev.* **2002**, *102*, 2497. d) Smith, B.M. *Chem. Soc. Rev.* **2008**, *37*, 470.

3) Desloges, W.; Neverov, A.A.; Brown, R.S. *Inorg. Chem.* **2004**, *43*, 6752.

4) Tsang, J.S.W.; Neverov, A.A.; Brown, R.S. *Org. Biomol. Chem.* **2004**, *2*, 3457.

5) a) Menger, F.M.; Tsuno, T. *J. Am. Chem. Soc.* **1989**, *11,* 4903. b) Lu, Q.; Singh, A.; Deschamps, J.R.; Chang, E.L. *Inorg.Chim. Acta.* **2000**, *309*, 82. c) Hartshorn, C.M.; Singh, A.; Chang, E.L. *J. Mater. Chem.* **2002**, *12*, 602. d) Hartshorn, C.M.; Deschamps, J.R.; Singh, A.; Chang, E.L *React. Funct. Polym.* **2003**, *55*, 219. e) Lykourinou-Tibbs, V.; Ercan, A.; Ming, L.-J. *Catal. Commun.* **2003**, *4*, 549. f) Wagner, G.W.; Bartram, P.W. *Langmuir*. **1999**, *15*, 8113. g) Beaudry, W.T.; Wagner, G.W.; Ward, J.R. *J. Mol. Catal.* **1994**, *93*, 221. h) Saltzman, S.; Mingelgrin, U.; Yaron, B. *J. Agric. Food Chem.* **1976**, *24*, 739. i) El-Amamy, M.M.; Mill, T. *Clays Clay. Miner.* **1984**, *32*, 67.

6) Gibson, G.T.T. PhD Thesis, Queen's University.

7) Lewis, R.E.; Neverov, A.A.; Brown, R.S. *Org. Biomol. Chem.* **2005**, *3*, 4082.

8) Melnychuk, S.A.; Neverov, A.A.; Brown, R.S. *Angew. Chem.* **2005**, *118*, 1799.

9) (a) Binnemans, K.; Lenaerts, P.; Driesen, K.; Görller-Warland, C. *J. Mater. Chem*. **2004**, *14*, 191. (b) Lenaerts, P.; Driesen, K.; Van Deun, R.; Binnemans, K. *Chem. Mater*. **2004**, *17*, 2148.

10) Akelah, A.; Sherrington, D.C. *Chem. Rev.* **1981**, *81*, 557.

11) Guyot, A.; Bartholin, M. *Prog. Polym. Sci.* **1982**, *8*, 277.

12) Chemin, A.; Deleuze, H.; Maillard, B. *Eur. Polym. J.* **1998**, *34*, 1395.

Chapter 5 - An Immobilized *Ortho*-palladated Dimethylbenzylamine Complex as an Efficient Catalyst for the Methanolysis of Phosphorothionate Pesticides

5.1 – Preface

With minor formatting changes, this chapter is largely as it was published in *Inorganic Chemistry* (Mohamed, M.F.; Neverov, A.A.; Brown, R.S. *Inorg. Chem.* **2009**, *48*, 1183). All experiments (including catalyst preparation, kinetics, and analytical data collection) were performed by Mark Mohamed. The manuscript was written by Mark Mohamed and R. Stan Brown. The published article is copyrighted by the American Chemical Society.

5.2 – Introduction

The sulfur-containing phosphorothionate triesters of general structure **5.1** comprise a family of compounds that are commonly used as agricultural pesticides having potent insecticidal and acaricidal properties while maintaining lower levels of toxicity toward mammals.[1,2] Due to their widespread use and persistence, the environmental accumulation of these toxic materials presents an ecological and health threat that has spurred much research into finding efficient chemical and biological decomposition strategies.[3,4] Current chemical methodologies for the decomposition of organophosphorus (OP) compounds rely primarily on hydrolytic and oxidative processes but only a few of these employ metal ions,[3] presumably because metal ion catalyzed hydrolysis of OP

substrates are relatively slow processes that also suffer from limited solubility of both the substrate and the active metal-hydroxo forms of the catalyst in water.

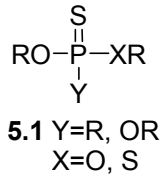

5.1 Y=R, OR
X=O, S

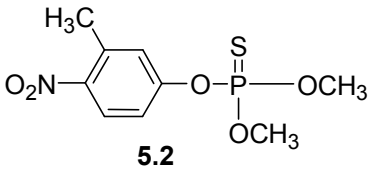

5.2

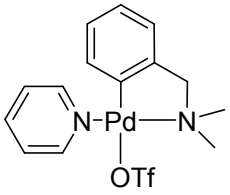

5.3 ($OTf=CF_3SO_3^-$)

Previous work in this laboratory demonstrated that neutral phosphate and phosphorothioate triesters[5,6], phosphonates[7] and phosphonothioates[8] are all cleaved rapidly in the presence of La(III) or a Zn(II)-complex of 1,5,9-triazacyclododecane in methanol to yield relatively non-toxic products where the XR group of **5.1** is replaced by an OCH_3 group. We have also demonstrated that the Cu(II):($^-OCH_3$) complex of 1,5,9-triazacyclododecane catalyzes the methanolysis of phosphorothionate (P=S containing) triesters with billion-fold acceleration relative to the methoxide-promoted background reaction at the ^s_spH[9] where the catalytic reaction is conducted.[10] These results prompted us to initiate a program to investigate the catalytic potential of immobilized metal:ligand complexes affixed to solid supports, and we have recently reported the initial results wherein the methanolysis of a series of neutral organophosphorus esters was promoted by some polystyrene-supported Zn(II) and Cu(II) complexes.[11] The latter polymer-supported catalysts do not approach the activity of the corresponding complexes in solution which is a general problem well known for supported catalysts,[12,13,14,15] and is usually attributed to surface and diffusion effects into the polymer matrix. However, the immobilized metal complexes still provide very good rate enhancements (up to 2.9 x 10^6-fold for the

methanolysis of fenitrothion (**5.2**) by a Cu(II):1,5,9-triazacyclododecane-fuctionalized polystyrene) relative to the background reaction at $^{s}_{s}$pH = 9.05.[16] Thus, having demonstrated the successful immobilization of transition metal catalysts on solid supports, and their use as effective catalysts for promoting the methanolysis of some pesticides, we directed our attention towards developing more active and efficient anchored complexes.

Previously we demonstrated that the palladacycle complex **5.3,** which had been shown to provide good catalysis of P=S OP materials in water,[17,18] is also an extremely efficient catalyst for the methanolysis of a series of phosphorothionate triesters including fenitrothion (**5.2**), where a 1.0 mM solution of catalyst at a near neutral $^{s}_{s}$pH = 8.75 in methanol accelerates the cleavage of **5.2** by 4.9 x 10^{9}-fold relative to the background methoxide promoted reaction at that $^{s}_{s}$pH.[19] Complex **5.3** is also effective for the methanolysis of other phosphorothionate substrates including dichlofenthion (**5.4**), coumaphos (**5.5**) and diazinon (**5.6**). A kinetic analysis of the $^{s}_{s}$pH -rate profile revealed that all these substrates react by a common mechanism involving formation of a transient complex (*cis* CH_3O^----Pd----(S=P)) where subsequent intramolecular delivery of the methoxide with Lewis acid assistance leads to a methanolysis product. However, despite its high efficiency, **5.3** is sparingly soluble in water and methanol, and also is expensive when used for the purposes envisioned. Thus, it seemed likely that anchoring this palladacycle on a solid support might provide a proficient, reusable, and cost effective heterogeneous catalyst for the decomposition of toxic P=S pesticide materials.

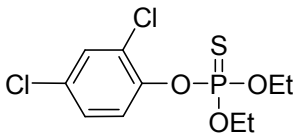

5.4

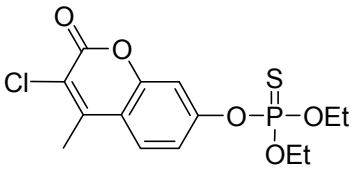

5.5

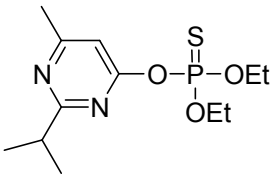

5.6

While many examples of immobilized palladium catalysts for diverse processes exist, these have been generally investigated as potential catalysts for C-C bond forming and related cross-coupling reactions,[20] and the majority employ covalently anchored phosphines or imines for attachment of palladium to the surface. Some examples of immobilized (SCS)-type pincer palladacycles have been reported,[21] however these complexes are known to be ineffective towards the methanolysis of phosphorothionate triesters.[22] The few examples of the immobilized *ortho*-palladated complexes that do exist have had variable success in their intended catalytic roles. In an example where the palladacycle was affixed to commercially available dicyclohexylphenyl phosphine functionalized polystyrene, there was an apparent turnover of the catalyst but no activity remained after the first run.[23] The *ortho*-palladated imine complexes developed by Nowotny *et al*.[24] and Bedford *et al.*[25] are thermally unstable in the organic media used and all the observed catalysis was found to be due to free palladium metal or nanoparticles in solution. More recently, Garcia *et al.* have reported that Suzuki-type cross-couplings could be promoted by an oxime carbapalladacycle immobilized on a variety of silica and polymeric surfaces.[26] While the SiO_2 anchored palladacycle showed no loss of activity after seven cycles,[26a] several of the polymeric materials exhibited decreased activity upon recycling.

Herein we report on a simple method to generate an immobilized equivalent of complex **5.3** on commercially available polystyrene and silica supports and show that these have

excellent catalytic activity and robustness for the methanolysis of phosphorothionate triesters **5.2** and **5.4-5.6** at ambient temperature and near neutral $^{s}_{s}$pH .

5.3 – Experimental

5.3.1 – Materials

Methanol (99.8% anhydrous), sodium methoxide (0.5 M solution in methanol), DMF (99.8%, anhydrous), K_2CO_3, Ag(OTf), $PdCl_2$, dimethylamine hydrochloride, dimethylamine (2.0 M solution in THF), and 4-benzylchloride functionalized silica gel (200-400 mesh, 1.2 mmolCl/g) were purchased from Sigma-Aldrich and used as supplied. Acetonitrile was purchased from Fisher Scientific. PL-CMS MP-Resin (>12% of cross linking with DVB, 2.8 mmolCl/g, porosity size 100 Å, particle size 150-300 μm) was purchased from Polymer Laboratories. Fenitrothion (**5.2**, *O,O*-dimethyl *O*-(3-methyl-4-nitrophenyl) phosphorothionate), dichlofenthion (**5.4**, *O,O*-diethyl *O*-(2,4-dichlorophenyl) phosphorothionate), coumaphos (**5.5**, *O,O*-diethyl *O*-(3-chloro-4-methyl-2-oxo-2H-chromen-7-yl) phosphorothionate), diazinon (**5.6**, *O,O*-diethyl *O*-(2-isopropyl-4-methyl-6-pyrimidinyl) phosphorothionate), and malathion (**5.8**, O,O-dimethyl-S-(l,2-dicarbethoxy)ethyl phosphorodithioate) were purchased from Chem Service Inc. and used as supplied.

The polystyrene and silica based catalysts (denoted PSPd and SiPd respectively) were prepared by the same general methodology, starting from macroporous chloromethylated polystyrene and 4-benzyl chloride functionalized silica gel respectively.

5.3.2 - Preparation of dimethylbenzylamine functionalized polystyrene: To a 2-necked round bottom flask was added 0.234 g (2.87 mmol) of dimethylamine hydrochloride and a small magnetic stir bar. The solid was dissolved in 20 mL of anhydrous DMF and 0.602 g (4.36 mmol) of K_2CO_3 was added to the solution. The solid carbonate remained largely undissolved at the bottom of the flask, and the mixture was allowed to stir at room temperature for two hours. At this point 0.489 g of PL-CMS MP-Resin (1.37 mmol Cl) was added to the reaction mixture along with an additional 0.19 g (1.37 mmol) K_2CO_3 and the flask was equipped with a reflux condenser and thermometer. The mixture was heated to 100 ˚C in an oil bath and gently stirred to avoid crushing the polymer for four days. The polymer was then filtered and washed with excess water to dissolve all residual K_2CO_3 followed by washing with 100 mL of methanol. The pale yellow polymer was immersed in a solution of 0.1 M sodium methoxide in methanol overnight to remove traces of acid and cap any residual chloromethyl functionality. The polymer was filtered, washed with methanol (100 mL) and dried in an oven at 60 ˚C for 24 hours.

5.3.3 - Palladation of dimethylbenzylamine functionalized polystyrene

To a Teflon centrifuge tube was added 0.11 g (0.64 mmol) $PdCl_2$ and 20 mL of anhydrous acetonitrile. The red solid was only sparingly soluble. To the mixture was added 0.33 g (0.13 mmol, 2 eq.) of Ag(OTf), whereupon an immediate formation of a thick beige precipitate (AgCl) ensued. A magnetic stir bar was added to the tube and the mixture was stirred vigorously for two hours until all of the red $PdCl_2$ was consumed. The solid precipitate was separated by centrifugation and the yellow liquid phase was

transferred to a 50 mL round bottom flask containing 0.22 g of the dimethylbenzylamine functionalized polystyrene prepared as above. Almost immediately after addition of the palladium solution, the pale yellow resin began to darken. The reaction flask was equipped with a small magnetic stir bar and a reflux condenser and the two-phase mixture was heated to reflux for 24 hours. After cooling, the black polymer was filtered and washed with 100 mL of methanol, followed by drying at 60 ˚C for 24 hours.

5.3.4 - Preparation of silica gel supported palladacycle

SiPd1: To a 2-necked round bottom flask was added 0.1195 g (1.47 mmol) of dimethylamine hydrochloride and a small magnetic stir bar. The solid was dissolved in 40 mL of anhydrous DMF and 0.328 g (2.37 mmol) of K_2CO_3 was added to the solution. The solid carbonate remained largely undissolved at the bottom of the flask, and the mixture was allowed to stir at room temperature for two hours. At this point 0.614 g of 4-benzylchloride functionalized silica gel (0.737 mmol Cl) was added to the reaction mixture along with an additional 0.11 g (0.8 mmol) K_2CO_3 and the flask was equipped with a reflux condenser and thermometer. The mixture was heated to 100 ^{o}C in an oil bath and gently stirred to avoid crushing the silica for four days. The silica was then filtered and washed with excess water to dissolve all residual K_2CO_3, followed by washing with 100 mL of methanol. The pale yellow silica was immersed in a solution of 0.1 M sodium methoxide in methanol overnight to remove traces of acid and cap any residual benzylchloride functionality. The silica was filtered, washed with methanol (100 mL) and dried in an oven at 60˚C for 24 hours. The palladium complex was formed analogously to what was described for the polystyrene supported catalyst above.

SiPd2: To a heavy-walled glass pressure tube fitted with a Teflon screw cap was added 0.25 g of 4-benzylchloride functionalized silica gel (0.3 mmol Cl) and the gel was suspended in 10 mL of a 2.0 M solution of dimethylamine in THF (0.02 mol dimethylamine, 67 eq.). The tube was sealed and heated in an oil bath at 80 ^{o}C for 72 hours after which the gel was filtered, washed with 100 mL of methanol and then suspended in a 7 mM solution of $NaOCH_3$ in methanol overnight to remove all traces of acid. The resulting gel was washed by Soxhlet extraction with THF overnight and then dried at 60 ^{o}C for 24 hours. The palladium complex was formed according to the procedure given above.

SiPd3: To a heavy-walled glass pressure tube fitted with a Teflon screw cap was added 1.0786 g of 4-benzylchloride functionalized silica gel (1.3 mmol Cl) and the gel was suspended in 20 mL of a 2.0 M solution of dimethylamine in THF (0.04 mol dimethylamine, 31 eq.). To the mixture was added 0.4768 g (1.3 mmol) Bu_4NI. The tube was sealed and heated in an oil bath at 80 ^{o}C for 72 hours after which the gel was filtered, washed with 100 mL of methanol and then suspended in a 7 mM solution of $NaOCH_3$ in methanol overnight to remove all traces of acid. The resulting gel was washed by Soxhlet extraction with $HOCH_3$ overnight and then dried at 60 ^{o}C for 24 hours. The palladium complex was formed analogously to what was described for the polystyrene supported catalyst.

5.3.5 - Analysis of palladium and nitrogen loading

Nitrogen microanalyses were performed by Canadian Microanalytical Services Ltd. in Delta, British Columbia. For palladium analysis, samples of the palladium loaded

material (0.01 g – 0.1 g) were weighed into crucibles and burned in a muffle furnace at 500 ˚C for four hours. The residual ash in the crucibles was dissolved in 4 mL of aqua regia (1 mL HNO_3 + 3 mL conc. HCl) and heated to 150 ˚C for four hours on a hot plate to solubilize the palladium. The acid solutions were diluted with distilled water in a volumetric flask (10 mL – 100 mL) and analyzed for palladium at the Queen's Analytical Services Unit using a Varian AX-Vista Pro Inductively Coupled Plasma – Optical Emission Spectrometer. Samples were analyzed by monitoring the palladium emission line at 360.955 nm. The palladium content was determined based on a four point calibration curve using indium and scandium as internal standards.

5.3.6 – Kinetics

All kinetics experiments with immobilized catalysts were conducted in 2.5 mL of a methanol solution buffered with *i*-Pr-morpholine (6.6 mM) at $^{s}_{s}$pH = 8.8 ± 0.4.[27] The rate of methanolysis of **5.2** (1 x 10^{-5} M) was monitored by observing the rate of loss of absorbance at 265 nm and the rate of appearance of the phenol product at 310 nm. The rate of disappearance of **5.4** (1 x 10^{-4} M) was followed at 220 nm and the appearance of product was observed at 295 nm. For substrates **5.5** and **5.6** (1 x 10^{-4} M and 1.5 x 10^{-4} M respectively) the rates of starting material disappearance were observed at 293 and 245 nm and appearance of product from **5.5** at 195 nm. All reactions were monitored using a Cary 100 UV-vis spectrophotometer with the cell compartment thermostatted at 25.0 ± 0.1 ˚C. In a representative example monitored by UV-vis spectrophotometry, 0.05 g of PSPd2 was added to a quartz cuvette. In a separate vial, 25 μL of a 1 x 10^{-3} M stock solution **5.2** in methanol was added to 2.5 mL of *i*-Pr-morpholine buffered (6.6 x 10^{-3} M)

methanol to give a final substrate concentration of 1 x 10^{-5} M. This solution was transferred to a UV-vis cuvette and immediately placed in the spectrometer to obtain a time-zero absorbance. Every minute, the cell was removed and manually shaken for 13 seconds (~30 times) and replaced in the spectrometer for a short time (one to five seconds to allow settling of the solid polymer) before collecting a new absorbance spectrum from 200-400 nm over 27 seconds. The reactions were run to completion and the pseudo-first order rate constants (k_{obs}) were determined by fitting the absorbance vs. time traces to a standard exponential model. As discussed later, the actual catalyzed reaction required agitation of the solutions and control experiments establish that the reactions are at least 100 times slower when the catalysts are settled to the bottom of the cuvettes. Thus, only the collective times during which the reaction mixtures were actually shaken were used for the absorbance vs. time profile.

Control experiments in which 0.05 g of non-functionalized chloromethylated polystyrene and 4-benzylchloride functionalized silica gel were used as catalysts for the methanolysis of **5.2** showed no conversion of starting material to product, confirming that the reactions observed when PSPd and SiPd are catalysts are due solely to the palladacycle complex and not to the solid matrix.

5.4 - Results and Discussion

5.4.1 - Preparation of Immobilized Palladacycle

The chloromethylated polystyrene and 4-benzyl chloride functionalized silica gels were chosen as solid supports based on their commercial availability and our previous success

in functionalizing various polystyrene based materials.[11] Chloromethylated polystyrene is an attractive support matrix due to its chemical inertness and structural stability[28] while silica gel has the advantage of a large surface area accessible to solvent. While past examples of immobilized palladacycle complexes have relied on grafting an already prepared complex onto the solid surface, the benzyl chloride moiety in both the commercially available functionalized polystyrene and silica gel is a convenient point of attachment for the core structure of the immobilized palladacycle. Nucleophilic substitution of the chloride by dimethylamine gave the N,N-dimethylbenzylamine species, which is the starting point for the analogous preparation of complex **5.3** in solution.[29] As shown in Scheme 5-1, treatment of the anchored N,N-dimethylbenzylamine with $Pd(CH_3CN)_2(OTf)_2$, followed by immersion in methanol, gave the catalytically active species **5.7**. The respective palladium and nitrogen contents of the solid materials as determined by atomic absorption spectroscopy and microanalysis are given in Table 5-1. The analyzed loadings achieved by direct functionalization are comparable to those previously reported[26a] for grafting of oxime carbapalladacycle on polystyrene. In comparison to the chloride content in the commercial chloromethylated polystyrene, the Pd loadings represent 10-20% conversion of the chloride to the palladacycle complex but the nitrogen loading is higher, and in the case of PSPd3 it is 55% of the stated Cl in the commercial polystyrene (2.8 mmol/g). The total Cl content of the commercial polymer represents the total chloride content so it is possible that a considerable fraction of the Cl is located at sites inaccessible to, or of reduced reactivity for, the substitution or palladation reactions. It is interesting that the Pd loading is only about 37% of the available N despite the fact that excess Pd reagent was used for all the

reactions. The reduced conversion to the palladium may be the result of the decreased reactivity of functional groups on rigid, highly cross-linked polymeric backbones,[30] or it may simply be a consequence of a slower reaction for the cyclopalladation reactions, but at this point we have not optimized the time-conversion profiles.

Scheme 5-1. Scheme for preparation of immobilized palladacycle (**5.7**)

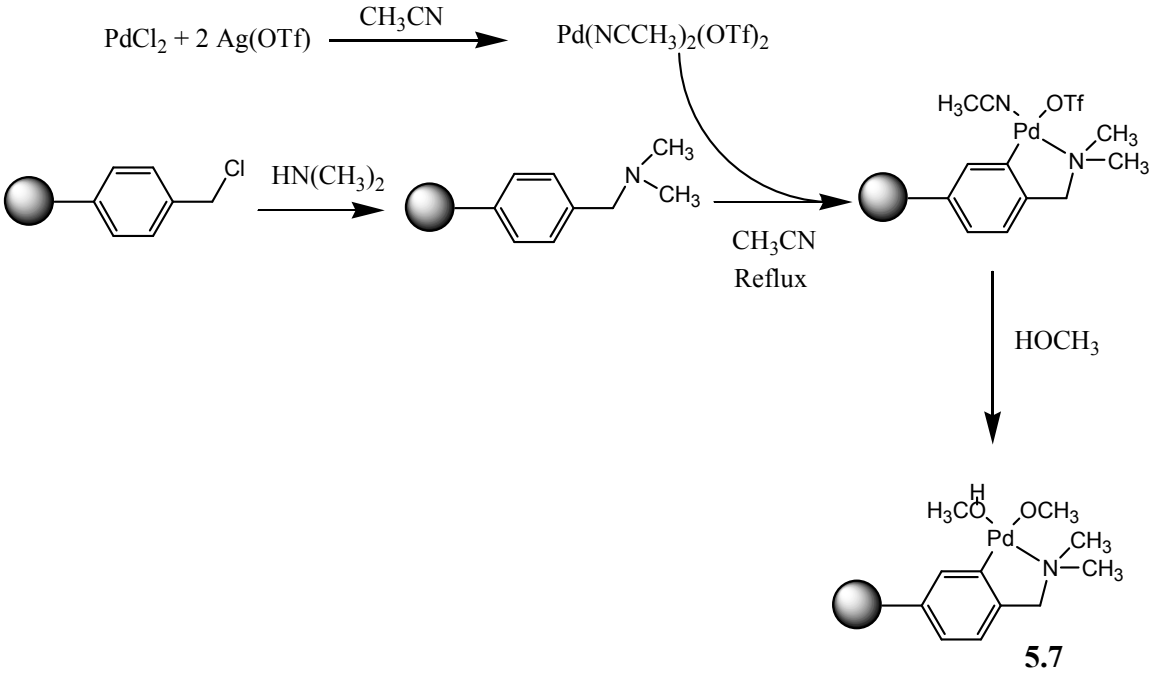

5.7

Three versions of silica supported catalyst were prepared as described in the experimental section where the palladium loading represented between 3% and 17% conversion of the reported 1.2 mmol/g chloromethylated starting material. As was the case with the polystyrene material, the nitrogen loading is invariably higher, being 42 to 88% of the available Cl, so the palladium loading is five to ten times less than the nitrogen loading for reasons that are not clear, but could be related to a slower palladation reaction. However, in the present study we have not optimized the palladium loading since, as will

be shown later, all these materials, surprisingly, exhibited the same general catalytic activity leading to the conclusion that there is no inherent advantage to create a more expensive, heavier loaded catalyst. Note that that the palladium analysis is for total palladium in all forms so cannot distinguish palladium in the form of active palladacycle, palladium black or nanoparticles, but later we show that even if Pd(0) is present, this material does not catalyze the reaction in question.

Table 5-1. Palladium and nitrogen content of immobilized catalysts as analyzed by Inductively Coupled Plasma – Optical Emission spectroscopy and microanalysis respectively

Catalyst	Pd source	Pd content (mmol/g) [a,b]	N content (mmol/g) [c]
PSPd1	Li_2PdCl_4	0.85 (0.57)	NA
PSPd2	$PdCl_2$	0.40 (0.21)	NA
PSPd3	$PdCl_2$	0.58	1.55
SiPd1	$PdCl_2$	0.036	0.5
SiPd2	$PdCl_2$	0.20	1.03
SiPd3	$PdCl_2$	0.075	0.74

[a] The value quoted is the Pd content before the material was used in a reaction. The value in brackets represents the Pd content after the first use of catalyst in solution.

[b] Error limits are considered to be ±15% of the reported value based on replicate measurements and detection instrument error.

[c] N loading determined by microanalysis; NA = not analyzed.

5.4.2 - Catalytic Studies

The catalytic activity of the materials was determined for the methanolysis of the phosphorothionate triesters **5.2**, **5.4**-**5.6**. The reaction rates were determined by measuring

the change in UV-vis absorbance for both the loss of starting material and formation of product in methanol solutions containing a known quantity of solid catalyst. The immobilized catalyst (0.009 - 0.090 g) was put into 2.5 mL of methanol solution, buffered at ${}^{s}_{s}pH = 8.8$ by *i*-Pr-morpholine (6.6×10^{-3} M). In each case the apparent concentration of the catalytic complex was determined as if the solid materials were completely dissolved in the reaction solution (denoted $[Pd]_T$) assuming that the Pd loading was completely in the form of palladacycle. Under these assumptions, the $[Pd]_T$ ranged between 8.9×10^{-5} M and 7.6×10^{-3} M when all experiments are considered.

As it is known that reproducible two-phase catalyzed reactions require a reproducible method of solution agitation, the simple manual procedure for determining the reaction kinetics described in the experimental section proved effective. This involved manual shaking of the cuvette for 13 seconds followed by placing the cell in the spectrophotometer for a few seconds, (1-5) to allow settling of the solids, followed by collection of the UV-vis spectrum from 200 to 400 nm over a 27 second period. The process was repeated every 60 seconds until the reactions were at least 95% completed. Magnetic stirring of the mixture was purposely avoided in order to prevent crushing of the solid catalyst which occurs quite readily with the silica catalyst even with a tiny stir bar, which in the latter stages of the reaction greatly increases the settling time of the solids. Control experiments established that the cleavage of the substrates occurs only while the solid catalyst is being actively agitated in the reaction mixture by shaking, and not when the catalyst is settled at the bottom of the cuvette. For example, when a 0.0426 g sample of the PSPd3 was placed in a cuvette with a 2.5 mL solution of 3×10^{-5} M **5.2** buffered at ${}^{s}_{s}pH = 8.8$, and the mixture was not shaken, contiguous UV-vis spectra do not

show any change. After sitting unshaken for 6 minutes, there was an absorbance change of $\Delta A = 0.0084$ at 272 nm (starting material wavelength). Compared to the total ΔAbs for complete conversion of starting material ($\Delta Abs = 0.1091$ at 272nm), the observed absorbance change represents $\Delta Abs/\Delta Abs_{total} = 0.0084/0.1091 = 7.7\%$ of the total absorbance change for the complete reaction or in terms of $\Delta Abs/dt = 0.0084/360$ s $= 2.3 \times 10^{-5}$ Abs/s. However, when the same mixture is shaken for 13 seconds, the absorbance change was $\Delta Abs = 0.031$, so the rate of change of absorbance was $\Delta Abs/dt = 0.031/13$ s $= 0.0024$ Abs/s, or 100 times greater than without shaking. In the absence of agitation, penetration of the reaction solution into the polymer matrix occurs only by slow diffusion of the solution across the liquid/solid interface. Active mixing of the solid catalyst in the reaction solution induces forced convection of the reaction mixture, thereby accelerating penetration of the solution across the phase boundary.

In view of the above, the Abs vs time plots that were used to determine the rate constants for the reactions reflect only the time period over which the reaction mixture was shaken (i.e. n x 13 sec., where n is the number of repetitions). A typical Abs vs. time plot for the methanolysis of **5.2** promoted by PSPd3 is shown in Figure 5-1, which also contains two data points for a second sample where the solution was continuously shaken for 120 seconds and then monitored by UV-vis spectrophotometry which are in excellent agreement with the data acquired from the mixtures shaken for the equivalent number of 13 second intervals. In all cases for each substrate and catalyst, the observed rate of change in absorbance followed good pseudo first-order behaviour, and when fit to a standard exponential model, gave the yielded first-order catalytic rate constants. These are normalized for 50 mg of catalyst, and the k_{obs} values are given in Tables 5-2 and 5-3.

The tables also contain the apparent second-order rate constants for the PSPd and SiPd catalyzed methanolysis of **5.2**, **5.4-5.6**, defined as $k_{obs}/[Pd]_T$.

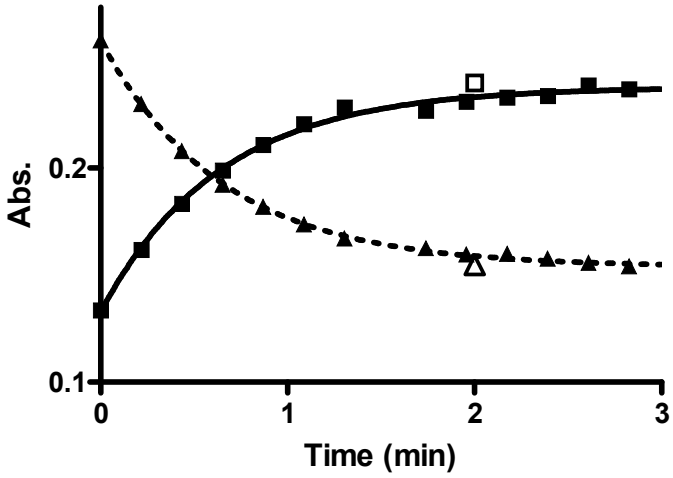

Figure 5-1. Absorbance vs. time curves for the disappearance of **5.2** (3 x 10^{-5} M) (▲, absorbance at 272 nm) catalyzed by 0.0426 g PSPd3 and for the appearance of 3-methyl-*p*-nitrophenol (■, absorbance at 310 nm) at T = 25 ˚C, $^{s}_{s}$pH = 8.8. The points (Δ) and (□) represent the absorbances at 272 nm and 310 nm respectively after the same catalyst was shaken with a 3 x 10^{-5} M solution of **5.2** continuously for 2 minutes at T = 25 ˚C, $^{s}_{s}$pH = 8.8. The time scale on the x-axis is corrected to reflect only the time of shaking as described in the text. Lines through the data are computed on the basis of fits to a standard exponential model for appearance of product (1.56 ± 0.06 min^{-1}) and disappearance of **5.2** (1.53 ± 0.03 min^{-1})

Table 5-2. First-order and apparent second-order rate constants for the methanolysis of phosphorothionate triesters catalyzed by polystyrene-bound palladacycle (PSPd2) in methanol buffered at $^{s}_{s}$pH = 8.8 by *i*-Pr-morpholine (6.6 x 10^{-3} M), T = 25˚C.

Substrate [a]	k_{obs} (s^{-1}) for 50 mg of polymer [b]	k_2 ($M^{-1}s^{-1}$) [c,d]	Solution k_2 ($M^{-1}s^{-1}$) [e]	k_2^{OMe} ($M^{-1}s^{-1}$)
5.2	2.68 x 10^{-2}	6.4	36.9	7.2 x 10^{-4}
5.4	2.15 x 10^{-2}	5.1	44.3	1.7 x 10^{-4}

5.5	2.07 x 10^{-2}	4.9	146.7	7.5 x 10^{-4}
5.6	1.63 x 10^{-2}	3.7	0.45	5.8 x 10^{-4}

[a] [**5.2**] = 1 x 10^{-5} M, [**5.4**] = 1 x 10^{-4} M, [**5.5**] = 1 x 10^{-4} M, [**5.6**] = 1.5 x 10^{-4} M

[b] For 50 mg of PSPd2 in 2.5 mL of solution, $[Pd]_T$ = 4.2 x 10^{-3} M. These kinetic data were gathered using the first use material where the Pd analysis was 0.40 mmol/g.

[c] Error limits are considered to be ± 20% based on errors in the determination of palladium loading and uncertainties in duplicate rate measurements

[d] k_2 is defined as $k_{obs}(s^{-1})/[Pd]_T(M)$

[e] Second-order rate constants for the methanolysis of substrates **5.2**, **5.4**-**5.6** catalyzed by **5.3** at $^{s}_{s}$pH 10.8 from ref. 19.

Table 5-3. First-order and apparent second-order rate constants for the methanolysis of phosphorothionate triesters catalyzed by silica-gel bound palladacycle (SiPd1) in methanol buffered at $^{s}_{s}$pH = 8.8 by *i*-Pr-morpholine (6.6 x 10^{-3} M), T = 25˚C.

Substrate [a]	$k_{obs}(s^{-1})$ for 50 mg of silica [b]	k_2 ($M^{-1}s^{-1}$) [c,d]	Solution k_2 ($M^{-1}s^{-1}$) [e]	k_2^{OMe} ($M^{-1}s^{-1}$)
5.2	6.22 x 10^{-2}	86.3	36.9	7.2 x 10^{-4}
5.2	4.8 x 10^{-2} [f]	12.4	36.9	7.2 x 10^{-4}
5.2	6.4 x 10^{-2} [g]	42.5	36.9	7.2 x 10^{-4}
5.4	4.13 x 10^{-2}	57.5	44.3	1.7 x 10^{-4}
5.5	4.07 x 10^{-2}	56.6	146.7	7.5 x 10^{-4}
5.6	2.38 x 10^{-2}	33.1	0.45	5.8 x 10^{-4}

[a] [**5.2**] = 1 x 10^{-5} M, [**5.4**] = 1 x 10^{-4} M, [**5.5**] = 1 x 10^{-4} M, [**5.6**] = 1.5 x 10^{-4} M

[b] For 50 mg of SiPd1 in 2.5mL of solution, $[Pd]_T$ = 7.2 x 10^{-4} M

[c] Error limits are considered to be ± 20% based on errors in the determination of palladium loading and uncertainties in duplicate rate measurements.

[d] k_2 is defined as $k_{obs}(s^{-1})/[Pd]_T(M)$

[e] Second-order rate constants for the methanolysis of substrates **5.2**, **5.4**-**5.6** catalyzed by **5.3** at $^{s}_{s}$pH 10.8 from ref. 19.

[f] The methanolysis reaction was catalyzed by SiPd2 (0.2 mmol/g Pd) for which 50 mg in 2.5 mL of solution gives $[Pd]_T = 4.0 \times 10^{-3}$ M.

[g] Methanolysis reaction promoted by SiPd3 (0.075 mmol/g Pd) for which 50 mg in 2.5 mL of solution gives $[Pd]_t = 1.44 \times 10^{-3}$ M

Plots of k_{obs} for the methanolysis of **5.2** catalyzed by PSPd2 and SiPd1 at $^{s}_{s}$pH = 8.8 as a function of the weight of catalyst (Figure 5-2) are, within experimental uncertainty, linear and show no obvious saturation kinetics over the weight range investigated which is consistent with the observations made for the methanolysis of **5.2** catalyzed by complex **5.3** in solution.[19]

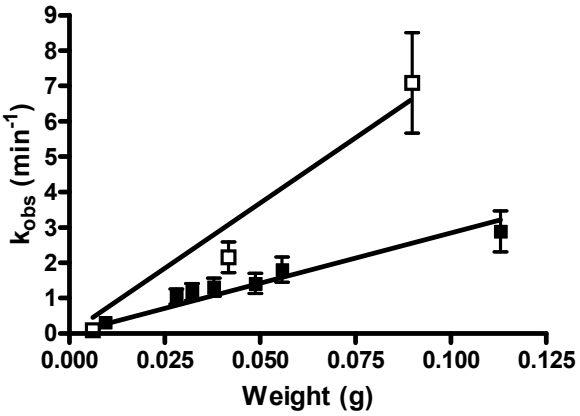

Figure 5-2. Pseudo first-order rate constant (k_{obs}) for the methanolysis of **5.2** (1×10^{-5} M) catalyzed by PSPd2 (■) and SiPd1 (□) vs. weight of catalyst at $^{s}_{s}$pH = 8.8, *i*-Pr-morpholine buffer (6.6×10^{-3} M), T = 25 ˚C.

The first three entries of Table 5-3 indicate that, while the experimental first-order rate constant (k_{obs}) for methanolysis of **5.2** promoted by the three variants of the SiPd catalyst are very similar, the computed second order constants based on total Pd content vary up to seven-fold as a consequence of the different amounts of $[Pd]_T$. Cursorily, this signifies

that there is no advantage to a higher palladium loading, and perhaps that the rate of the reaction is not limited by a chemical step but probably by diffusion or surface effects. Despite the lower palladium content of the silica based catalyst (SiPd1), the first-order rate constants for the methanolysis of all substrates were greater by roughly a factor of 2-3 than that provided by the polystyrene supported catalyst. When corrected for the Pd loading to determine the apparent second-order rate constants for the catalyzed reaction, the silica catalyst is about two to ten-fold better than the polystyrene one due to the ~10-fold less amount of Pd on the silica based catalyst, but the difference in reactivity is not strikingly large for the substrates investigated. Perhaps the greater activity of the silica based catalysts is due to the larger concentration of accessible reactive sites on the surface of the silica particles in comparison to the polystyrene beads. Another important factor could be that the surface of the silica support is very hydrophilic which may be of catalytic benefit in bringing the substrate to the surface, and also in allowing the methanol solvent to surround the catalytic groups on the surface while the opposite could be true for the hydrophobic surface of the polystyrene based catalysts.[31] Although the functionalization of the commercial chloromethylated polystyrene was performed in DMF and the cyclopalladation performed in acetronitrile (two solvents which are known to swell polystyrene), the solvolysis reactions are conducted in non-swelling methanol, and its hydrophobic surface may present a barrier to allowing the methanol solvent close to the surface-attached catalytic groups and those in the interior which are even less accessible.

The fact that the three silica supported catalysts have very similar activity, as measured by the pseudo first-order rate constant for methanolysis of **5.2,** while the total analyzed

loading of the palladium is quite different, can arise from two likely effects. One of these could be that there is a variable ratio of catalytically active/nonactive palladium in the three samples, with the larger loading arising from more of the nonactive forms that are occluded or attached to the solid support. This is probably also the case with the polystyrene catalysts which are visibly black when made and where the Pd analyses show that considerable Pd is leached from the polymer after the first use, but the overall activity does not change much. We acknowledge the probability of Pd(0) and/or palladium nano-particle formation on the surface of the solid materials as evidenced by the black colour of the catalysts. The Pd(0) formation may be the result of the reduction of palladium(II) by trace amounts of methanol remaining after washing the N,N-dimethylbenzylamine functionalized solids prior to palladation. However, even if formed, Pd(0) is not catalytically active. As a control experiment, unfunctionalized silica gel, which has no point of attachment for a palladacycle, was soaked in methanol overnight and then dried overnight at 60 ˚C and atmospheric pressure (the same drying procedure described for the other solid catalysts). This silica was then subjected to the same palladation conditions described in the experimental section. The resulting silica was found to be dark grey, presumably as a result of Pd(0) formation and when 0.043 g of this silica was introduced into a cuvette containing a solution of 3×10^{-5} M **5.2** with the usual shaking procedure, no change was observed in the UV spectrum over the course of five minutes.

A second likely possibility for the similar activity of the three silica supported catalysts stems from the fact that the rate-limiting step for the overall conversion of starting material to product involves a non-chemical process such as surface penetration or

diffusion. While the second-order rate constant for the methanolysis of substrates **5.2**, **5.4**-**5.6** in solution (given in Tables 5-2 and 5-3) range between 0.45 $M^{-1}s^{-1}$ for diazinon **5.6** and 146.7 $M^{-1}s^{-1}$ for coumaphos **5.5** (a 326-fold difference), the apparent second-order rate constants for methanolysis of the same substrates promoted by the supported catalysts reactions differ only by factors of ~1.3 and 1.7 for PSPd2 and SiPd1 respectively, and none of the reactivities of **5.2**, **5.4**-**5.6** follow the trend observed in solution. This too supports the contention that the rate-limiting process does not depend on the nature of the substrate. Interestingly, the second order rate constants computed for the methanolysis of substrates **5.2**, **5.4** and **5.6** catalyzed by SiPd1 are greater than the second order rate constants for the methanolysis in homogeneous solution catalyzed by **5.3** and in the case of PSPd2, the rate constant for its reaction with diazinon exceeds that of the solution reaction by about 8-fold. The reported apparent second-order rate constants in Tables 5-2 and 5-3 are lower limits since the computed values depend on the $[Pd]_T$, which is undoubtedly higher than the concentration of active species due to the presence of an inactive Pd(0) form. Nevertheless, the increased second-order rate constant for the heterogeneous reaction may be the result of an effect whereby substrate is concentrated on the catalyst surface. Hartshorn *et al.* also observed such phenomena when examining the hydrolysis of bis(*p*-nitrophenyl) phosphate and methyl parathion catalyzed by copper(II) containing polymers.[32]

It is notable that the solid supported palladacycles operate at near neutral $^{s}_{s}pH$ values in methanol where the background methoxide reactions are very slow. This is an attractive feature of the system for removal of this sort of pesticide from sensitive surfaces which

may corrode easily under highly alkaline conditions. Comparing the methoxide (k_2^{OMe} = (7.2 ± 0.2) x 10^{-4} $M^{-1}s^{-1}$)[10] and solid promoted reactions of fenitrothion (**5.2**) at ${}^{s}_{s}pH$ = 8.8, 50 mg of PSPd2 or SiPd1 provides a 3.7 x 10^9-fold and 8.6 x 10^9-fold acceleration when in excess of the substrate. When conducted in methanol buffered with 2,2,6,6-tetramethylpiperidine at ${}^{s}_{s}pH$ = 11.5, the methanolysis of **5.2** catalyzed by both SiPd1 and PSPd3 were increased by only a factor of two relative to the same reaction at ${}^{s}_{s}pH$ = 8.8. This suggests that the catalytically active complex, postulated as **5.7** having an associated lyoxide ($^{-}OCH_3$) by analogy with what we determined for the solution reaction mediated by **5.3**[19] and what was proposed by Gabbai and co-workers for a palladacycle operating in basic water with methyl parathion,[18] has a kinetic ${}^{s}_{s}pK_a$ of 8.8 or somewhat lower, and exists in its active form over a wide ${}^{s}_{s}pH$ range. This is an important distinction from the free catalyst **5.3** in solution where the reported ${}^{s}_{s}pK_a$ for formation of the active form is 10.8.[19] Indeed, these solid systems which bear a great number of ionizing sites must act as a large polybasic acid that undergoes numerous dissociations over a very wide ${}^{s}_{s}pH$ range.[33] In fact, if the rate-limiting step for these catalyzed reactions is that of a non-chemical process such as surface diffusion or penetration, it is not required that all the palladacycles exist in an active Pd-$^{-}OCH_3$ form; only a sufficient number are required to be present and react with the substrate more rapidly than it is presented to the catalytic domain.

5.4.3 - Catalytic Turnover

A turnover experiment was performed in order to demonstrate that the solid materials are indeed catalytic. A small amount of SiPd1 catalyst in 2.5 mL of methanol (6.2 mg, 8.9 x 10^{-5} M = $[Pd]_T$) was used to catalyze the methanolysis of 3.4 x 10^{-4} M **5.2** ([**5.2**] = 3.8$[Pd]_T$) buffered at ${}^{s}_{s}pH$ = 8.8 with *i*-Pr-morpholine (6.6 x 10^{-3} M). The UV-vis absorbance showed a complete loss of substrate and release of product with good first-order kinetics (k_{obs} = 0.092 min^{-1}) and no observed product inhibition. In this case, for the entire reaction under turnover conditions, the acceleration for the degradation of **5.2** relative to the background reaction at ${}^{s}_{s}pH$ = 8.8 was 2.1 x 10^{8}-fold. The data do point out, however, that the reactions conducted under turnover conditions are somewhat slower than when the catalyst is in excess of substrate, a phenomenon also observed for the methanolysis of **5.2** promoted by **5.3** under turnover conditions.[19,34] Thus the observed turnover second-order rate constant for methanolysis of fenitrothion of 17.2 $M^{-1}s^{-1}$ (based on the total amount of Pd on 6.5 mg of silica) is about five times lower than that determined for the kinetic determination with an excess amount (50 mg) of functionalized silica given in Table 5-3, entry 1, (k_2 = 86 $M^{-1}s^{-1}$). The reduction in the observed rate of reaction with increasing substrate concentration might be indicative of a saturating transport phenomenon.

5.4.4 - Catalyst Recycling

The oft-quoted advantages of polymer/solid supported catalysts are the ability to store and to reuse the catalyst when recovered from the reaction mixture[20,21,35.] As a control

experiment to test the effects of catalyst storage, the methanolysis of **5.2** was conducted using two batches of PSPd2, one of which was dried and stored in air, and a second that was stored for five days in *i*-Pr-morpholine buffer (6.6 x 10^{-3} M) at $^{s}_{s}$pH = 8.8. A reaction was conducted in which 0.0488 g of PSPd2, soaked in buffer, was used to catalyze the methanolysis of **5.2**. The catalyst was soaked in *i*-Pr-morpholine buffer (6.6 x 10^{-3} M) at $^{s}_{s}$pH = 8.8 in a quartz cuvette for five days. After this period, the buffer solution was decanted and the catalyst was washed with three portions of clean methanol (3mL each). To the cell was then added 2.5 mL of a 1 x 10^{-5} M solution of **5.2** in *i*-Pr-morpholine buffer (6.6 x 10^{-3} M) at $^{s}_{s}$pH = 8.8. This experiment gave the same observed rate constant (within experimental error) for the methanolysis of **5.2** as obtained with catalyst which was dried and stored in air (see Table 5-2).

The reusability of the immobilized catalysts was demonstrated by performing a series of sequential methanolysis reactions with the same sample of catalyst. Shown in Figure 5-3 are ten consecutive reactions with 1 x 10^{-5} M fenitrothion promoted by both PSPd2 and SiPd1. Each experiment involved following the time course of the reaction to completion, removal of the reaction solution from the cuvette by careful pipetting, washing the solid material in the cuvette with five portions of clean methanol (3 mL each) each of which was removed by careful pipetting, and then charging the remaining solid with 2.5 mL of buffer along with inoculation with 1 x 10^{-5} M fenitrothion and remonitoring the reaction.

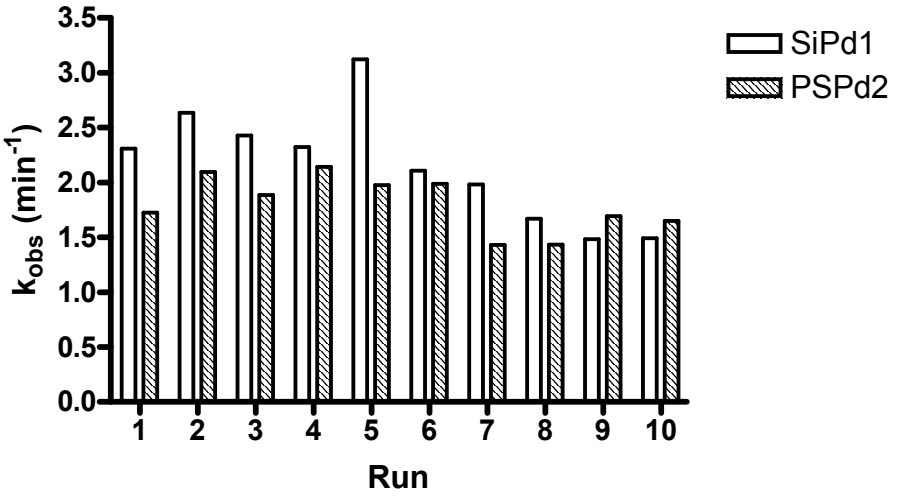

Figure 5-3. Pseudo first-order rate constants (k_{obs}) for the methanolysis of **5.2** (1 x 10^{-5} M) catalyzed by PSPd2 (0.0558 g) and SiPd1 (0.0418 g) at $^{s}_{s}$pH = 8.8 and T = 25˚C. Average k_{obs}(PSPd2) = 1.79 ± 0.26 min^{-1}. Average k_{obs}(SiPd1) = 2.16 ± 0.52 min^{-1}.

Given the relatively crude assessment of the activity as a function of time, both catalysts show a good stability toward subsequent use. It is possible that, during the washing cycles, some loss of active, but more flocculent, solid could have occurred which might account for the gradual diminution and apparent plateauing of activity. As shown in Table 5-1, the polystyrene based catalysts (PSPd) typically undergo some 30-50% loss of palladium upon the first use of the material, but the Figure 5-3 data indicate there is not much of a loss of the catalytic activity of the remaining material. This is consistent with desorption of a catalytically inactive palladium species which was chemi- or physisorbed into the polymer matrix. In the case of the silica based materials, the palladium contents before and after the first reaction do not differ which is probably a consequence of having the loosely adsorbed Pd removed during the washing procedures prior to any kinetic experiments.

5.4.5 - Control experiment showing putative solution palladium is not active

To further demonstrate the truly heterogeneous nature of the catalysts and to confirm the robustness of the immobilized palladium species, leeching experiments were conducted to show that all of the observed catalysis is due to immobilized palladium, and not due to palladium free in solution. Samples of PSPd3 and SiPd1 (0.035 g and 0.033 g respectively) were added to separate UV cuvettes and to each was added 2.5 mL of a 1 x 10^{-5} M solution of **5.2** in *i*-Pr-morpholine buffer (6.6 x 10^{-3} M) at $^{s}_{s}$pH = 8.8. The reactions were monitored and allowed to progress to ~50% completion at which point the reaction solution was carefully removed from the UV/vis cell and transferred to a clean cuvette. The cuvettes containing the reaction solution were again placed in the spectrometer and the reactions were monitored over the next 15 minutes. During this time, no change was observed in the UV spectrum of either reaction solution indicating that in the absence of solid catalyst, the reactions proceed only at their slow background rate. Reintroduction of the reaction solutions into the cuvettes containing the solid catalyst and carrying out the shaking/monitoring the UV-vis spectra, as described above for the solid catalyzed reactions, showed a continuation of the expected reaction until all of the substrate had disappeared.

5.4.6 - Methanolysis of Malathion

The structures of substrates **5.2**, and **5.4**-**5.6**, with chromophoric leaving groups, makes their reactions convenient to study using UV-vis spectrophotometry, but these are not as widely used as some other P=S pesticides such as malathion (**5.8**), which is the most

commonly used organophosphorus insecticide in the United States[36] for applications ranging from protection of agricultural crops to the treatment of head lice. While it has relatively low toxicity in humans, the major oxidative metabolite and contaminant in the commercial product is malaoxon (**5.9**) which is roughly 60-times more toxic for mammals. The wide-spread use of malathion, the toxicity of its metabolite and its slow rate of spontaneous hydrolysis makes it an appealing target for catalytic degradation.

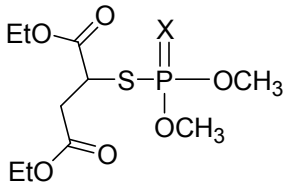

5.8 X=S
5.9 X=O

Since malathion does not contain a chromophore, its catalyzed methanolysis reactions were followed using ^{31}P NMR. A solution of malathion (5.15 x 10^{-3} M) was prepared in an NMR tube in 0.8 mL of a 1:1 mixture of normal methanol containing *i*-Pr-morpholine buffer (6.6 x 10^{-3} M) and CD_3OD. The substrate appears in the ^{31}P spectrum at δ96.43 ppm. The catalyst (PSPd3, 0.0436 g) was added to the NMR tube, giving $[Pd]_T$ = 31.6 x 10^{-3} M, and the tube was shaken for 30 seconds. After 5 minutes the ^{31}P spectrum was recorded and showed a new signal corresponding to the methanolysis product (*O,O,O*-trimethyl phosphorothionate) emerging at δ74.26 ppm (lit.[37] 73.91 ppm). Collection of the ^{31}P spectrum was repeated after 14 minutes and 24 minutes (relative peak intensities (starting material/product): 5 minutes = 1.00/0.26, 14 minutes = 0.696/1.00, 24 minutes = 0.274/1.00). After 32 minutes, the substrate peak at δ96.43 ppm was completely replaced by the product peak at δ 74.26 ppm. An analogous experiment in which 0.0426 g of

SiPd1 was used as the catalyst ($[Pd]_T$ = 1.9 x 10^{-3} M) showed an initial conversion of starting material to product, but failed to decompose all of the substrate after 30 minutes suggesting catalyst inhibition (relative peak intensities (starting material/product): after 15 minutes = 1.00/0.31, after 30 minutes = 1.00/0.38). This is consistent with an earlier ^{31}P NMR experiment using PSPd2 which rapidly decomposed an amount of malathion equal to half of the palladium content. In this experiment, 0.0378 g of PSPd2 was added to an NMR tube containing a solution of 5.15 x 10^{-3} M malathion prepared as described above, which showed the starting material peak at δ96.41 ppm in the ^{31}P NMR spectrum. The tube was shaken for 30 seconds every ten minutes and after a total of 60 minutes the ^{31}P NMR was collected and showed that the starting material peak at δ96.41 ppm was completely replaced by the product peak at δ74.25 ppm. Addition of a second aliquot of malathion (5.15 x 10^{-3} M) generated its customary signal at δ96.41 ppm, however the ^{31}P spectrum recorded 60 minutes after the addition of the second portion of substrate and shaking the sample as was done for the first aliquot, showed no decrease in the starting material and no additional product signal was observed. After a period of 96 hours (4 days), 64% of the substrate was converted to product and after 264 hours (11 days), the ^{31}P NMR showed no sign of starting material and the product peak at δ74.26 ppm.

The incomplete conversion by SiPd1 and the prolonged reaction time for the methanolysis of the second portion of malathion by PSPd2 is attributed to inhibition by the thiol/thiolate product. In the case of substrates **5.2**, **5.4**-**5.6** we do not observe product inhibition, even in the presence of excess substrate since the leaving groups are all substituted phenols where the hydroxyl group oxygen is a hard ligand and does not bind strongly to the soft[38] palladium centre. In the case of malathion however, the leaving

group is diethyl thiomalate which irreversibly binds to palladium via sulfur. As expected, analysis of the reaction solution from the catalyzed methanolysis of malathion by mass spectrometry showed the presence of the *O,O,O*-trimethyl phosphorothionate product at m/z = 156 with 34% intensity, but not the diethyl thiomalate. The fact that a less than a stoichiometric amount of malathion strongly inhibits the polystyrene-bound palladacycle supports our earlier hypothesis that the metal containing sites have variable accessibility to solvent and substrate, such that only the accessible ones are inhibited by the reaction products.

5.5 – Conclusion

We have shown here that derivatization and palladation of commercially available chloromethylated polystyrene and 4-benzylchloride functionalized silica gels leads to efficient heterogeneous catalysts for the methanolysis of phosphorothionate triesters where the departing group does not contain a free thiolate. The materials both show good activity towards the methanolysis of fenitrothion (**5.2**), dichlofenthion (**5.4**), coumaphos (**5.5**), and diazinon (**5.6**), all of which are commercially available P=S pesticides. The catalytic activity is shown to be somewhat greater for catalyst immobilized on silica gel, probably due to the former's higher surface area and hydrophilic nature making it more accessible to solvent than its polystyrene counterpart. In the best case, the palladacycle immobilized on silica gel accelerates the methanolysis of **5.2** by a factor of 8.6×10^9 compared to the background reaction at the same ${}^{S}_{S}\mathrm{pH}$. However, this result is obtained only when the heterogeneous catalyst is in excess of the substrate, and in cases where the

substrate is in excess to the catalysis, there is a small, but noticeable drop in activity for reasons that are not clear but might be related to transport phenomena. Both the polystyrene and silica gel based catalysts show good stability over the course of several sequential reactions and show no product inhibition with substrate **5.2**.

A surprising aspect of this work is that silica based catalysts having different amounts of total analyzed palladium show roughly the same activity toward the methanolysis of **5.2**, and in fact very similar reactivities toward different substrates despite the fact that the solution based reactions of these vary by more than 300-fold. This suggests that the rate limiting steps for these reactions are not chemical ones, but rather steps having to do with surface diffusion and penetration. One benefit of this phenomenon is that creating more expensive, higher loaded catalysts does not appear to be of any benefit in accelerating the rates of the observed reactions.

A major shortcoming of the palladacycle catalysts as used here concerns their inhibition by the products of methanolysis of malathion. Presumably, the inhibitor is the thiolate anion which suggests that it might be possible to employ oxidizing agents to divert the latter into disulfides or S=O products that will not be inhibitory. Further work along these lines is underway and will be reported in due course.

5.6 - References and Footnotes

1) a) Toy, A.; Walsh, E.N. *Phosphorus Chemistry in Everyday Living*. American Chemical Society, Washington, DC, 2nd ed., 1987, ch.18-20. b) Quin, L. D. *A Guide to Organophosphorus Chemistry.* Wiley, New York, 2000. c) Gallo, M.A.; Lawryk, N.J. *Organophosphorus Pesticides. The Handbook of Pesticide Toxicology.* Academic Press,

San Diego, CA, 1991. d) Chernier, P. J. *Survey of Industrial Chemistry.* VCH, New York, 2nd ed, 1992, pp. 389-417.

2) Hassall, K. A. *The Biochemistry and Uses of Pesticides.* VCH, Weinheim, 2nd ed., 1990, pp. 269-275.

3) Morales-Rojas, H.; Moss, R. S. *Chem. Rev.* **2002**, *102*, 2497.

4) Shimazu, M.; Chen, W.; Mulchandani, A. ACS Symposium Series **2004**, *863*, 25-36.

5) Tsang, J. S.; Neverov, A. A.; Brown, R. S. *J. Am. Chem. Soc.* **2003**, *125*, 7602; b) Tsang, J. S. W.; Neverov, A. A.; Brown, R. S. *Org. Biomol. Chem*. **2004**, *2*, 3457.

6) Liu, T.; Neverov, A. A.; Tsang, J. S. W.; Brown, R. S. *Org. Biomol. Chem.* **2005**, *3*, 1525.

7) Lewis, R. E.; Neverov, A. A.; Brown, R. S. *Org. Biomol. Chem.* **2005**, *3*, 4082.

8) Melnychuk, S. A.; Neverov, A. A.; Brown, R. S. *Angew. Chem. Int. Ed.* **2006**, *45*, 1767.

9) For the designation of pH in non-aqueous solvents we use the forms recommended by the IUPAC, *Compendium of Analytical Nomenclature. Definitive Rules 1997* 3rd ed., Blackwell, Oxford, U. K. 1998.

10) Neverov, A .A.; Brown, R. S. *Org. Biomol. Chem.* **2004**, *2*, 2245.

11) Didier, B.; Mohamed, M. F.; Csaszar, E.; Colizza, K. G., Neverov, A. A.; Brown, R. S. *Can. J. Chem.* **2008**, *86*, 1.

12) Menger, F. M.; Tsuno, T. *J. Am. Chem. Soc.* **1989**, *111*, 4903.

13) (a) Lu, Q.; Singh, A.; Deschamps, J. R.; Chang, E. L. *Inorg. Chem. Acta* **2000**, *309*, 82; (b) Hartshorn, C. M.; Singh, A.; Chang, E. L. *J. Mater. Chem.* **2002**, *12*, 602; (c)

Hartshorn, C. M.; Deschamps, J. R.; Singh, A.; Chang, E. L. *Reactive & Functional Polymers* **2003**, *55*, 219.

14) (a) Srivatsan, S. G.; Verma, S. *Chem. Eur. J.* **2001**, *7*, 828; (b) Srivatsan, S. G.; Parvez, M.; Verma, S. *Chem. Eur. J.* **2002**, *8*, 5184; (c) Chandraskhar, V.; Athmoolan, A.; Srivatsan, S. G.; Shanmuga Sundaram, P.; Verma, S.; Steiner, A.; Zacchini, S.; Butcher, R. *Inorg. Chem.* **2002,** *41*, 5162; (d) Srivatsan, S. G.; Verma, S. *Chem. Commun.* **2000**b, 515.

15) Hanafy, A. I.; Lykourinou-Tibbs, V.; Bisht, K. S.; Ming, L.-J. *Inorg. Chim. Acta* **2005**, *358*, 1247.

16) Since the autoprotolysis constant is $10^{-16.77}$, neutral ${}^{s}_{s}\mathrm{pH}$ in methanol is 8.38: see Bosch, E.; Rived, F.; Rosés, M.; Sales, J. *J. Chem. Soc., Perkin Trans.* **1999**, *2*, 1953.

17) Various Pd and Pt N,N-dimethylbenzylamine metallocycles and related species and their use for the hydrolysis of sulfur containing OP materials have been described prior to our work; (a) Ryabov, A. D.; Kazankov, G. M.; Kurzeev, S. A.; Samuleev, P. V.; Polyakov, V. A. *Inorg. Chim. Acta*. **1998**, *280*, 57; (b) Kurzeev, S. A.; Kazankov, G. M.; Ryabov, A. D. *Inorg. Chim. Acta*. **2000**, *305*, 1; (c) Kazankov, G. M.; Sergeeva, V. S.; Efremenko, E. N.; Alexandrova, L.; Varfolomeev, S. D.; Ryabov, A. D. *Angew. Chem. Int. Ed.* **2000**, *39*, 3117; (d) Kazankov, G. M.; Sergeeva, V. S.; Borisenko, A. A.; Zatsman, A. I.; Ryabov , A. D. *Russ. Chem. Bull. Int. Ed.* **2001**, *50*, 1844.

18) Recent reports by Gabbaï et al.[18] have also found structurally similar palladacycle complexes to be effective catalysts for the hydrolysis of the phosphorothionate methyl parathion: a) Kim, M.; Liu, Q.; Gabbaï, F.P. *Organometallics*. **2004**, 23, 5560. b) Kim, M.; Picot, A.; Gabbaï, F.P. *Inorg. Chem.* **2006**, 45, 5600.

19) Lu, Z.-L.; Neverov, A. A.; Brown, R. S. *Org. Biomol. Chem.* **2005**, *3*, 3379. From the data presented in Table 4 of ref. 19, the k_2 value for methanolysis of **5.2** (2.0×10^{-5} M) promoted by complex **3** (2.0×10^{-5} M) at ${}^{s}_{s}\mathrm{pH}$ 8.75 is 35 $M^{-1}s^{-1}$. It is of note in ref.19 that when turnover experiments are conducted with 7.3 x 10^{-3} M **5.2** and 1.5 x 10^{-4} M **5.3** at ${}^{s}_{s}\mathrm{pH}$ 10.8 in triethylamine buffer, the k_2 value is 36.9 $M^{-1}s^{-1.}$

20) Leadbeater, N. E.; Marco, M. *Chem. Rev.* **2002**, *102*, 3217.

21) a) Bergbreiter, D. E.; Osburn, P. L.; Wilson, A.; Sink, E. M. *J. Am. Chem. Soc.* **2000**, *122*, 9058; b) Bergbreiter, D. E.; Osburn, P. L.; Liu, Y.-S. *J. Am. Chem. Soc.* **1999**, *121*, 9531; c) McNamara, C. E.; King, F.; Bradley, M. *Tetrahedron Lett.* **2004**, *45*, 8239.

22) Lu, Z.-L.; Neverov, A.A.; Brown, R.S. unpublished data.

23) Bedford, R. B.; Coles, S. J.; Hursthouse, M. B.; Scordia, V. J. M. *J. Chem. Soc. Dalton Trans.* **2005**, 991.

24) Nowotny, M.; Hanefeld, U.; van Koningsveld, H.; Maschmeyer, T. *Chem. Comm.* **2000**, 1877.

25) Bedford, R. B.; Cazin, C. S. J.; Hursthouse, M. B.; Light, M. E. Pike, K. J.; Wimperis, S. *J. Organometal. Chem.* **2001**, *633*, 173.

26) a) Baleizão, C.; Corma, A.; Garcia, H.; Leyva, A. *J. Org. Chem.* **2004**, *69*, 439; Corma, A. ; Das, D.; Garcia, H. ; Leyva, A. *J. Catal.* **2005**, *229*, 322 ; c) Corma, A. ; Garcia, H. ; Leyva, A. *J. Catal.* **2006**, *240*, 87.

27) For the measurement of ${}^{s}_{s}\mathrm{pH}$ in methanol see: Gibson, G.; Neverov, A. A.; Brown, R. S. *Can. J. Chem.* **2003**, *81*, 495 and references therein.

28) Chauvin, Y.; Commereuc, D.; Dawans, F. *Prog. Polym. Sci.* **1977**, *5*, 95.

29) Ryabov, A.; Polyakov, V.A.; Yatsimirsky, A.K. *J. Chem. Soc., Perkin Trans. 2*. **1983**, 1503.

30) Guyot, A. *Pure Appl. Chem.* **1988**, *60*, 365.

31) Corma, A.; Garcia, H. *Topics in Catalysis,* **2008**, *48*, 8.

32) Hartshorn, C.M.; Singh, A.; Chang, E.L. *J. Mater. Chem.* **2002**, 12, 602.

33) As is known for polybasic acids bearing numerous ionizing sites, the pKa values are spread over several pH units due to statistical effects and, more importantly, electrostatic effects.

34) When in excess of substrate, the k_2 value determined for reaction of **5.2** with **5.3** at $^{s}_{s}$pH 10.8 by UV-visible spectrophotmetry is 1880 $M^{-1}s^{-1}$, while that determined under turnover conditions by ^{1}H NMR is 36.9 $M^{-1}s^{-1}$. The drop in reactivity was atrtributed[19] to the large concentration of inhibitory buffer in the NMR experiment which was required to control the $^{s}_{s}$pH, as well as the larger concentrations of substrate (7 x 10^{-2} M) and catalyst which can alter the solution properties. It is possible, however, that the diminution of rate is attributable to a saturation binding of substrate and catalyst.

35) a) Bergbreiter, D.E. *Chem. Rev.* **2002**, *102*, 3345; b) Dijkstra, H.P.; Slagt, M.Q.; McDonald, A.; Kruithof, C.A.; Kreiter, R.; Mills, A.M.; Lutz, M.; Speck, A.L.; Klopper, W.; Van Klink G.P.M.; Van Koten,G. *J. Catal.* **2005**, *229*, 322.

36) Bonner, M.R.; Coble, J.; Blair, A.; Beane Freeman, L. E.; Hoppin, J. A.; Sandler, D. P.; Alavanja, M. C. R. *Am. J. Epidemiol.* **2007**, *166*, 1023.

37) Greenhalg, R.; Shoolery, J. N. *Anal. Chem.* **1978**, *50*, 2039.

38) Smith, B.; March, J. *Advanced Organic Chemistry.* Fifth Ed., Wiley Interscience, New York, **2001**, pp. 338-342 and references therein.

Chapter 6 – Summary and Conclusions

At the outset of this work, we were motivated by the simple question: How do we make phosphoryl transfer faster? We were interested to know the answer to this question from a purely academic point of view (as it pertains to the fundamental question of how enzymes carry out these reactions), and also from a practical perspective for the development of catalysts which can rapidly cleave organophosphorus toxins. The projects that followed have led to a greater understanding of the components of small-molecule enzyme mimics which give rise to high catalytic activity towards the cleavage of phosphate diesters. They have also culminated in the preparation of immobilized transition metal catalysts which are not only capable of rapidly decomposing poisonous neutral phosphate esters, but are also simple to prepare and fully recyclable.

In Chapter 2, we have described a detailed kinetic study in which two sets of dinuclear Zn(II) complexes were prepared in order to determine the effect of the presence of oxyanionic bridging groups between the metal centers on the catalytic activity towards the methanolysis of the RNA analog 2-hydroxypropyl-*p*-nitrophenyl phosphate (HPNPP). The $Zn(II)_2$ complexes of **2.6** and **2.7** were compared to assess the effect of a bridging phenoxide ligand, while the $Zn(II)_2$ complex of **2.8** was prepared to determine the effect of the 2-propoxy group compared to the previously studied complex of **2.4**. Detailed kinetic studies of the cleavage of HPNPP including k_{obs} vs [catalyst] plots and $^{s}_{s}$pH-rate profiles were performed for each system along with potentiometric titration experiments to determine the acid dissociation constants for the catalytically relevant groups. The

results show that inclusion of the phenoxy bridging group in **2.7**:$Zn(II)_2$ reduces the second-order catalytic rate constant (k_2^{cat}) for cleavage of HPNPP by a factor of 160 relative to that of **2.6**:$Zn(II)_2$, while the incorporation of a propoxy group in **2.8**:$Zn(II)_2$ reduces its efficacy by 3.7 x 10^4 times relative to **2.4**:$Zn(II)_2$. Energetics calculations reveal that **2.6**:$Zn(II)_2$ offers a 3.7 kcal/mol greater stabilization of the reaction transition state for the cleavage of HPNPP than does **2.7**:$Zn(II)_2$ and that **2.4**:$Zn(II)_2$ affords 6.5 kcal/mol greater transition state stabilization than does **2.8**:$Zn(II)_2$. The analyses show that the reduction in the transition state stabilization experienced with the complexes having permanently bridging oxyanion groups stems almost entirely from a weaker binding of the phosphate and catalyst, and a reduced catalytic rate constant. These results indicate that the presence of a bridging oxyanion ligand between the metal centres, a common structural element required for the successful formation of many small molecule dinuclear catalysts that show cooperative activity in water, significantly impairs the catalytic efficiency for cleavage of HPNPP.

Chapter 3 describes a structure-function relationship study aiming to elucidate the role of hydrogen-bond donating substituents in dinuclear complexes which cleave HPNPP. We have prepared a family of dinuclear ligands (**3.7 – 3.13**) which contain hydrogen-bonding and non hydrogen-bonding functionality and we have assessed the ability of their $Zn(II)_2$ complexes to catalyze the cleavage of HPNPP. We conducted k_{obs} vs. [catalyst] plots for all complexes as well as $^{s}_{s}$pH-rate profiles to determine the acid-base properties of the catalysts. The kinetic data demonstrates that while all complexes with substituents in place of hydrogen (**3.8 – 3.11**, and **3.13**) are more active than the corresponding

unfunctionalized complexes (**3.7** and **3.12**), the complexes bearing hydrogen-bonding substituents (**3.8** and **3.9**) are no more active than complexes with simple alkyl substituents (**3.10**, **3.11**, and **3.13**). All of the functionalized complexes exhibit similar kinetic parameters (k_{cat} and K_m) which suggests that hydrogen-bonding and non hydrogen-bonding substituents have identical effects on both substrate binding and transition state stabilization. These results show that the incorporation of hydrogen-bonding substituents in small-molecule enzyme mimics, a practice which has seen increasing popularity, may not have an easily analyzed effect. While we have not definitively ruled out hydrogen-bonding as a mode of activation, our findings suggest that it is not the only factor at play and that the general change in local dielectric constant, polarity, hydrophobicity, and sterics upon introduction of (any) substituents around metal ions has a beneficial effect.

Chapters 4 and 5 are related to our efforts to develop solid-supported transition metal catalysts for the destruction of the toxic organophosphorus esters of the type which are commonly used as pesticides and chemical warfare agents. Our initial work (Chapter 4) focused on the development of immobilized zinc species for the cleavage of phosphonates which simulate the G- and V-agents. We successfully grafted the Zn(II) complex of 1,10-phenanthroline (**4.4**) onto a variety of chloromethylated polystyrene resins and used these insoluble catalysts for the methanolytic cleavage of the G-agent mimic **4.7** and the V-agent stimulant **4.8**. We found that all of the heterogeneous catalysts were able to accelerate the degradation of the two substrates by at least 10^4-fold relative to the background reaction at near neutral $^{s}_{s}\mathrm{pH}$. The catalysts were reusable at least ten

times and we investigated the use of the materials as a column packing in a continuous circulating system, which conferred an additional 40% to the rate of cleavage of **4.7**.

Although the catalysts developed in Chapter 4 were effective for simulants of chemical warfare agents (which are all P=O materials), they were not ideal for the methanolysis of presticides having a P=S group. Inspired by our previous work which had shown that cyclopalladated complexes are highly effective catalysts for the methanolysis of phosphorothionate pesticides, we investigated solid-supported catalysts to develop immobilized variants of the palladium species which had been studied in homogeneous solution. We have disclosed this work in Chapter 5. We first developed a simple strategy to form the active palladacycle complex on the polymer surface by first reacting a chloromethylated polystyrene or benzylchloride functionalized silica gel with dimethylamine, followed by metallation. The solid-supported palladium catalysts were used to promote the methanolysis of a series of P=S pesticides (fenitrothion **5.2**, dichlofenthion **5.4**, coumaphos **5.5**, and diazinon **5.6**). Both the polystyrene and silica gel based catalysts showed excellent activity and robustness for the methanolysis of the substrates. The silica gel supported catalysts were found to be slightly superior, possibly as a result of a higher surface modification accessible to the reaction solvent. For the methanolysis of fenitrothion, a silica gel based catalyst was found to accelerate the reaction by a factor of 8.6×10^9-fold relative to the background reaction at $^{s}_{s}\text{pH} = 8.8$. Interestingly, despite a large difference in the rates of catalyzed cleavage of the substrates in solution, in the presence of the solid catalysts prepared here the observed rates are much less variable. This suggests to us that the rate-limiting step for the overall process is one which involves surface penetration of the polymer and mass transport of the substrate

from solution into the polymer matrix. We have also observed that beyond a certain point, increasing the metal-loading of the materials does not give any additional activity which is further evidence for some non-chemical step being rate-limiting.

In addition to catalyzing the cleavage of substrates **5.2** and **5.4-5.6**, the solid supported material is also effective against the widely used pesticide malathion (**5.8**). While it does cleave malathion, the reactions are not catalytic due to poisoning of the catalysts, presumably by the diethyl thiomalate leaving group which irreversibly binds to palladium via sulfur.